

NUTRIENT AND CONTAMINANT EXPORT DYNAMICS IN
A LARGER-ORDER MIDWESTERN WATERSHED:
UPPER WHITE RIVER, CENTRAL INDIANA, USA

Michael David Wayne Stouder

Submitted to the faculty of the University Graduate School
In partial fulfillment of the requirements
for the degree
Master of Science
in the Department of Earth Sciences
Indiana University

August 2010

Accepted by the Faculty of Indiana University, in partial fulfillment of the requirements for the degree of Master of Science.

Lenore P. Tedesco, Ph.D., Chair

Philippe G. Vidon, Ph.D.

Master's Thesis
Committee

Pierre-Andre Jacinthe, Ph.D.

Acknowledgements

I would like to thank my family, especially my parents and grandparents, for their support throughout my academic career. Their encouragement to pursue my passion for the earth sciences and a level of higher education has allowed me to bear the trials and tribulations and relish in the victories that I have met along the way. Along with my family, I would also like to thank my friends for humoring me with their heartfelt attempts at taking interest in my work and providing the little pushes I needed to rekindle my enthusiasm and progress forward with my research.

I would also like to express my gratitude toward my research committee including Lenore Tedesco, Philippe Vidon, and Pierre Jacinthe. In addition to their patience, support, and guidance offered throughout this project, it was their instruction during my seven years at IUPUI that introduced me to and developed my passion for environmental geology and allowed me to promote public awareness of critical environmental issues through my work. Thank you to Joe Johnstone for teaching me the ropes and aiding me both in the field and the laboratory. Also, thank you to everyone at the IUPUI Center for Earth and Environmental Science (CEES) including Bob Hall, Bob Barr, Vince Hernly, and interns Mark Sparks, Jacob Lemon, and Ryan McAtee for your help and guidance in all aspects of this project.

Finally, I would like to thank the Central Indiana Water Resources Partnership (CIWRP) and Veolia Water Indianapolis, LLC for project funding and the laboratory analyses provided by Mark Gray's team.

ABSTRACT

Michael David Wayne Stouder

NUTRIENT AND CONTAMINANT EXPORT DYNAMICS IN A LARGER-ORDER MIDWESTERN WATERSHED: UPPER WHITE RIVER, CENTRAL INDIANA, USA

The transport of excess nutrients, sediment, and other contaminants to surface waters has been shown to cause a number of environmental and human health concerns. An understanding of the export pathways that these contaminants follow to surrounding water bodies is crucial to the anticipation and management of peak concentration events. Several studies have demonstrated that the majority of annual contaminant loading in the Midwest occurs during periods of elevated discharge. However, many studies use a limited number of sampling points to determine concentration patterns, loadings, and fluxes which decreases accuracy. Through high-resolution storm sampling conducted in a 2945 km² (1137 mi²) area of central Indiana's Upper White River Watershed, this research has documented the complex concentration signals and fluxes associated with a suite of cations, nutrients, and contaminants and isolated their primary transport pathways. Additionally, by comparing the results of similar studies conducted on smaller areas within this watershed, differences in concentration patterns and fluxes, as they relate to drainage area, have also been documented.

Similar to the results of previous studies, NO₃⁻ concentrations lacked a well-defined relationship relative to discharge and was attributed to primarily subsurface contribution. DOC was exported along a shallow, lateral subsurface pathway, TP and

TSS via overland flow, and TKN through a combination of both. Near or in-channel scouring of sediment increased DOC, TKN, TP, and TSS concentrations during Storm 2. Atrazine export was attributed to a combination of overland and subsurface pathways. 2-MIB and geosmin derived from different sources and pathways despite being produced by similar organisms. 2-MIB concentration patterns were characterized by dilution of an in-stream source during Storm 1 and potential sediment export during Storm 2 while in-stream concentrations or a sediment source of geosmin was rapidly exhausted during Storm 1. Many of the concentration patterns were subject to an exaggerated averaging effect due to the mixing of several larger watersheds, especially during Storm 1.

This research illustrates the need for high-frequency sampling to accurately quantify contaminant loads for total maximum daily load (TMDL) values, developing best management practices (BMPs), and confronting the challenges associated with modeling increasingly larger-scale watersheds.

Lenore P. Tedesco, Ph.D., Committee Chair

Table of Contents

Introduction	1
Nutrients and Contaminants	
<i>Nitrogen</i>	8
<i>Phosphorus</i>	10
<i>Dissolved Organic Carbon</i>	12
<i>Atrazine</i>	13
<i>Taste and Odor Compounds</i>	15
Significance, Objectives, and Hypothesis	17
Study Area	
<i>Basin Characteristics</i>	21
<i>Climate</i>	21
<i>Geology</i>	22
<i>Streamflow</i>	23
<i>Land Use</i>	24
Research Approach	
<i>30-year Streamflow Summary</i>	25
<i>Instrumentation and Sample Collection</i>	25
<i>Sample Processing and Analytical Methods</i>	27
Data Analysis	
<i>Hydrology and Precipitation</i>	30
<i>Concentrations, Loads, Timing Relationships, and Export Patterns</i>	32
Results	
<i>Hydrologic Response</i>	34
<i>Univariate Concentration Statistics and Error Analysis</i>	37
<i>Concentration Patterns</i>	41
<i>Loadings and Yields</i>	48
Discussion	
<i>Export Patterns</i>	49
<i>Influence of Scale</i>	59
Summary and Conclusions	63
Tables	67
Figures	78
References	96
Curriculum Vitae	

List of Tables

- Table 1. Summary of land use in Upper White River Watershed
- Table 2. Storm event descriptions and sampling summary
- Table 3. Analytical methods, detection limits, and method descriptions
- Table 4. Locations and descriptions of precipitation gages
- Table 5. Comparison of total daily precipitation data sources
- Table 6. Comparison of 2007-2008 streamflow to 30-year normal (1971-2000)
- Table 7. Summary of precipitation events and hydrological responses
- Table 8. Comparison of antecedent discharge data sources
- Table 9. Mean, geometric mean, median, and maximum concentration values
- Table 10. Minimum, maximum, mean, and median error percentages
- Table 11. Total loads, yields, and yield rates

List of Figures

- Figure 1. Map of the Upper White River Watershed
- Figure 2. Linear regression of discharge to contributing watershed area ratios
- Figure 3. Hydrograph of study period
- Figure 4. Hydrograph of average daily discharge and daily contributing precipitation
- Figure 5. Double-mass curve
- Figure 6. 30-year discharge recurrence interval and exceedance probability curves
- Figure 7. Box plots of ion concentrations
- Figure 8. Box plots of nutrient concentrations
- Figure 9. Box plots of contaminant concentrations
- Figure 10. Ion concentration curves
- Figure 11. Nutrient concentration curves
- Figure 12. Contaminant concentration curves

Introduction

Since European settlement in the 1600s, the United States has been subjected to mass deforestation, the implementation of widespread subsurface artificial drainage networks for agricultural purposes, large mining and resource extraction operations, water diversion, and exponential growth in urbanized areas and industrialization. As a result of deforestation and subsurface drainage systems, the natural hydrologic processes that existed prior to settlement in much of the United States have been fundamentally altered, especially in the glaciated Midwest (Barr et al., 2002). Additionally, without riparian and wetland areas to act as natural buffers to river systems, their ability to provide critical ecosystem functions including runoff and sedimentation control, nutrient cycling, water filtration, flood regulation, stream flow and temperature maintenance, groundwater recharge, and habitat preservation has been compromised (Kauffman et al., 1997). Now, as global populations have continued to grow and industrialization, urbanization, and resource extraction and consumption have all intensified, so too have many of the same water quality concerns in addition to a number of new and unique problems. The recent spike in urbanization is associated with increased areas of impervious surface, the channelization and straightening of streams, and homogenization of stream bed sediments (Booth and Jackson, 1997). These changes have caused higher peak discharges and flashier event flows, reduced groundwater-surface water exchange, reduction in groundwater recharge and hyporheic zone size, scouring and increased channel erosion, and reduced biotic richness (Burns et al., 2005; Bernhardt and Palmer, 2007). In addition to the hydrological and geomorphological repercussions caused by the anthropogenic alteration of the landscape, these modifications have also contributed to

the accelerated loading and transport of nutrients, sediment, and other contaminants from urban and agricultural areas due to the inherent inability of altered basins to store water on the landscape or remediate contaminant loads. Unfortunately, while the effects of surface water degradation are felt on a local scale, they are often the result of poor management practices from upstream sources.

When speaking of water quality issues in the United States, perhaps the most commonly discussed area of concern lies in the effects of the agricultural dominated land use in the Midwest and its effects on the surface waters within the Mississippi River Basin. The Mississippi River Basin is the third largest river system on Earth and, in total, drains more than 1,245,000 square miles, or 41% of the contiguous United States, including a majority of the Midwest. In addition to the significant physical alteration of the banks and floodplain of the Mississippi River and many of its tributaries, the primarily nonpoint source pollution associated with the Mississippi River's drainage basin has fueled detrimental influxes of nutrients, sediment, and other contaminants to the Gulf of Mexico (Goolsby et al., 2001; Alexander et al., 2008; Robertson et al., 2009). Large nitrogen and phosphorus loads traveling downstream from sources of agricultural and urban land use have been associated with the eutrophication of inland lakes and coastal waters (Carpenter et al., 1998; Goolsby et al., 2001; Royer et al., 2006). Eutrophication, or elevated nutrient levels occurring in surface water bodies, in turn leads to an increase in primary productivity in the system in the form of algal blooms and excessive plant growth, especially in the late summer months. With the death and subsequent decomposition of these organisms, dissolved oxygen is utilized and may

cause concentrations to drop to reduced levels. As levels continue to drop, aquatic species are subject to increasing levels of stress and may ultimately be unable to survive.

While municipal and industrial wastewater treatment has improved due to more stringent regulations in recent years, agricultural and urban nonpoint pollution is perhaps the most difficult to regulate and control (Kronvang et al., 2005; Reinhardt et al., 2006). Studies involving the treatment of nonpoint source pollution, including stormwater and agricultural runoff, are not as common and as a result are not understood to the degree of other contaminant sources (Mitsch and Gosselink, 2000). Unlike others, nonpoint sources are highly variable in contaminant type and concentration and are dependent on seasonal variation and land usage (Beaulac and Reckhow, 1982; Castillo et al., 2000; Randall and Mulla, 2001; Coulter et al., 2004; Poor and McDonnell, 2007; Christopher et al., 2008). Nutrients such as nitrogen (N) and phosphorus (P), in the form of artificial and inorganic fertilizers, are commonly applied to agricultural land and urban landscapes in order to increase productivity. Organic wastes, such as manure or sewage sludge, are also sources of these nutrients and are commonly applied for similar purposes or may derive from confined animal feeding operations. However, in areas such as the Midwestern United States, where agricultural land usage is commonly dominant, runoff potential is high, and streams may have little to no buffer zone, substantial amounts of these substances are able to make their way into groundwater as well as surrounding lakes, rivers, and streams.

A 2009 study implemented a previously published Spatially Referenced Regression On Watershed attributes (SPARROW) model (Alexander et al., 2008) in order to estimate and rank the total nitrogen (TN) and total phosphorus (TP) incremental

yields and delivered incremental yields from the 818 Hydrologic Unit Code (HUC) 8 watersheds that make up the Mississippi River Basin (Robertson et al., 2009). The 818 HUC8 watersheds drained a median area of 3,400 km² (1,313 mi²) and, after ranking each of the 818 watersheds according to their incremental and delivered incremental yields, nearly all of the top 150 ranked watersheds were located in the area known as the Corn Belt or near the Mississippi River. The highest yields for TN occurred in northern Illinois and central Indiana, and the highest yields of TP were from watersheds along the Mississippi River, northern Kentucky, and distributed through Missouri, Illinois, and Indiana (Robertson et al., 2009).

One of the primary factors contributing to the difficulty in mitigating the nutrient and contaminant loads entering stream systems lies in their variable methods of export and flow pathways. Nutrients and other contaminants may be deposited in streams via differing pathways including runoff, artificial drainage networks, shallow, lateral subsurface flow, groundwater, or atmospheric deposition. As a result, in order to successfully control the influx of harmful substances into surface water systems, it is essential to isolate which of these pathways are most commonly utilized by each contaminant. Nutrient and contaminant pathways are based on a number of factors and may be highly site-specific according to land use, topography, underlying geology, soil type and moisture conditions, or extent of drainage networks (Bachman et al., 1998; Brown et al., 1999; Kladivko et al., 2004; Craig et al., 2008). Runoff and shallow, lateral subsurface pathways are generally more direct and able to rapidly transport water to surrounding bodies (Craig et al., 2008). As a result, these pathways may act as significant contributors of both dissolved and particulate-bound nutrients and contaminants,

especially in wet conditions or if the pathway is not intersected by a riparian zone or areas of organic-rich soils (Lindsey et al., 1998; Brown et al., 1999; Craig et al., 2008). Riparian zones have been shown to slow runoff potential and sediment transport as well as support biotic uptake of many dissolved constituents due to elevated levels of organic matter (Osborne and Kovacic, 1993). Elevated runoff potential is associated with heavy rainfall, large areas of impervious surface, sparse vegetation, low permeability soils, and saturated hill slopes, while lateral flow is common in areas with steep slopes and thin soils overlying impermeable surfaces such as rock and clay (Craig et al., 2008). While groundwater flow pathways are generally more indirect and associated with longer residence times and the potential to interact with areas that promote remediation, removal of dissolved constituents may still be low depending on the hydrogeological setting (Craig et al., 2008).

Perhaps one of the largest, and least understood, pathways of nutrients and contaminants in the Midwest are the extensive drainage networks implemented in many of the agricultural areas. For example, 37% of the cropland in the Corn Belt and Great Lakes regions of the United States is artificially drained by surface channels, subterranean tiles, or a combination of both (Fausey et al., 1995; Kovacic et al., 2000). According to a study conducted by the U.S. Department of Agriculture, Indiana ranked second amongst U.S. states in total land area altered by the use of (sub)surface drainage systems with approximately 50% of all cropland in Indiana being affected, 70% of which is by tile drainage (U.S. Department of Agriculture, 1987; Baker et al., 2006). In the Eagle Creek Watershed, located within the Upper White River Watershed in central Indiana, research has shown that at least 75% of the cropland is artificially drained

(Babbar-Sebens et al., unpublished data). These networks act as a major conduit of nutrients and agricultural chemicals as they rapidly redirect nutrient loads to surface waters (Dinnes et al., 2002). Contaminated waters from preferential flow paths in the soil are collected by these extensive drainage networks which promote lateral transport and decrease the potential for sorption through contact with the subsurface matrix (Gächter et al., 1998; Stamm et al., 1998; Reinhardt et al., 2005). One study showed that in the Upper Embarras River Watershed of central Illinois, artificial drainage tiles drain between 70-85% of the cropland (David et al., 1997; Kovacic et al., 2000) and contributed 75-91% of the total nitrogen load in 1995 and 68-82% in 1996 (Kovacic et al., 2000). Additionally, from 1995 to 1996, an estimated 46-59% of the load of dissolved phosphorus was exported by tile drainage (Xue et al., 1998; Kovacic et al., 2000).

Another of the major issues affecting improved understanding of nutrient and contaminant export pathways lies in the infrequent sampling methodology used in many studies to characterize long-term periods rather than high-resolution sampling of large-scale hydrological events. A number of studies have shown that large majorities of annual nutrient and contaminant fluxes occur during periods of elevated discharge. A phosphorus mass balance of Eagle Creek Reservoir in the Upper White River Watershed in central Indiana between 2003 and 2005 showed that 60-77% of the total phosphorus load was delivered to the reservoir during event flows greater than or equal to the 80th percentile (Pascual et al., 2006). Another study conducted in a rural watershed in New York found that 75% of total phosphorus was transported during the highest 10% of flow (Johnson et al., 1976). It was found in another central Indiana watershed that 71-85% of annual DOC load was transported at high flows amounting to only 20% of the total time

(Dalzell et al., 2007). Finally, 82% of nitrate export and 95% of soluble reactive phosphorus export was found to occur at high flows ($\geq 75\%$ percentile) in agricultural Midwestern watersheds (Royer et al., 2006). Unfortunately, many studies that utilize infrequent, long-term sampling methods may characterize discharge events with only one or two points, if they are not missed completely, which affects the ability to accurately document nutrient loading and fluxes (Williams et al., 2004). A comparison of high-resolution storm sampling and fortnightly sampling during a two year period found that annual loads of suspended solids and particulate phosphorus were underestimated between -24% and -331% for suspended sediment and between -8.6% and -151% for particulate phosphorus (Kronvang et al., 1997). During storm events, loads were underestimated between -3% and -69% for suspended sediment and -2% to -51% for particulate phosphorus (Kronvang et al., 1997). As a result, while long-term sampling methods may be useful in other respects, obtaining a detailed understanding of the nutrient and contaminant signals associated with the most significant periods of export is not possible without the use of high-resolution storm sampling.

Finally, a third major issue affecting improved understanding of nutrient and contaminant export pathways can be attributed to the differences in concentration signals that occur as the drainage area of the watershed changes. As watershed scale increases, the number of contributing tributaries and other sources, as well as the complexity in the timing at which their contributions arrive at the stream, also increase. This increase in signal complexity increases the difficulty in developing models that are able to accurately predict the timing and contributions of nutrient and contaminant loads and fluxes during these significant storm events.

Nutrients and Contaminants

Nitrogen

In aquatic environments, nitrogen may occur in one of two forms; organic or inorganic. In streams, the majority of nitrogen export occurs as dissolved inorganic nitrogen including nitrate, nitrite, and ammonium which are generally the forms of primary concern as they are more easily utilized by algae and other organisms. Total Kjeldahl Nitrogen (TKN) is used to classify the remaining fraction of total nitrogen which is made up of all forms of organic nitrogen in addition to sediment-bound ammonia. It has been found that approximately one-third of terrestrial nitrogen inputs are subsequently exported (Howarth et al., 2002) and, as a result, increased export of nitrate has been found to correlate with the percentages of agricultural and urban land use in watersheds (Beaulac and Reckhow, 1982; Howarth et al., 2002; Poor and McDonnell, 2007).

The primary sources and pathways of nitrogen export have been found to be highly variable. Studies in forested watersheds of New York (Inamdar et al., 2004) and Spain (Butturini and Sabater, 2002) found that nitrate was primarily contributed by groundwater sources. Another study of two similar forested watersheds in the Adirondack Mountains of New York found that, despite their close proximity to one another, nitrate was contributed primarily from a groundwater source for one and a shallow surface source for the other (Christopher et al., 2008). In Indiana, high concentrations and loads of nitrate have been found to derive from subsurface tile drainage systems (Kladivko et al., 1991, 2004; Baker et al., 2006). A study conducted in Illinois found that tile drain systems served as the primary mode of export from the agricultural watersheds while

contributions from overland flow were not as significant (Royer et al., 2006). Another study of two first-order watersheds, located within the Upper White River Watershed in central Indiana, found that nitrate was likely transported with groundwater either as tile drain flow or direct subsurface flow (Wagner et al., 2008). While studies of TKN are less common, it too has been found to contribute heavily to annual nitrogen loads in some watersheds and has been associated with export by overland flow (Cooke and Cooper, 1988).

Other factors relating to climate, landscape, and geology may affect the impact of nitrogen on surface waters. For example, several studies have reported the majority of nitrate loss occurring during the winter and spring months (Snyder et al., 1998; Kladivko et al., 2004; Willet et al., 2004; Royer et al., 2006). Export of TKN was also found to be highest during the winter and spring months as saturated soils promoted overland flow and the export of sediment (Cooke and Cooper, 1988). A study in a small urban watershed found that the majority of total dissolved nitrogen was exported during baseflow (Hook and Yeakley, 2005). Another study of three agricultural watersheds found that, while a high proportion of nitrate was exported at baseflow (25-37%), the majority was exported during stormflow (Vanni et al., 2001). One study conducted in a bedrock-dominated, forested watershed in central Ontario illustrated the impact that topography may play on variation in nitrate concentrations among similar adjacent watersheds (Creed and Band, 1998).

The ability of an ecosystem to perform biogeochemical processes such as denitrification has also been found to affect the susceptibility of a surface water body to eutrophication. The reduction of nitrate (NO_3^-) to N_2 is known to occur in riparian areas

(Schipper et al., 1993; Devito et al., 2000; Dosskey et al., 2002) and stream sediments (Inwood et al., 2005) where favorable anaerobic conditions and sources of organic matter may periodically exist. However, if these environments are not present, preferential flow pathways bypass organic-rich deposits within them, or other variables such as temperature, steep slopes, or low residence times hinder the reactions, these processes may not be able to occur as efficiently.

Phosphorus

Forms of phosphorus in streams are generally grouped into two categories. Soluble reactive phosphorus (SRP) is composed primarily of orthophosphates and is the form most easily utilized by algae and other organisms. The remaining fraction of total phosphorus is made up of P bound to sediments including both organic P and insoluble inorganic P.

Like nitrogen, the sources and export pathways associated with phosphorus are complex and varied among different streams. Particulate-bound phosphorus (PP) has been found to be the primary contributor to phosphorus loads in a number of studies. One study of a rural watershed in New York found that PP accounted for 78% of total export and that less than 1% of all soluble P applied as fertilizer or manure left the watershed in a dissolved form (Johnson et al., 1976). In Finland, 73-94% of phosphorus in runoff was associated with particulate matter (Uusitalo et al., 2003). Studies of PP export patterns have yielded various results. PP loads are most commonly associated with transport by overland flow. Studies in agricultural watersheds of Illinois have shown that PP was exported almost exclusively by overland flow (Royer et al., 2006) and that a majority of

annual PP load was transported during events associated with large sediment loads carried by overland flow (Gentry et al., 2007). Other studies, however, have found stream bank erosion to act as the primary contributor of sediment and particulate phosphorus in watersheds. A number of European studies, including one study in Denmark, found that stream bank and bed erosion had attributed to 66-89% of suspended sediment and 75-89% of PP delivery to the stream (Kronvang et al., 1997). Tile drainage systems have also been found to be significant contributors of PP to streams, especially during elevated discharge (Gentry et al., 2007). Tile drainage systems have also been found to be significant, if not the primary source, of SRP in a number of studies though overland flow may also act as a significant contributor (Royer et al., 2006; Gentry et al., 2007).

Other factors may play a role in the export of phosphorus in watersheds. In one study conducted in Michigan, geology and proximity to wastewater treatment plants were found to potentially influence SRP concentrations (Castillo et al., 2000). Seasonal variations in export of phosphorus have been documented in a number of studies, especially as they relate to frequency of storm events, the presence of saturated soils, and overland flow (Johnson et al., 1976; Kronvang et al., 1997; Royer et al., 2006; Gentry et al., 2007). One study found streamflow P concentrations to correlate more closely with surface runoff and soil P content in near-stream (within 60 m) areas (Sharpley et al., 1999). A study of the effects of dredging on agricultural ditches found that, when dredged, the ability to remove introduced P from the water column was reduced and concentrations remained higher for a longer period of time compared to pre-dredging conditions (Smith et al., 2006). Another study found that the presence of cattle in a mixed agricultural watershed strongly influenced the levels of phosphorus in surface waters,

compared to a watershed associated with mostly row crop agriculture, due to the flushing of animal waste that had accumulated during the winter season (Cooke and Prepas, 1998).

Dissolved Organic Carbon

Organic carbon in streams refers to any decomposed plant matter, as well as fungal and microbial biomass and metabolites that may exist, whether dissolved or bound to sediments (Dalzell et al., 2005). Because the dissolved forms of organic carbon (DOC) are more readily available for biological uptake, it is this fraction that has been linked to biological processes in aquatic ecosystems. When introduced to surface waters, DOC has been shown to influence heterotrophic productivity and respiration in streams thereby influencing the rates of carbon cycling (Dalzell et al., 2005).

Elevated levels of DOC have been associated with the presence of riparian and wetland areas where organic matter accumulates in surficial soil layers (Inamdar et al., 2004, 2006). In one study, riparian areas were found to contribute 70-74% of the DOC to a small urban stream during stormflow and 90% during baseflow (Hook and Yeakley, 2005). As a result of bioaccumulation at or near the soil surface, near-surface soil runoff, macropore flow, and overland flow transport of DOC have been documented as primary pathways in a number of studies (Inamdar et al., 2004, 2006; Hood et al., 2006; Wagner et al., 2008). The activation of these pathways is often influenced by hydrological conditions and, as a result, periods of elevated discharge, precipitation, and antecedent moisture conditions have been documented as primary factors influencing DOC export (Inamdar et al., 2004, 2006; Hook and Yeakley, 2005; Royer and David, 2005; Dalzell et

al., 2005, 2007; Hood et al., 2006; Vidon et al., 2008). As soil moisture increases and the groundwater table rises, new pools of DOC are accessed and mobilized in a process known as flushing (Inamdar et al., 2006; Vidon et al., 2008). One study found that export of DOC was ninety times higher during floods compared to baseflow in an Indiana agricultural watershed (Dalzell et al., 2005). The influence of DOC in surface waters may also be exacerbated by near surface soils containing carbon associated with higher aromaticity and lignin contents than those transported to streams via mineral soil layers during baseflow (Vidon et al., 2008). Algal blooms located within the stream have also been documented as potential DOC sources, especially during the summer months (Royer and David, 2005).

Atrazine

Streams draining areas dominated by agricultural land use also transport a suite of synthetic organic compounds in the form of herbicides, fungicides, and insecticides. While some pesticides are naturally occurring, such as pyrethrins, most are laboratory-created to ensure that the targets have had no previous exposure and therefore no opportunity to evolve resistance (Ricklefs, 2001). While they are successful in their usage, they may be transported to and accumulate in other areas of the ecosystem and negatively affect native populations of flora and fauna.

One such pesticide of increasing concern is atrazine. Atrazine is an effective herbicide used primarily on corn crops for both pre- and post-emergent weed control and has become one of the most frequently applied herbicides in the United States. Currently banned in Europe, atrazine has been implicated as a carcinogen and has gathered recent

attention as a potential cause of a number of other human and environmental health impacts including low birth weights (Ochoa-Acuña et al., 2009), birth defects (Winchester et al., 2009), and endocrine disruption (U.S. Geological Survey, 1999). A number of studies have documented the mobility and persistence of atrazine in agricultural environments where it is heavily utilized (Hyer et al., 2001; Baker et al., 2006). A 1999 report summarizing the findings of a U.S. Geological Survey study conducted on the water quality of twenty large watersheds across the United States for the National Water Quality Assessment Program found that the White River Watershed in Indiana had the highest concentrations and number of EPA guideline exceedances for herbicides than any of the other watersheds (U.S. Geological Survey, 1999).

Atrazine has been found to follow a number of export pathways including atmospheric deposition, soil water, tile drainage networks, overland flow, and groundwater (Hyer et al., 2001; Kladivko et al., 2001; Baker et al., 2006; Hancock et al., 2008). A study conducted in an agricultural ditch in central Indiana found that atrazine was detected in 84.6% of rainfall samples and 100% of all soil water, tile drain, overland flow, and in-stream samples (Baker et al., 2006). In general, concentrations and export rates were found to be higher immediately following spring applications as the loads, located at or near the soils surface, are subject to flushing and transport by overland flow associated with periods of elevated precipitation and discharge (Hyer et al., 2001; Kladivko et al., 2001; Baker et al., 2006). Additionally, the application of pesticides has been found to correlate with their occurrence in humans, both of which peaked during the spring (Winchester et al., 2009). A review of thirty studies of pesticide transport in tile drains found that drain spacing also affected the transport of atrazine from agricultural

areas and, while intermittent periods of high concentration did occur in tile drains, mass losses were generally an order of magnitude lower than those recorded from surface runoff (Kladivko et al., 2001).

Taste and Odor Compounds

Geosmin and 2-Methylisoborneol (2-MIB) are two organic compounds that are commonly associated with the presence of strong tastes and odors in surface water bodies and drinking water that they produce. These compounds may drastically affect the quality of drinking water as humans are able to detect these compounds at extremely low concentrations (i.e. parts per trillion) and they are relatively resistant to both chemical and biological degradation thereby allowing them to persist in these environments (Westerhoff et al., 2006; Peter and von Gunten, 2007; Jüttner and Watson, 2007). Both compounds are primary influences on soil odor and are known to derive from a suite of aquatic microorganisms, as well as sources within terrestrial ecosystems, industrial waste treatment facilities, and drinking water treatment plants (Buttery and Garibaldi, 1976; Jüttner, 1990; Jüttner and Watson, 2007). Aerobic, filamentous, actinomycete bacteria, including a number of those belonging to the *Streptomyces* and *Nocardia* genera, have been documented as significant producers of both geosmin and 2-MIB (Jüttner and Watson, 2007). Studies have linked high runoff events with the export of actinomycete bacteria, geosmin, and 2-MIB into surface waters, especially those associated with large-scale livestock operations (Jüttner and Watson, 2007). One study conducted on a major Canadian river found that annual occurrence of odors in tap water were linked to actinomycetes exported to surface waters during snowmelt and runoff (Jensen et al.,

1994; Jüttner and Watson, 2007). Cyanobacteria, commonly referred to as blue-green algae, have also been linked to the production of geosmin and 2-MIB and are generally considered to be the most common source of the taste and odor compounds in photic, aquatic environments (Jüttner and Watson, 2007). Elevated levels are often associated with the presence of significant algal blooms and/or the subsequent deaths and decomposition of the organisms, but a number of cyanobacterial producers are nonplanktonic, benthic, epiphytic, or present in soil (Watson, 2004; Jüttner and Watson, 2007). Other organisms, including fungi, amoebas, and liverworts have been associated with the production of taste and odor compounds (Jüttner and Watson, 2007). Fungi present in biofilms lining activated filtration systems and distribution pipes in water treatment facilities have been linked to elevated levels of geosmin in a number of studies, especially when they are disturbed and subsequently exported (Jüttner and Watson, 2007).

Significance, Objectives, and Hypothesis

This study focuses on accomplishing three primary objectives to contribute to the understanding of nutrient and contaminant export in Midwestern watersheds including a) capturing nutrient and contaminant concentration patterns and loadings associated with two significant spring storm events in a large agricultural Midwestern watershed located in central Indiana, b) gaining an understanding of the primary sources and flow pathways through which these constituents travel throughout the duration of the storm events, and c) comparing the concentration patterns exhibited by the study basin with those observed in similar studies of smaller-order streams in the same watershed and determine what influence, if any, scale has on their export.

Through high-resolution sampling, it is possible to obtain a detailed illustration of the relationships that exist between discharge and the concentrations, fluxes, and loadings of a suite of ions, nutrients, suspended sediment, atrazine, and taste and odor compounds during storm events. This is crucial as a number of studies have shown that storm events contribute the largest percentages of annual nutrient and contaminant loads, especially during the spring (Johnson et al., 1976; Pascual et al., 2006; Royer et al., 2006; Dalzell et al., 2007). By capturing multiple storms, it may be possible to determine whether concentration patterns remain consistent from one event to another and, if they do not, attempt to determine what possible causes may explain the variances.

A number of techniques have been developed for understanding both the relative contributions of pre-event (old) and event (new) water as components of discharge (Burns et al., 2001; Worrall et al., 2003) and the mechanisms of runoff generation and response (Worrall et al., 2003). Most commonly, these techniques include the use of

isotope or chemical tracer data in conjunction with a multi-component mixing model (Burns et al., 2001; Worrall et al., 2003). These models are used under the assumptions that the precipitation (i.e. new event water component) will be characterized by a different signature than that of the old pre-event groundwater, that these differences are consistent throughout the watershed, and that the tracers mix conservatively in the catchment during the event thereby providing an accurate representation of stream runoff (Burns et al., 2001). While these methods have been successfully utilized in a number of smaller watersheds, as catchment scale increases so too does the variability in underlying soils and geology thereby reducing the likelihood that each of the model prerequisites will be fulfilled.

While hydrograph separations may be unable to be successfully utilized in larger watersheds, a number of studies have documented the value of cations and anions for use as qualitative tracers. Soil-water chemistry is controlled by residence time and cation exchange and, in turn, controls the composition of the stream water (Bonnell et al., 1993; Brown et al., 1999; Worrall et al., 2003). As the mean length of the subsurface pathway of water increases, concentrations of cations and anions increase until a point of steady state equilibrium is achieved (Burns et al., 1998). Magnesium (Mg^{2+}) and calcium (Ca^{2+}) concentrations have been shown to increase with soil depth thereby linking them to deeper, groundwater pathways (Inamdar et al., 2004). During storm events, Mg^{2+} and Ca^{2+} are generally diluted with increased discharge as more new event water mixes with the displaced groundwater (Hill, 1993; Inamdar et al., 2004). Other studies have documented similar patterns with sodium (Na^+) (Hill, 1993), sulfate (SO_4^{2-}) (Brown et al., 1999), and chloride (Cl^-) (Brown et al., 1999; Sidle et al., 1999; Devito et al., 2000).

Potassium (K^+), on the other hand, has been associated with stable or elevated concentrations during elevated discharge attributed to mixing of throughfall and groundwater in saturated overland flow (Hill, 1993; Hood et al., 2006). By comparing the concentration patterns of cations and anions during storm events to those of nutrients and contaminants of concern, it is possible to identify their contributing sources as well as the primary flow pathways through which they travel during these events.

At a series of sites in Indiana's Upper White River Basin, research has documented the transport pathways of nutrients and contaminants to streams and has shown differences in the concentration patterns and response time of streams based on drainage area and network complexity. One of these study sites is located on Eagle Creek, near Zionsville, IN, and is associated with a drainage area of 267 km^2 (103 mi^2). Another study examines two subwatersheds of Eagle Creek, both with drainage areas of less than 13 km^2 (5 mi^2). A comparison of these two previous studies has shown that with increased scale and network complexity, concentration patterns relative to discharge are generally smoother and occur more regularly while exhibiting decreases in the abruptness and uniqueness of their timing. This shift is indicative of a decrease in the influence of smaller contributing watersheds on concentration patterns, due to an averaging effect, and a general increase in ecosystem stability as defined by variability in concentration over time. In turn, the results of this study, from a site located on the trunk of the Upper White River near Fishers, IN and associated with a drainage area of approximately $2,945 \text{ km}^2$ ($1,137 \text{ mi}^2$), will be compared to those of the previous studies. Concentration patterns are expected to follow similar trends characterized by increased smoothness and pattern regularity and decreases in the abruptness and uniqueness of their timing.

This in-depth collection of scaled studies focused on the Upper White River Watershed holds particular significance due to its role as a major contributor of total nitrogen and total phosphorus to the Gulf of Mexico. According to a 2009 report, the Upper White River watershed was ranked as 91st of 818 HUC8 watersheds located in the Mississippi River Basin for total phosphorus delivered incremental yield and 30th for total nitrogen delivered incremental yield (Robertson et al., 2009).

This study will illustrate the importance of high-frequency sampling during storm events in accurately characterizing nutrient and contaminant concentration patterns and loads as a majority of annual fluxes occur during these periods of elevated flow. Additionally, this study will act as a reference point for the differences in nutrient and contaminant export behavior observed across scale in a single Midwestern river basin thereby drawing attention to the challenges associated with modeling increasingly larger-scale watersheds. While studies of nutrient export dynamics are increasingly common, they often focus on smaller watersheds in forested catchments rather than those watersheds that are either larger or in urban/agricultural settings. As a result, studies aimed towards the understanding of the nutrient and contaminant export pathways and changes in concentration signal across scale, in watersheds from a variety of landscape settings, contribute to a much needed collection of knowledge that may aid in the development of BMP's, aid in the understanding, anticipation, and management of peak concentration events, and shed light on the difficulty in modeling systems of increased complexity and scale.

Study Area

Basin Characteristics

The Upper White River Watershed is a HUC 8 watershed located in central Indiana and consists of 17 smaller HUC 10 watersheds. The hydrologic unit code (HUC) system utilized by the USGS subdivides the United States into successively smaller hydrologic units which are classified into four levels: regions, sub-regions, accounting units, and cataloging units (Seaber et al., 1987). The hydrologic units are arranged within each other, from the smallest to the largest, and each is identified by a unique hydrologic unit code consisting of two to eight digits based on the four levels of classification (Seaber et al., 1987). The area associated with the 146th Street study site drains approximately 40%, or 2945 km² (1,137 mi²), of the north-easternmost portion of the Upper White River Basin, including its headwaters (Figure 1).

Climate

Central Indiana is located in a humid-continental climate characterized by well-defined summer and winter seasons, large annual temperature changes, and highly variable weather patterns. Mean annual temperatures range from approximately 10.6-12.8° C (51-55° F) with mean monthly temperatures of approximately -2.8° C (27° F) in January and 23.9° C (75° F) in July according to 1961-1990 data (Shampine, 1977; Schnoebelen et al., 1999). Mean annual precipitation for the state of Indiana ranges from approximately 96.5 cm (38 in) in the northernmost part of the state to 111.8 cm (44 in) in the southernmost part of the state with the majority of the study basin associated with 101.6 cm (40 in) of annual precipitation. In Indiana, cooler months are generally

associated with precipitation events with lower intensities and longer durations while, in the warmer months, precipitation events with higher intensities and shorter durations are more common (Schnoebelen et al., 1999). Due to the direct influence of precipitation levels on mean annual runoff trends in central Indiana, a similar pattern of increased runoff from north to south exists (Schnoebelen et al., 1999). In the northernmost portion of the White River Basin, mean annual runoff totaled approximately 30.5 cm (12 in) while the southernmost portion of the basin saw approximately 43.2 cm (17 in) (Schnoebelen et al., 1999). Within the study basin itself, mean annual runoff only ranges from 30.5 cm (12 in) in the north and 35.6 cm (14 in) in the south (Schnoebelen et al., 1999). Expressed as a percentage of mean annual precipitation, mean annual runoff ranges from 30% in the northernmost portion of the White River Basin and 40% in the south (Schnoebelen et al., 1999). Evapotranspiration is estimated to total 66 cm (26 in) (Clark, 1980; Schnoebelen et al., 1999).

Geology

The study basin lies entirely in the Tipton Till Plain of central Indiana. The bedrock underlying this area consists almost entirely of Silurian limestone and dolomite with small areas of Ordovician Maquoketa Group shale and limestone and Devonian Muscatatuck Group limestone and dolomite also included. The underlying bedrock of this area is overlain completely by varying thicknesses of loam to sandy loam, Wisconsinan-age till glacial deposits with small patches of clay, silt, and sand, Wisconsinan-age lake deposits and fingers of sand, silt, and some gravel from Holocene alluvium and Pleistocene glacial outwash (Schneider, 1966; Shaver et al., 1986; Gray et al., 1987;

Gray, 1989; Soller, 1993; Schnoebelen et al., 1999). The soils of the Upper White River Basin are divided into thirteen regions based on parent material, vegetation, and topography (Franzmeier et al, 1989; Schnoebelen et al., 1999), but can be clustered to form four primary groups. These four groups are comprised of those soils that were developed from loess or glacial till, those developed along floodplains, those developed from bedrock, and those developed from lake deposits (Schnoebelen et al., 1999). The majority of the study basin is covered by soils developed from loess and glacial tills with some smaller areas of those associated with floodplains occurring along stream channels. The glacial soils originate from a calcareous parent material and are often associated with poor natural drainage, high base content, and high fertility (Ulrich, 1966; Schnoebelen et al., 1999). It is these soils that have attracted the widespread agricultural land use in this area and, as a result of the poor drainage, most estimates of tile-drainage percentage come from these classes. Soils associated with floodplains are also fertile and associated with a high base content but have much better drainage than the clay-rich glacial soils due to their larger percentages of silts and sands (Ulrich, 1966; Schnoebelen et al., 1999).

Streamflow

Under natural conditions, streamflow in the northernmost small to moderate drainage basins of the White River, including all of those included in the 146th Street study basin, generally exhibit well-sustained baseflow and moderate peak flows relative to those watersheds lying farther to the south which may be dry at baseflow and associated with higher peak flows (Schnoebelen et al., 1999). These differences between north and south are the result of the types of materials exposed at the surface. In the

north, flat, thick glacial deposits allow rainfall to pond and infiltrate thereby moderating runoff and peak flows. Additionally, these thick glacial deposits are able to support aquifers that regulate sustained baseflows to surrounding streams. In the south, however, steeper slopes, thin glacial deposits, older, more compact tills, and bedrock all contribute to increased runoff, flashier flow events, and an inability to maintain flow during drier periods (Schnoebelen et al., 1999). While this may accurately describe the general behaviors of the different landscapes of the White River Watershed under natural conditions, anthropogenic influences (i.e. artificial drainage systems, urbanization) have altered natural drainage patterns in many areas thereby complicating this simplistic conceptualization.

Land Use

Land use percentages were derived from a 2007 land cover/crop data provided by U.S. Department of Agriculture's National Cartography and Geospatial Center. The study basin was determined to be predominantly corn/soybean rotation row-crop agriculture (66%) and 21% herbaceous which includes pasture, lawns, and golf courses (Table 1). A majority of this area, especially in the case of the agricultural portion, is artificially drained by subsurface tiles. The remaining portion of the study basin is covered primarily by mid-high density urban areas (5%), which drain cities including Muncie, Anderson, and Noblesville, IN, and forested areas (4%).

Research Approach

30-year Streamflow Summary

While the USGS stream gaging station at 146th Street (03350800) was only more recently implemented and, as a result, does not have thirty years of collected data, other nearby sites in the White River such as Noblesville, IN (03349000) and Nora, IN (03351000) were examined for their utility in providing streamflow records for the study site. Ratios of average daily discharge values between October 28, 2007 and October 27, 2008 and contributing watershed areas were determined for the USGS sites at Noblesville, IN and Nora, IN. Linear regression analyses were performed on these ratios and those calculated for the 146th Street site in order to determine if a significant relationship existed and if equivalent average daily discharge values could be extrapolated for the study site. Results of plotting the Nora, IN site against the study site were the most significant and provided an R^2 value of 0.99 (Figure 2). As a result, the best-fit line equation provided by this analysis was determined to be suitable for extrapolating 30-year streamflow records for the 146th Street study site.

Instrumentation and Sample Collection

In order to collect high temporal resolution storm samples, Teledyne ISCO portable auto-samplers (Model 6712) were deployed in the Upper White River near the intersection of 146th Street and Allisonville Road in Fishers, IN (Figure 1). The auto-samplers were housed in an elevated, locked, protective wooden case built specifically for the purpose of this project. This site was chosen in part based on the fact that it is also a USGS water monitoring site which provided both discharge and gage height readings at

15-minute intervals throughout the sampling process. Additionally, at the end of the auto-sampler's water intake hose, a YSI Multi-Parameter Water Quality Probe (Model 600XLM) was deployed to provide temperature, specific conductance, dissolved oxygen, pH, and depth readings throughout the sampling process.

Two storms were sampled in May and June of 2008. Storms were chosen based on their exceedance of the 80th percentile for discharge at the study site, based on thirty years of USGS historical daily streamflow records for the individual days of the year, as well as their close temporal proximity following the spring applications of fertilizers and pesticides to cropland in the Upper White River Watershed. The streamflow site at Nora, IN was used to determine the streamflow percentile of the study site.

Sampling of each storm began after the first exceedance of baseflow in the channel and continued until a typical baseflow had again been achieved. In a basin of this size, significant storms may last several weeks and include multiple events. In the case of this study, the first sampled storm lasted from May 7th to May 26th, 2008 and the second from June 3rd to June 19th, 2008. Both storms included three well-defined events each characterized by their own distinct peaks in discharge.

The first storm was sampled at four to five hour intervals from May 7th through the crest of the third event on May 15th when sampling frequency was decreased to ten hour intervals until the channel had nearly returned to baseflow on May 23rd. After this point in time, daily grab samples were collected for an additional three days to document fluxes during post-event return to baseflow. Duplicate grab samples were collected and analyzed once for approximately every ten samples collected. In total, sixty-two samples

were collected for the first storm with an additional six acting as duplicates for a total of sixty-eight sample analyses (Table 2; Figure 3).

The second storm was sampled at five hour intervals from June 3rd through June 15th at which point single daily grab samples were collected through June 19th. Sampling ceased slightly before the river returned completely to baseflow. In total, fifty-three samples were collected for the second storm with an additional five acting as duplicates for a total of fifty-eight sample analyses (Table 2; Figure 3). Due to the fact that both of the captured storms were characterized by three distinct peaks in discharge before returning to baseflow conditions, data analysis was completed for each individual event, in addition to analyzing each storm in its entirety in order to more fully understand the nature of nutrient and contaminant export patterns. Storms were divided into individual events for analysis by separating the hydrograph at the points of lowest discharge between each peak (Table 2).

Sample Processing and Analytical Methods

Each of the collected water samples consisted of five 0.5 L aliquots which were collected in either a) acid-washed bottles or b) sterile disposable sample bags. For each sample, two of the five aliquots were collected in containers with 2.0 mL of 11N H₂SO₄ in order to lower the pH to ≤ 2.0 and preserve the DOC, Total P, and TKN fractions. The remaining three aliquots were not acidified and were used for analyzing NO₃⁻, TSS, atrazine, 2-MIB, geosmin, and major cations and anions including Mg²⁺, Na⁺, SO₄⁻, Cl⁻, and K⁺.

Once collected, samples were immediately refrigerated, processed, and transferred to the Veolia Water Indianapolis laboratory for analysis within twenty-four hours. For processing, a portion of the acidified sample was filtered with Whatman 0.7 μm glass filters for the DOC analysis and placed in a 40 mL acidified, dark-brown glass vial. The remaining portion of the acidified sample was left unfiltered and transferred to a 250 mL acidified, HDPE plastic container for Total P and TKN analysis. An unfiltered, non-acidified portion of each sample was transferred to a 40 mL, dark-brown glass vials containing sodium sulfite for atrazine, 2-MIB, and geosmin analysis. The remaining portion of the unfiltered, non-acidified sample was transferred to two acid-washed, HDPE plastic bottles including a 250 mL volume for the cation and anion analyses and at least a 500 mL volume for TSS analysis. Analytical methods and analyses are presented in Table 3.

Due to instrument failure, initial analysis of DOC failed to meet QA/QC standards. As a result, frozen aliquots of the original filtered/acidified storm samples were thawed in November 2008, transferred to 40 mL acidified, dark-brown glass vials, and delivered to the Veolia Water Indianapolis laboratory for reanalysis. Due to budget constraints, only approximately 50% of the original storm samples were submitted for reanalysis of DOC. For Events 1-1, 1-2, and 1-3, there were nine, eight, and seventeen samples, respectively. A single duplicate analysis was run for each event totaling thirty-seven sample analyses for Storm 1. For Events 2-1, 2-2, and 2-3, there were eleven, six, and twelve samples, respectively. A single duplicate analysis was run for each event totaling thirty-two sample analyses for Storm 2. While the freezing of DOC samples may

affect the accuracy of the analyses at high concentrations (> 15 mg/L), this is generally not the case at concentrations below 15 mg/L (Vidon et al., 2008).

Data Analysis

Hydrology and Precipitation

Discharge data collected at 15-minute intervals by the USGS monitoring station located at the study site was used to plot hydrographs (discharge vs. time) of the two sampled events in addition to determining basic hydrological statistics including mean stormflow, peak discharge, and baseflow discharge during each of the events. The time to peak of each event was determined by calculating the length of time between the noticeable increase in discharge at the beginning of the events and the subsequent peaks in discharge. Antecedent discharge was calculated for the watershed by determining the ratio of the total volumes of water discharged by the watershed during the 7, 30, and 90-day periods of time preceding each event and the area of the watershed. The runoff ratio of each event was calculated by determining the ratio of the volume of water discharged by the watershed over the duration of the event and the volume of water delivered by precipitation to the watershed during the same period of time. Finally, the storm recurrence interval and probability of exceedance were calculated for each event. This was accomplished by comparing the average daily discharge values associated with each event peak to all USGS average daily discharge values recorded during 1971-2000 for the 146th Street study site as extrapolated from the Nora, IN station.

Hourly precipitation data was also necessary for fully characterizing the two storms and their events. In smaller study basins, a few precipitation gages located near the study site may be able to collect sufficient data to characterize rainfall patterns, but a study conducted on a basin of this size required multiple gages dispersed throughout the study area. Six weather stations from the NOAA network were chosen based on their

distribution throughout the watershed and the completeness of the data from the period of October 28, 2007 - October 27, 2008 (Table 4; Figure 1). Unfortunately, the regularity of data collection between the six stations was highly variable. Each station was characterized by a collection of rainfall rate (in/hr) readings collected sporadically over the duration of the study period. Data collection ranged between one to thirty minutes between readings and, therefore, a total number of hourly readings ranging from two to forty between stations.

For each of the six stations, the arithmetic means of all rainfall rates contained within each hour were calculated to determine hourly rainfall totals for the months of May and June, 2008. These values were then averaged amongst the six sites in order to obtain overall hourly precipitation totals for the entire Upper White River Watershed. Through totaling these values, daily precipitation values were also able to be calculated. In order to obtain a sense of validity of this method, total daily rainfall values for the Upper White River Watershed, as calculated from the rainfall rate values, were compared to the daily precipitation totals reported directly by NOAA and averaged across each of the six stations (Table 5). The daily precipitation totals both calculated from hourly rainfall rates and reported directly by NOAA were averaged and the error percentages calculated for each day in the months of May and June. Error ranged from 1.72% to 100% for May and 0.72% to 77.78% for June. Median values of error for May and June were 9.97% and 9.43%, respectively. For the combined months of May and June, the median value of error for was 9.62%.

The calculated arithmetic mean of all available data from the six weather stations was used to produce a precipitation graph for the basin between October 28, 2007 and

October 27, 2008 and was plotted along the hydrograph of USGS daily mean discharge values for the same time period (Figure 4). Data for four significant points on the daily mean discharge hydrograph were missing from the 146th Street data set, but values were able to be extrapolated from the complete Nora, IN data set. A double-mass curve was formulated for the Upper White River basin at 146th Street during October 28, 2007 - October 27, 2008 by plotting cumulative daily precipitation against cumulative average daily discharge (Figure 5).

Precipitation data was used to calculate antecedent precipitation by determining the total amount of precipitation that fell during the 7, 30, and 90-day periods preceding the storm events. Precipitation intensity and bulk precipitation were also calculated by determining the amount of precipitation falling hourly for the duration of each storm event and the total amount of precipitation that fell during the storm event, respectively. Due to the extended periods of time during which these storms took place, a number of precipitation events occurred in the Upper White River Watershed during the length of each of the two sampling periods. However, for each of the six storm peaks, a single, more significant rainfall event was the primary contributor for each of the significant increases in discharge and, for the purposes of this study, these will be the only events that are described and discussed.

Concentrations, Loads, Timing Relationships, and Export Patterns

Storm sample ion, nutrient, and contaminant concentration data was utilized in several ways. The statistical analysis software SigmaPlot was used to run a suite of univariate statistical analyses on concentration data from each storm event in addition to

creating box plot graphs as visual interpretations of their results. Statistical analyses included determination of mean, geometric mean, median, 25th/75th percentile values, min/maximum values, and the presence of suspected outliers.

In addition to statistical analyses, loading measurements were calculated for all ions, nutrients, and contaminants using the simple load estimation technique. This involves associating each complete 4-, 5-, 10-, etc. hour period with the preceding measured concentration and combining the totals for the entire duration of the event in order to determine kg/event. From loading calculations, yields (i.e. the mass of the substances entering the stream per unit area of drainage basin) were able to be calculated and reported as kg/ha. Finally, by dividing yield values by the number of hours for each event, rates of export to the river were able to be determined and reported as kg/ha/hr.

Concentration curves (i.e. concentration vs. time) for each ion, nutrient, and contaminant were plotted against the appropriate hydrograph for visual interpretation of concentrations as they relate to discharge and time throughout the duration of the storms. Sample analyses that were returned as being below the detectable limit were plotted as half of the difference between the detection limit and zero (Table 3). Error percentages were calculated for all ions, nutrients, and contaminants from the results of the duplicate samples by dividing the difference between the two sample values and their averaged value. Univariate statistics were then performed on these values to provide the range (minimum and maximum), mean and median error percentages associated with each storm and the entire study period as a whole.

Results

Hydrologic Response

A summary of the 30-year streamflow records for the 146th Street Upper White River study site is presented in Table 6. Monthly streamflow averages tended to be higher during the winter and spring months (December - May) than the summer and autumn months (June - November). Between 1971 and 2000, monthly streamflow averages ranged between 8.18 m³/s in October and 58.24 m³/s in March. Streamflow records for 2007 and 2008 prior to the study period (May - June, 2008) are characterized by two drastically different periods in regards to discharge. The period of May - November, 2007 was characterized by a period of low average monthly discharges ranging from 20.2% to 52.3% of the 30-year normal values. This period was followed by a dramatic increase in average monthly discharges between December 2007 and the beginning of the sampling period. Average monthly streamflow values between December 2007 and April 2008 ranged from 228.3% to 107.8% of the 30-year normal values with three of the months having values over 200.0% (i.e. December, February, and March). The study period between May and June, 2008 was characterized by average monthly discharge values of 51.8 m³/s and 81.3 m³/s, or 144.3% and 231.7% of the 30-year normal values, respectively (Table 6).

While both storms exceeded the 80th percentile flow at the study site, the event recurrence curve (Figure 6) determined that events characterized by equivalent maximum average daily discharge values on days of peak discharge were repeated on intervals ranging from 11.3 days for Event 1-1 to 73.1 days for Event 2-3 (Table 7). This result demonstrates that flows of this magnitude, often associated with increased concentrations

and loadings of nutrients and contaminants in surface waters, are occurring in the Upper White River Watershed on an annual, and even monthly, basis.

Rainfall intensities were calculated from the average hourly precipitation values for the Upper White River Watershed for the events of primary contribution. The three events of primary contribution for Storm 1 spanned from May 7, 20:00 pm - May 9, 2:00 am, May 11, 2:00 am - 22:00 pm, and May 14, 1:00 am - 9:00 am for Events 1-1, 1-2, and 1-3, respectively. The three events of primary contribution for Storm 2 spanned from June 3, 5:00 am - June 4, 11:00 am, June 6, 19:00 pm - June 7, 17:00 pm, and June 9, 13:00 pm - June 10, 11:00 am for Events 2-1, 2-2, and 2-3, respectively. Results of this analysis are summarized in Table 7. Average rainfall intensities for each of the six events ranged from 1.10 mm/hr for Event 1-1 to 2.63 mm/hr for Event 1-3, with maximum hourly intensity for each peak ranging from 4.09 mm/hr for Event 1-3 to 9.18 mm/hr for Event 2-3. Bulk precipitation values for each of the events of primary contribution were also calculated from the hourly precipitation values for the Upper White River Watershed by totaling the precipitation contributing to each discharge peak (Table 7). Bulk precipitation values ranged from 21.04 mm for Event 1-3 to 57.95 mm for Event 2-1. Due to a lack of hourly data, antecedent precipitation totals for the 7, 30, and 90-day periods prior to each event were calculated by rounding the beginning of each of the six increases in discharge to midnight of the nearest day and totaling the calculated total daily precipitation values that had been averaged across each of the six NOAA weather stations (Table 7). The 7-day antecedent precipitation values ranged from 9.8 mm for Event 2-1 and 104.9 mm for Event 2-3. The 30-day values ranged from 68.9 mm for Event 1-1 and 174.3 mm for Event 2-3. Finally, the 90-day values ranged from 346.4 mm for Event 1-1

to 401.9 for Event 1-3. The 30-year (1971-2000) monthly precipitation normal values for the central and east-central regions of Indiana, as reported by the Indiana State Climate Office through Purdue University's Department of Agronomy (Indiana State Climate Office, 2003), were averaged and compared to the results obtained from the six NOAA stations. The 30-year precipitation normal values for May and June were reported as 111.9 and 106.7 mm, respectively. When taken from the total daily precipitation values calculated from the hourly readings averaged for each of the stations, monthly precipitation values for May and June, 2008 in the Upper White River Watershed were 115.1 mm and 176.0 mm, or 102.9% and 165.0% of the 30-year normal values, respectively. When taken from the total daily precipitation values reported directly by NOAA and averaged across the each of the six stations, monthly precipitation values for May and June, 2008 were 132.1 mm and 198.0 mm, or 118.0% and 185.6% of the 30-year normal values, respectively.

Again, due to a lack of 15-minute USGS discharge data, antecedent discharge totals for the 7, 30, and 90-day periods prior to each event were calculated by rounding the beginning of each of the six increases in discharge to midnight of the nearest day and totaling the average daily discharge values for the study site as reported by the USGS (Table 7). For those antecedent discharge calculations for which 15-minute data was available, values were calculated and compared to those obtained through the method of rounding to midnight of the nearest day (Table 8). Percent differences between the calculated values only ranged from 0.001% to 0.01% thereby validating the method of rounding to midnight. The 7-day antecedent discharge values ranged from 0.025 mm/hr, for Events 1-1 and 2-1, to 0.162 mm/hr for Event 2-3. The 30-day values ranged from

0.042 mm/hr for Event 1-1 to 0.092 mm/hr for Event 2-3. Finally, the 90-day values ranged from 0.088 mm/hr for Event 2-2 to 0.107 mm/hr for Event 1-1.

Pre-event flow values were determined just prior to the significant increase in discharge that defined the beginning of the storm and were 0.021 and 0.022 mm/hr for Storm 1 and Storm 2, respectively. For each of the six events, the amount of time between each trough and the subsequent peak in discharge (i.e. time to peak), mean stormflow, and peak discharge are each summarized in Table 7. Time to peak ranged from 23.5 hours for Event 1-3 to 86.25 hours for Event 2-1. Mean stormflow ranged from 0.074 mm/hr for Event 1-3 to 0.175 mm/hr for Event 2-2. Peak discharges ranged from 0.116 mm/hr for Event 1-1 to 0.304 mm/hr for Event 2-3. Finally, runoff ratios for each event of primary contribution were calculated and are summarized in Table 7. Values for this analysis ranged from 0.145 for Event 1-1 to 0.746 for Event 1-3.

Univariate Concentration Statistics and Error Analysis

Univariate statistical analyses and box plot graphs of the ion concentrations for magnesium (Mg^{2+}), sodium (Na^+), sulfate (SO_4^-), and chloride (Cl^-) showed little difference in maximum concentrations between Storms 1 and 2, except in the case of SO_4^- (Table 9; Figure 7). This discrepancy can be attributed to a single, outlying point recorded for Storm 2 (Figure 7). Maximum concentrations for Mg^{2+} , Na^+ , SO_4^- , and Cl^- were 29.44 mg/L, 32.76 mg/L, 58.60 mg/L, and 45.48 mg/L, for Storm 1 and 29.7 mg/L, 34.10 mg/L, 79.8 mg/L, and 42.35 mg/L for Storm 2, respectively (Table 9; Figure 7). Median concentrations of Mg^{2+} , Na^+ , SO_4^- , and Cl^- were greater for Storm 1 than Storm 2 with values of 21.43 mg/L, 17.07 mg/L, 34.65 mg/L, and 30.26 mg/L for Storm 1 and

17.23 mg/L, 11.45 mg/L, 23.40 mg/L, and 21.05 mg/L for Storm 2, respectively (Table 9; Figure 7). The results of K^+ concentration analysis varied from those obtained from the other ions. Maximum K^+ concentrations were higher for Storm 2 (4.74 mg/L) than Storm 1 (3.10 mg/L) (Table 9; Figure 7). Additionally, median concentrations were higher for Storm 2 with values of 2.64 mg/L and 3.29 mg/L for Storms 1 and 2, respectively (Table 9; Figure 7).

Univariate statistical analyses and box plot graphs of the nutrient concentrations for nitrate (NO_3^-), dissolved organic carbon (DOC), total phosphorus (TP), and total Kjeldahl nitrogen (TKN) showed much more variation between storms than what was observed in the ions with NO_3^- being the only nutrient with maximum and median concentrations similar between Storms 1 and 2. Storm 1 had a median NO_3^- concentration of 4.84 mg/L and a maximum concentration of 6.17 mg/L while Storm 2 had a median NO_3^- concentration of 4.60 mg/L and a maximum concentration of 6.24 mg/L (Table 9; Figure 8).

DOC, TP, and TKN concentrations were found to be elevated during Storm 2 relative to Storm 1, especially in the case of TP. Storm 1 had median and maximum DOC concentrations of 4.19 mg/L and 5.85 mg/L, respectively, while Storm 2 had median and maximum concentration of 5.24 mg/L and 7.30 mg/L (Table 9; Figure 8). Storm 1 had median and maximum TP concentration of 0.23 mg/L and 0.39 mg/L, respectively, while Storm 2 had a median concentration of TP of 0.35 mg/L, or nearly equivalent to the maximum concentration achieved during Storm 1 (Table 9; Figure 8). Storm 2 had a maximum TP concentration of 0.81 mg/L, or approximately double the maximum concentration achieved during Storm 1 (Table 9; Figure 8). Finally, Storm 1 had median

and maximum TKN concentrations of 1.37 mg/L and 2.21 mg/L, respectively, while Storm 2 had a slightly higher median TKN concentration of 1.56 mg/L and a higher maximum concentration of 3.23 mg/L (Table 9; Figure 8).

Like the nutrients, the contaminant concentrations for total suspended solids (TSS), the herbicide atrazine, and the taste and odor compounds 2-MIB and geosmin were varied between Storms 1 and 2. Storm 2 had highly elevated concentrations of TSS relative to Storm 1. Storm 1 had median and maximum TSS concentrations of 31.0 mg/L and 77.6 mg/L, respectively, while Storm 2 had a median concentration of 71.1 mg/L or nearly equivalent to the maximum concentration achieved during Storm 1 (Table 9; Figure 9). Storm 2 had a maximum TSS concentration of 218.7 mg/L, or approximately triple the maximum concentration achieved during Storm 1 (Table 9; Figure 9). Atrazine concentrations were also elevated for Storm 2 relative to Storm 1. Median and maximum atrazine concentrations were 4.5 µg/L and 14.7 µg/L for Storm 1 and 5.7 µg/L and 23.5 µg/L for Storm 2, respectively (Table 9; Figure 9).

2-MIB concentrations between storms were unique in that, while Storm 1's median concentration of 4.58 ng/L was greater than Storm 2's median concentration of 4.03 ng/L, Storm 2 had much higher maximum concentration levels than those achieved in Storm 1 (Table 9; Figure 9). This can be attributed to a small number of outlying points occurring during Storm 2 (Figure 9). Storm 2 had a maximum concentration of 57.18 ng/L nearly tripling the maximum concentration of 19.6 ng/L achieved during Storm 1 (Table 9; Figure 9). Geosmin concentrations were also unique between storms in that they were greatly reduced during Storm 2 relative to Storm 1. The median and maximum geosmin concentrations for Storm 1 were 8.13 ng/L and 24.91 ng/L,

respectively, or approximately double the median and maximum concentrations of 4.56 ng/L and 10.56 ng/L calculated for Storm 2 (Table 9; Figure 9). Additionally, only one sampled point from Storm 2 exceeds the median concentration of 8.13 ng/L calculated for Storm 1 (Figure 9).

The majority of both mean and median error values associated with each of the five cations/anions were below 1% (Table 10). Exclusions included mean SO_4^- error values calculated at 1.14%, 4.80%, and 3.17% for Storms 1, 2, and the collective study period, respectively, and a mean Cl error value of 1.35% calculated for Storm 1 (Table 10). In all cases, these elevated values can be attributed to elevated values calculated from a single duplicate pair that skewed the mean value. This is supported by the low median percent error values (< 1%) associated with each of these cases (Table 10).

The majority of both mean and median nutrient and contaminant error values were also low (< 5%) including all NO_3^- , DOC, TKN, and geosmin values for Storms 1, 2, and the collective study period (Table 10). The three TP mean error values ranged from 5.35% to 7.67% for Storms 1 and 2, respectively (Table 10). TSS mean and median error values were all below 5%, both for Storm 2 and with the storms combined, excluding the highest value of 7.07% as the mean value for the collective study period (Table 10). However, the three duplicate TSS calculations for Storm 1 produced mean and median error values of 17.33% and 22.22%, respectively (Table 10). Mean atrazine error values ranged from 7.65% to 9.21% and median values from 6.25% to 7.33% for Storms 2 and 1, respectively (Table 10). 2-MIB mean and median error values were all below 5%, both for Storm 2 and with the storms combined, excluding the highest value of 13.31% as the mean value for the collective study period (Table 10). However, the

three duplicate 2-MIB calculations for Storm 1 produced mean and median error values of 28.45% and 35.73%, respectively (Table 10).

Concentration Patterns

Concentration-discharge curves found that, for both storms, Mg^{2+} , Na^+ , SO_4^- , and Cl^- concentrations were all diluted (i.e. decreased) as discharge increased (Figure 10). For Storm 1, these concentration patterns were characterized by single curves and concentrations reaching their lowest values at, or just after, the highest rate of discharge for the storm during Event 1-2 (Figure 10). Concentrations gradually increased after this point and through the receding limb until ultimately reaching near pre-event levels toward the end of the sampling period (Figure 10). The concentration patterns for Storm 2 were slightly different for these ions in that the curves were characterized by a minimum concentration occurring just before the peak in discharge of Event 1-1, an increase in concentration coinciding with the peaks in discharge for Event 1-2 in the cases of Na^+ and SO_4^- , or with the troughs separating Events 2-2 and 2-3 in the cases of Mg^{2+} and Cl^- , and another decrease in concentration, for all parameters, reaching their lowest levels just after the peak in discharge for Event 2-3 (Figure 10). After this point, each of these four parameters began increasing in concentration through the receding limb of Event 2-3 and the end of the sampling period, but did not return to pre-event levels (Figure 10). For each of the four parameters, highest concentrations generally occurred during pre-event flows, though peaks in SO_4^- and Cl^- occurred during the rising limb of Event 1-1 (Figure 10).

Concentration curves for K^+ generally exhibited increases in concentration with increases in discharge, though the patterns were not as well-defined as the other ions. The K^+ concentration curve for Storm 1 was characterized by a single, well-defined peak in concentration occurring on the receding limb of Event 1-1 and a smaller peak occurring on the receding limb of Event 1-2 (Figure 10). After this point, concentration began to steadily drop before gradually increasing again during the latter-half of the receding limb of Event 1-3 and returning to pre-event levels (Figure 10). The K^+ concentration curve for Storm 2 exhibited two peaks in concentration occurring with discharge for Event 2-1 and with, or just after, peak in discharge for Event 2-3 (Figure 10). These peaks were separated by a steady drop in concentration through the receding limb of Event 2-1 and all of Event 2-2 before again increasing during the rising limb of Event 2-3 (Figure 10). Concentrations decreased during the receding limb of Event 2-3 and dropped below pre-event levels before the end of the sampling period (Figure 10). The maximum K^+ concentrations occurred on the receding limb of Event 1-2 for Storm 1 and at the peak in discharge of Event 2-1 for Storm 2 (Figure 10).

NO_3^- , DOC, TP, and TKN displayed various responses both amongst each other as well as between Storms 1 and 2 (Figure 11). NO_3^- concentrations for Storm 1 were characterized by a single, well-defined peak occurring on the receding limb of Event 1-1 followed by stable, but elevated, concentrations and smaller peaks occurring with, or just before, the peak in discharge of Event 1-2 and with, or just after, the peak in discharge for Event 1-3 (Figure 11). Unfortunately, it is unknown if the missing data points on the concentration curve for Event 1-3 were associated with higher concentrations than those that make up the small peak preceding them. Following the gap in data, nitrate

concentrations dropped steadily through the receding limb of Event 1-3, but did not return to pre-event levels before the end of the sampling period (Figure 11).

The concentration pattern for NO_3^- exhibited during Storm 2 was much different than that of the first storm. During Event 2-1 of Storm 2, NO_3^- concentrations peaked on the rising limb before dropping slightly and exhibiting another small concentration peak on the receding limb just after peak in discharge for the event (Figure 11). Concentrations during Event 2-2 increased during the rising limb, approached the peak concentration for Storm 2 at the point of peak discharge, and remained nearly constant through the receding limb (Figure 11). Event 2-3 was characterized by a dilution trend (i.e. a decrease in concentration associated with an increase in discharge). Concentrations dropped through the rising limb of the event and minimum concentrations for the event were achieved at the point of peak in discharge (Figure 11). Concentrations rose and peaked early in the receding limb of Event 2-3 before steadily dropping through the latter-part toward, but not reaching, pre-event levels (Figure 11).

The DOC concentration curve for Storm 1 was characterized by two nearly equivalent peaks in concentration on the receding limbs of Events 1-1 and 1-2 before steadily dropping back to pre-event concentrations through Event 1-3 and the final receding limb (Figure 11). The maximum DOC concentration for Storm 1 occurred during Event 1-1 (Figure 11).

The DOC concentration curve for Storm 2 was characterized by two nearly equivalent peaks in concentration with, or just before, the peak in discharge for Event 2-1 and with, or just after, the peak in discharge for Event 2-3 (Figure 11). Concentrations dropped throughout the receding limb of Event 2-3, but did not return to pre-event levels

before the end of the sampling period (Figure 11). The maximum DOC concentration for Storm 2 occurred during Event 2-1 (Figure 11).

TP concentrations for Storm 1 were characterized by two peaks occurring with discharge for Events 1-1 and 1-2 (Figure 11). Concentrations did not show a well-defined peak for Event 1-3, but stay elevated through the majority of the event before suddenly dropping to pre-event levels on the receding limb (Figure 11). The maximum TP concentration for Storm 1 occurred during Event 1-2 coinciding with the point of highest discharge for Storm 1 (Figure 11).

TP concentrations for Storm 2 were characterized by three sharp concentration increases, to levels that were double those achieved during Storm 1, occurring on the rising limb of Event 2-1 as well as on the rising limb and with peak in discharge during Event 2-3 (Figure 11). Concentrations for Event 2-1 continued to drop through the peak in discharge, the receding limb, and all of Event 2-2 before the second rapid increase on the rising limb of Event 2-3 (Figure 11). After this increase, a sharp drop followed by a sharp increase in concentration, associated with peak in discharge for Event 2-3, occurred before concentrations again dropped rapidly through the receding limb and back to pre-event levels prior to the end of the sampling period (Figure 11). The maximum TP concentration for Storm 2 occurred during Event 2-1 (Figure 11).

TKN concentrations for Storm 1 were characterized by three peaks occurring on the receding limbs of Events 1-1, 1-2, and 1-3 (Figure 11). Concentrations decreased to pre-event levels on the receding limb of Event 1-3 (Figure 11). The maximum TKN concentration for Storm 1 occurred during Event 1-2 near the point of maximum discharge for Storm 1 (Figure 11).

TKN concentrations for Storm 2 were characterized by two prominent peaks occurring on the rising limbs of Events 2-1 and 2-3 (Figure 11). Concentrations dropped through the peaks in discharge and receding limbs of these two events (Figure 11). Event 2-2 was characterized by concentrations that were both slightly elevated and relatively constant through the entire event (Figure 11). Concentrations dropped through the peak in discharge and receding limb of Event 2-3 to pre-event levels prior to the end of the sampling period (Figure 11). The maximum TKN concentration for Storm 2 occurred during Event 2-1 (Figure 11).

Similar to the those displayed by the suite of nutrients, the concentration curves associated with TSS, atrazine, 2-MIB and geosmin all displayed various responses both amongst each other as well as between Storms 1 and 2. TSS concentrations for Storm 1 were characterized by three peaks occurring with, or just before, peaks in discharge for Events 1-1, 1-2, and 1-3 (Figure 12). Concentrations dropped steadily after the third peak and through the receding limb of Event 1-3 before returning to pre-event levels prior to the end of the sampling period (Figure 12). The maximum TSS concentration for Storm 1 occurred during Event 1-2 just before the point of highest discharge for Storm 1 (Figure 12).

TSS concentrations for Storm 2 were characterized by two sharp increases, to levels that were more than double those achieved during Storm 1, occurring on the rising limbs of Events 2-1 and 2-3 (Figure 12). Concentrations for Event 2-1 spiked and dropped rapidly twice during the rising limb (Figure 12). Event 2-2 was characterized by a smaller peak on the rising limb followed by an equivalent drop in concentration (Figure 12). Finally, Event 2-3 was characterized by a sharp increase in concentration on the

rising limb followed by a drop to an elevated level where concentrations remained steady through the peak in discharge (Figure 12). Following the peak in discharge, concentrations dropped nearly uninterrupted and approached pre-event levels prior to the end of the sampling period (Figure 12). The maximum TSS concentration for Storm 2 occurred during Event 2-1 (Figure 12).

Atrazine concentrations for Storm 1 were characterized by three peaks occurring with, or just after, peaks in discharge for Events 1-1, 1-2, and 1-3 (Figure 12). Concentrations dropped steadily following the third peak to nearly pre-event levels prior to the end of the sampling period (Figure 12). The maximum atrazine concentration for Storm 1 occurred during Event 1-2 just after the highest peak in discharge for Storm 1 (Figure 12).

The atrazine concentration pattern for Storm 2 varied a great deal compared to that of Storm 1. The concentration pattern for Storm 2 seemed to exhibit a flushing effect as it was characterized by a single, elevated peak occurring with discharge during Event 2-1, before dropping significantly (Figure 12). Concentration stabilized through Event 2-2, dropped again, and peaked only slightly with, or just after, the peak in discharge during Event 2-3 (Figure 12). Following the third peak in concentration, atrazine dropped to nearly pre-event levels prior to the end of the sampling period (Figure 12). The maximum atrazine concentration for Storm 2 occurred during Event 2-1 (Figure 12).

The taste and odor compounds 2-MIB and geosmin were found to have varied signals both between one another as well as between storms. 2-MIB concentrations for Storm 1 were characterized by elevated levels during pre-event flows followed by three well-defined peaks on the receding limbs of Events 1-1, 1-2, and 1-3 (Figure 12). Peak 2-

MIB concentrations for each event occurred at, or just before, the points of lowest discharge between events (Figure 12). These peaks were sharp in nature and, as discharge began to increase during the rising limbs of Events 1-1, 1-2, and 1-3, 2-MIB levels dropped almost immediately to levels below the detectable limit (Figure 12). After the third peak in 2-MIB concentration, occurring on the receding limb of Event 1-3, concentrations trended upwards as the end of the sampling period approached and reached levels nearly double those occurring during the three preceding events (Figure 12). The maximum 2-MIB concentration for Storm 1 occurred on the latter-part of the final receding limb during Event 1-3 (Figure 12).

In contrast, the 2-MIB pattern for Storm 2 was characterized by highly-elevated concentrations, measured during pre-event flows, immediately followed by a sudden drop and rise before maintaining a somewhat elevated 2-MIB concentration (5-10 ng/L) throughout the rising limb and peak in discharge of Event 2-1 (Figure 12). Concentrations rapidly spiked and dropped during the receding limb of Event 2-1 before dropping to reduced levels and producing two negligible concentration peaks on the receding limbs of Events 2-2 and 2-3 (Figure 12). After the third peak in concentration, 2-MIB levels increased slightly to concentrations approaching those characterizing the two preceding peaks and were maintained until the end of the sampling period (Figure 12). The maximum 2-MIB concentration for Storm 2 occurred just prior to the beginning of Event 2-1 (Figure 12).

The geosmin concentrations pattern for Storm 1 seemed to exhibit a flushing effect characterized by a single, elevated peak in concentration occurring on the rising limb of Event 1-1 before dropping significantly and exhibiting no noticeable peaks

throughout Events 1-2 and 1-3 (Figure 12). Geosmin concentrations appeared to increase slightly during the receding limb of Event 1-3 and through end of the sampling period (Figure 12). The maximum geosmin concentration for Storm 1 occurred on the rising limb of Event 1-1 (Figure 12).

In contrast, the geosmin concentration pattern associated with Storm 2 was characterized by a lack of well-defined peaks and levels that remained relatively constant throughout the storm with only slight elevations in concentration associated with increases in discharge (Figure 12). The maximum geosmin concentration for Storm 2 occurred during Event 2-1 (Figure 12).

Loadings and Yields

While Storm 1 occasionally exhibited concentrations higher than those of Storm 2, loadings were almost exclusively higher for Storm 2 relative to Storm 1. NO_3^- , DOC, TP, and TKN loadings for Storm 1 were 2.13 kg/ha, 1.85 kg/ha, 0.10 kg/ha, and 0.57 kg/ha, respectively and 2.65 kg/ha, 3.19 kg/ha, 0.28 kg/ha, and 0.90 kg/ha for Storm 2, respectively (Table 11). Similarly, TSS, atrazine, and 2-MIB loadings for Storm 1 were 15.87 kg/ha, 2.66×10^{-3} kg/ha, and 2.45×10^{-6} kg/ha respectively and 56.69 kg/ha, 4.62×10^{-3} kg/ha, and 3.18×10^{-6} kg/ha for Storm 2, respectively (Table 11). The only parameter that loaded higher for Storm 1 than Storm 2 was geosmin with values of 3.78×10^{-6} kg/ha and 2.58×10^{-6} kg/ha, respectively.

Discussion

Export Patterns

The concentration patterns of the major cations and anions used in this study as qualitative aids in determining streamwater sources and nutrient and contaminant flow pathways were similar to the findings of other comparable studies (Hill, 1993; Brown et al., 1999; Sidle et al., 1999; Devito et al., 2000; Inamdar et al., 2004; Hood et al., 2006; Vidon et al., 2008). During both storms, Mg^{2+} , Na^+ , SO_4^- , and Cl^- concentrations generally decreased in the channel as stream discharge increased and minimum concentrations of each ion were generally achieved at or near the points of highest discharge (Figure 10). Additionally, the rates of discharge associated with the peaks of Events 2-1 and 2-3 of Storm 2 were higher than any achieved during Storm 1 and were also associated with the lowest concentrations of these ions than any other points during the study period (Figure 10). In contrast, maximum concentrations remained similar between storms (Table 9). These concentration patterns correspond to previously published conclusions linking these four ions to deeper soil sources and groundwater pathways (Hill, 1993; Brown et al., 1999; Sidle et al., 1999; Devito et al., 2000; Inamdar et al., 2004; Hood et al., 2006). In central Indiana, high concentrations of Ca^{2+} and Mg^{2+} are common in groundwater due to the presence of calcareous glacial tills derived from limestone bedrock (Tedesco et al., 2005). The high solubility of other cations and anions, including Na^+ , SO_4^- , and Cl^- , attributes them to transport via subsurface pathways as well. In the cases of all these ions, when increases in new event water mix with displaced groundwater during periods of elevated discharge, subsequent dilution in the channel is

common (Hill, 1993; Brown et al., 1999; Sidle et al., 1999; Devito et al., 2000; Inamdar et al., 2004; Hood et al., 2006).

The patterns associated with K^+ were also generally consistent with the findings of other tracer-based studies that reported stable or elevated concentrations associated with increases in discharge attributed to increased contribution by overland flow and shallow, lateral subsurface flow (Hill, 1993; Hood et al., 2006; Vidon et al., 2008). During Storm 1, K^+ remained stable throughout all three events which can be observed in the range of the concentrations of less than 1.0 mg/L (Figures 9-10). However, the peaks in concentration on the receding limb of Events 1-1 and 1-2 indicate that a subsurface pathway (i.e. groundwater, macropores, shallow subsurface flow, or tile drainage) may be a significant contributor of K^+ during this event (Figure 10). During the latter-half of the final receding limb of Storm 1, K^+ concentrations increase slightly as discharge continues to decrease which may also suggest subsurface influence. In contrast, Storm 2 was associated with almost consistently higher discharge and concentrations of K^+ than Storm 1, and concentrations of K^+ during Storm 2 ranged more than twice that of Storm 1 (Figures 9-10). Additionally, two well-defined peaks in K^+ concentration occur more closely with the peaks of highest discharge during Events 2-1 and 2-3 (Figure 10), and the inverse relationship relative to the concentrations of Mg^{2+} , Na^+ , SO_4^- , and Cl^- are also more well-defined (Figure 9). However, while the peak in K^+ concentration appears to occur with the peak in discharge during Event 2-1 which may indicate that overland flow transport of K^+ is a more significant contributor during Storm 2, there is a slight delay during Event 2-3 which places the K^+ peak on the receding limb and, like Storm 1, may indicate subsurface influence (Figure 10).

While the differences between Storms 1 and 2 in regard to K^+ concentration patterns relative to discharge may suggest a shift in modes of export, the similarities in the runoff ratios between storms (Table 7) suggest that elevated K^+ concentrations during Storm 2 cannot be attributed to an increase in export via overland flow alone, but must also be related to the elevated levels of discharge within the channel. Similar patterns were found associated with those nutrients and contaminants which are also generally attributed to export via shallow, lateral subsurface or overland flow pathways (i.e. DOC, TP, TKN, TSS) throughout this study and are each discussed in more detail below. These drastic differences in K^+ , DOC, TP, TKN, and TSS concentrations between Storms 1 and 2 may be attributed to the inundation of near-channel areas with increased stream discharge and/or channel bank and bed erosion. According to a calculation of bankfull discharge, based upon the nearby state of Ohio's regional curve (Sherwood and Huitger, 2005), this stage is achieved at approximately $234 \text{ m}^3/\text{s}$ ($8273 \text{ ft}^3/\text{s}$), or $0.286 \text{ mm}/\text{hr}$, at the point of the 146th Street study site. The bankfull stage defines the point at which a stream breaches its natural banks or levees and activates its adjacent floodplain (Wolman and Leopold, 1957; Sherwood and Huitger, 2005). The levels of discharge at, or near, the bankfull stage are commonly associated with elevated levels of suspended sediment, and those nutrients and contaminants that may be bound to them, due to the increased erosion taking place in the channel (Leopold and Maddock, 1953; Wolman and Miller, 1960; Sherwood and Huitger, 2005). During Storm 1, the maximum discharge of $0.223 \text{ mm}/\text{hr}$ occurred during Event 1-2 (Table 7) and thus did not exceed the calculated bankfull discharge. However, Events 2-1 and 2-3 of Storm 2, those same two events associated with sizable increases in K^+ , DOC, TP, TKN, and TSS loads relative to Storm 1, were

also associated with peak discharges of 0.288 and 0.304 mm/hr (Table 7), respectively, thereby exceeding the calculated bankfull discharge.

In general, concentration patterns for each of the four nutrients (NO_3^- , DOC, TP, and TKN) seemed to match those associated with K^+ most closely. Like K^+ , the nitrate concentration pattern associated with Storm 1 is characterized by a single strong increase in concentration, along with the increase in discharge during Event 1-1, and a delayed peak occurring on the falling limb of Event 1-1 (Figure 11). Additionally, for both K^+ and NO_3^- , Events 1-2 and 1-3 are characterized by stable, elevated concentrations through the peak in discharge of the final event before steadily dropping through the final receding limb, though K^+ concentrations do increase slightly before the end of the storm. This pattern of NO_3^- peaking on the receding limb of Event 1-1 suggests that primary export initially occurred with subsurface flow. Similar NO_3^- concentration patterns were reported in a parallel study conducted during the same three events that make up Storm 1 in a 274 km² portion of the Eagle Creek Watershed, one of the Upper White River Watershed's HUC 10 subwatersheds (Johnstone et al., 2010). During the events of Storm 1, NO_3^- concentrations in Eagle Creek regularly peaked after peaks in discharge and delivery was attributed to primarily subsurface pathways (Johnstone et al., 2010). The smaller NO_3^- concentration inflections occurring during Events 1-2 and 1-3 occur with the peak in discharge indicating a possible increase in contribution via an overland or a preferential flow pathway such as tile drains. This is possible considering the increasing runoff ratios that were achieved as Storm 1 progressed (Table 7). Like the Eagle Creek study, NO_3^- concentrations were able to remain stable at elevated concentrations throughout the three events of Storm 1 indicating a large NO_3^- pool available for flushing.

This is attributed to the recent spring nutrient applications occurring just prior to the beginning of sampling.

NO_3^- concentration patterns for Storm 2 were highly varied from those of Storm 1. Event 2-1 was associated with a peak in NO_3^- concentration occurring on the rising limb indicating a rapid contribution delivered by overland flow or a direct subsurface pathway in the form of tile drains (Figure 11). However, the three remaining NO_3^- peaks occurring during Storm 2 each suggest that subsurface pathways were again the dominant contributors. In addition to the peak in nitrate occurring on the rising limb, the receding limb of Event 2-1 is characterized by a small peak in nitrate suggesting subsurface contribution (Figure 11). Additionally, while NO_3^- appears to peak with discharge during Event 2-2, which may suggest some contribution via overland flow, concentrations remain elevated throughout the duration of the receding limb indicating primarily subsurface contribution (Figure 11). The sudden increase in NO_3^- concentrations associated with Event 2-2 may also indicate the activation of new hydrological area and subsequent nitrate source as the result of increasing antecedent moisture conditions (Sidle et al., 2000). Finally, NO_3^- concentrations show considerable dilution with discharge during Event 2-3 before peaking on the receding limb; both of which are indicative of subsurface contribution (Figure 11). Similar to Storm 1, NO_3^- concentrations were able to remain elevated throughout the entirety of the Storm 2 sampling period indicating a large available pool. However, the dilution pattern exhibited during Event 2-3 may also suggest the contributing NO_3^- source(s) were beginning to show signs of exhaustion.

The inconsistent nature of the NO_3^- concentration patterns observed during this study indicate that discharge does not appear to play as significant of a role in influencing

its export compared to other factors. These results are similar to other studies of NO_3^- that have been conducted in the Midwest (Vanni et al., 2001; Wagner et al., 2008; Johnstone et al., 2010). In each of these studies, no consistent relationship linking the export of NO_3^- and discharge were able to be established and, in turn, other factors such as seasonal variation, NO_3^- availability, and hydrologic controls were highlighted as potential influences. In the case of this study, while any potential seasonal variation is not applicable, the exhaustion of the available flushing pool as provided by the spring applications over the span of the six storm events and the potential activation of new hydrological areas as described by Sidle et al. (2000) may account for some of the variation observed in the NO_3^- patterns over the course of the study period.

DOC concentration signals for both storms were much more closely related to those produced by K^+ than those of NO_3^- . Like NO_3^- , Storm 1 was characterized by peaks in concentration occurring after the peaks in discharge. In the case of DOC, these peaks occurred on the receding limbs of Events 1-1 and 1-2 before dropping steadily through Event 1-3 to pre-event concentrations (Figure 11). This pattern suggests primarily subsurface contribution as indicated by the results of one study conducted in the Catskill Mountains of New York in which DOC concentrations were found to be consistently higher on the receding limbs relative to the rising limbs of the hydrographs (Brown et al., 1999). This pattern of DOC export was attributed to an increased shallow subsurface contribution of O-horizon soil water (Brown et al., 1999). In central Indiana, the impermeable nature of the compacted till packages underlying surface soils may promote similar shallow, lateral subsurface contribution of O-horizon soil water as described in the study conducted by Brown et al. (1999). The DOC concentration patterns during

Storm 2 were nearly identical to those of K^+ and were characterized by two strong peaks occurring in close proximity to the peaks in discharge indicating delivery may be the result of overland flow (Figure 11). Again, like K^+ , while this indicates that overland flow transport of DOC is a more significant contributor during Storm 2, and the peak in DOC concentration appears to occur with the peak in discharge during Event 2-1, there is a slight delay during Event 2-3 which places the DOC peak on the receding limb and, like Storm 1, may indicate subsurface influence. Additionally, the increased concentrations and discharges associated with Storm 2 relative to Storm 1 may be the result of the inundation of near-channel areas with elevation in water levels and/or channel bank and bed erosion as described above.

Though all exhibiting somewhat erratic concentration signals, the export patterns of TP, TKN, and TSS appear to be closely related to K^+ , as well as one another, for both Storms 1 and 2. Like K^+ , each of the three concentration signals were characterized by much more modest peaks during Storm 1 relative to Storm 2 (Figures 11-12). During Storm 1, TP peaked with discharge during Events 1-1 and 1-2, indicating contribution via overland flow, but seemed to show signs of dilution and subsurface export during Event 1-3 (Figure 11). While K^+ did not appear to be exported via overland flow during Events 1-1 and 1-2 of Storm 1, due to the peaks in concentration occurring on the receding limbs, the patterns of dilution noted in the concentration curves of K^+ and TP during Event 1-3 are similar. The TKN concentration curve during Storm 1 was similar to that of K^+ in that concentrations peaked on the receding limbs of Events 1-1 and 1-2 thereby indicating contribution via subsurface pathways (Figure 11). Unlike the K^+ and TP curves, TKN concentrations peaked a third time on the receding limb of Event 1-3 rather

than exhibiting dilution and no concentration peak. Finally, TSS concentrations regularly peaked on the rising limbs of each of Storm 1's three events indicating rapid export of sediments to the channel as the result of an overland flow export pathway (Figure 12).

The concentration patterns exhibited by TP, TKN, and TSS during Storm 2 were much more consistent between one another. Each of the three curves were generally characterized by strong peaks on the rising limbs of Events 2-1 and 2-3 separated by a smaller peak, also occurring on the rising limb, during Event 2-2 (Figures 11-12). This pattern of rapid transport to the channel via an overland flow pathway, the inundation of near-channel areas with elevation in water levels, and/or channel bank and bed erosion is consistent with the findings of a number of parallel studies that have found the largest percentages of exported TP and TKN to be bound to sediment (Johnson et al., 1976; Cooke and Cooper, 1988; Uusitalo et al., 2003; Royer et al., 2006; Gentry et al., 2007).

Each of the three remaining contaminants (i.e. atrazine, 2-MIB, and geosmin), were each characterized by radically different concentration signals both amongst one another as well as between Storms 1 and 2. Atrazine concentrations during Storm 1 regularly peaked with or just after the peak in discharge for each of the three events (Figure 12). While atrazine concentrations tended to peak near peaks in discharge, which is indicative of overland transport, the elevated nature of the atrazine concentrations occurring on the receding limbs of Storm 1 likely indicate significant subsurface contribution such as tile drain flow. This is especially highlighted in the elevated concentrations that persist through the receding limb of Event 1-1. During Storm 2, peak atrazine concentration again occurs with peak in discharge during Event 2-1 indicating contribution via overland flow. However, concentrations steadily drop through both

Events 2-2 and 2-3 and only temporarily level out on the receding limbs after increases in discharge indicating primarily subsurface export (Figure 12). The results of this study are similar to those reported from nearby Leary Weber Ditch where atrazine was also found to be transported via a combination of overland flow and tile drains (Baker et al., 2006). Additionally, this pattern indicates that the Event 2-1 exhausted the sink contributing to elevated atrazine concentrations in the channel and, despite the elevated discharges associated with Event 2-3, concentrations were unable to climb.

The unique pattern exhibited by 2-MIB indicated significant dilution with increased discharge. Through each of the three rising limbs and peaks in discharge during Storm 1, 2-MIB concentrations remained at below detectable limits, but, just as discharge began to drop on the receding limbs, 2-MIB concentrations rose and peaked at the points of lowest discharge separating Events 1-1 and 1-2 and Events 1-2 and 1-3 (Figure 12). Additionally, concentrations generally increased throughout the entire receding limb of Event 1-3. This pattern may be indicative of in-stream production of 2-MIB by cyanobacteria and/or other organisms during periods of low discharge and subsequent dilution with new water during periods of high flow. Algal blooms have been linked to elevated levels of taste and odor compounds and may be the primary source in photic, aquatic environments (Jüttner and Watson, 2007). During Event 2-1 of Storm 2, the 2-MIB concentration pattern seems to indicate a secondary source contributing 2-MIB to the channel. Except for a lone, highly-elevated 2-MIB reading that occurs prior to Event 2-1, concentrations remain low until the receding limb where three highly-elevated 2-MIB readings occur and form a sharp, short-lived concentration peak (Figure 12). This sudden, sharp increase in 2-MIB concentration, like DOC, TP, TKN, and TSS, may be

linked to either the transport of sediment to the stream or the scouring of sediment within or near the channel. Periods of high terrestrial runoff have also been shown to contribute the export of actinomycete bacteria and other organisms associated with elevated levels of taste and odor compounds (Jensen et al., 1994; Jüttner and Watson, 2007). It is therefore reasonable to assume that the suspension of sediments in the vicinity of the channel would have a similar effect on concentration patterns. Unlike Storm 1, concentrations drop to near pre-event conditions following this initial peak on the receding limb of Event 2-1 potentially indicating that, similar to atrazine, the contributing secondary 2-MIB source had been extinguished. However, this pattern may also relate to 2-MIB concentrations stemming from in-stream production being diluted by the increase in discharge during Storm 2 relative to Storm 1.

Finally, the geosmin concentration pattern during Storm 1 acted similarly to that of atrazine during Storm 2 in that a single concentration peak occurred during the first event before concentrations dropped to a stable, lower concentration through the remainder of Storm 1 and, additionally, Storm 2 (Figure 12). The geosmin peak occurring on the rising limb of Event 1-1 prior to the peak in discharge may indicate a very rapid transport of this compound to the channel via overland flow or the dilution of an in-stream source. Like 2-MIB concentrations during Storm 2, these elevated concentrations may be indicative of transport of material associated with taste and odor producing organisms to the channel, but the slight increase in concentration on the receding limb of Event 1-3 may be indicative of the dilution of an in-stream source. While this peak, acting as the only point in either storm where geosmin concentrations are elevated, may indicate a very rapid exhaustion of the source, the elevated discharge rates occurring

through Events 1-2, 1-3, and all of Storm 2 may have also restricted geosmin concentration from increasing. However, the low discharge rates associated with Event 1-1, and the radically different signals relative to 2-MIB, suggest that the two compounds are each deriving from different sources and pathways in the Upper White River Watershed despite being associated with production by similar organisms.

Influence of Scale

In addition to this study, two similar projects have been conducted on smaller watersheds within the Upper White River Basin to examine nutrient transport pathways (Wagner et al., 2008; Johnstone et al., 2010). Along with these past studies, this research has been able to provide insight into the influence of watershed scale on nutrient concentration patterns during high flow events. The first of these studies (Wagner et al., 2008) investigated export dynamics of cations, NO_3^- , and DOC during spring storm events in both a mixed land use subwatershed (6.7 km^2) and agricultural subwatershed (10.9 km^2) of the Eagle Creek Watershed located near the western edge of the Upper White River Basin (Figure 1). The second of these studies (Johnstone et al., 2010) investigated seasonal differences in export dynamics of a suite of cations, nutrients, and contaminants within a 267 km^2 area of the Eagle Creek Watershed.

Marked differences in nutrient concentration patterns were noted between the three watersheds suggesting that patterns were influenced by watershed scale. In the case of the smaller watersheds (Wagner et al., 2008), some cation concentration patterns (i.e. Ca^{2+} , Cl^-) were often erratic, or noisy, in nature and exhibited high inter-storm variability. Additionally, reported concentration curves commonly showed a lack of pattern

regularity between storms. At times, the background variations in concentration occurring prior to and after storm events were as high as those associated with variations in discharge. This high variability made it difficult to interpret the influence of discharge on concentration patterns and determine the timing of peak concentrations. Some cations (i.e. Mg^{2+} , Na^+ , K^+), however, did show a more well-defined and regular response to increases in discharge. In contrast, nutrient concentration patterns reported by Johnstone et al. (2010) for the larger watershed (267 km^2) were more well-defined. Relationships between concentrations and discharge were more constant and showed limited variation from storm to storm despite seasonal differences. This difference in transport pattern between the two watershed scales was attributed to an averaging, or smoothing, effect as a result of many first-order streams mixing together and subsequently dampening the sensitivity of the signals (Johnstone et al., 2010). Finally, in contrast to the two previous studies, the concentration patterns observed in the Upper White River Watershed (2945 km^2) seem to exhibit an intensified version of the averaging effect due to the mixing of a number of larger-order streams. While there is generally a lack of inter-storm variability, and the relationships of concentration and discharge are evident, the cation and anion curves have been smoothed to a degree in which individual event peaks are difficult to be distinguished from one another. This trend is particularly evident in the case of cations and anions (Mg^{2+} , Na^+ , SO_4^- , Cl^-) known to be associated with subsurface tracers (Storm 1, Figure 10).

The differences in nutrient and contaminant patterns amongst the three studies suggest that the transport of these constituents may be more complex than the cations and anions and, additionally, may not each be affected in similar ways as scale increases.

Like the cations and anions, the NO_3^- concentration patterns reported by Wagner et al. (2008) showed a great deal of inter-storm variability and lacked of pattern regularity between storms. However, unlike the cations and anions, the results of both Johnstone et al. (2010) and this study show that while the smoothing of concentration signals is evident compared to Wagner et al. (2008), the pattern regularity does not appear to improve in either the Upper Eagle Creek or Upper White River Watersheds. This is evident in the erratic nature in which NO_3^- peaks relative to discharge during both Storm 1 and Storm 2 (Figure 11). Johnstone et al. (2010) proposed that the large inter-storm variability associated with the relationship between NO_3^- and discharge that can be seen in smaller watersheds is the primary reason for the weak relationship that is maintained in larger watersheds.

Other nutrients and contaminants acted more similarly between storms in addition to maintaining similar concentration patterns across all scales. DOC concentration patterns reported by Wagner et al. (2008) were generally lacking in the signal noise that was associated with some of the other solutes. Additionally, DOC was found to peak very regularly with discharge for a majority of the sampled events. A similar degree of smoothness and pattern regularity was associated with the DOC concentration patterns reported in Johnstone et al. (2008). The similarities in DOC pattern and regularity shared by the two previous studies are not evident in this research. While Wagner et al. (2008) found that DOC concentrations tended to be higher on the receding limbs of storm events and Johnstone et al. (2010) reported a peak in DOC concentration after the peak in discharge during one of the storms, the DOC concentration patterns associated with the Upper White River Watershed were not representative of those seen in both of the

previous studies. DOC concentration patterns for Storm 1 were irregular, without pattern regularity, and generally peaked after peak discharge despite occurring simultaneously with three of the events studied in Johnstone et al. (2010) (Figure 11). Additionally, the DOC patterns associated with Storm 1 and Storm 2 were drastically different from one another though this is likely attributed to the sizable differences in discharge that occurred during the two sampling periods. Similar differences existed between the results of Johnstone et al. (2010) and this study regarding TP and TKN concentration patterns during sampled events. While concentration patterns for both nutrients in the Upper Eagle Creek Watershed were similar to DOC in their smoothness, pattern regularity, and tendency to peak with discharge, those in the Upper White River were noisy and, while TP tended to peak with discharge for Storm 1, TKN peaked after peak in discharge. During Storm 2, both TP and TKN generally peaked prior to discharge and is likely the result of the elevated levels of discharge in the channel (Figure 11). The same storm reported by Johnstone et al. (2010) in which DOC peaked after discharge was also associated with TP and TKN peaks prior to peaks in discharge.

Summary and Conclusions

The results of this study have captured the complexity of nutrient and contaminant export dynamics associated with periods of elevated discharge and the importance of high-resolution storm sampling in capturing and interpreting their concentration patterns. Two storms were sampled for a suite of nutrients and contaminants in the Upper White River Watershed, located in central Indiana, directly after spring applications to the areas of corn and soybean row crops that cover approximately 66% (1944 km²) of the basin. NO₃⁻ concentrations were found to have no well-defined relationship with discharge, but showed patterns consistent with subsurface contribution via preferential flow pathways such as macropores or tile drains. This lack of consistent concentration pattern relative to discharge was consistent with the findings of other similar studies conducted in the Upper White River Basin (Wagner et al., 2008; Johnstone et al., 2010). DOC concentration patterns indicated transport via a shallow, lateral subsurface pathway. TKN showed signs of transport via a combination of shallow, lateral subsurface flow and overland flow while TP and TSS were confined to primarily overland flow. High DOC, TKN, TP, and TSS levels during Storm 2 were all determined to be influenced by the erosion of sediment near or in the stream channel due to event discharge exceeding calculated bankfull discharge. Atrazine concentrations were determined to originate from a combination of sediment-bound fraction transported by overland flow as well as a dissolved fraction transported via a subsurface pathway such as tile drains. The taste and odor compounds 2-MIB and geosmin were determined to originate from different sources and pathways in the Upper White River Watershed. In-stream production of 2-MIB during periods of low discharge and subsequent dilution with new water during storm

events controlled concentrations during Storm 1 while potential transport of sediment to, or scouring of sediment in or near the channel, controlled 2-MIB concentrations during Storm 2. Rapid flushing of in-stream geosmin or the transport of sediment via overland flow during Storm 1 raised geosmin concentrations, but the contributing source was rapidly exhausted and concentrations remained low throughout the remainder of the sampling period.

By comparing the results of other similar studies conducted in the Upper White River Basin, watershed scale was also determined to be a factor in the concentration patterns observed during storm events. NO_3^- concentration patterns were generally less erratic as scale increased due to an averaging effect caused by the mixing of a number of smaller watersheds, but a consistent concentration to discharge relationship was not recorded in any of the watersheds. A well-defined DOC pattern relative to discharge was evident and remained relatively smooth and consistent in the two smaller watersheds, but was not evident in the Upper White River study. TP and TKN patterns were much smoother and consistent in the mid-sized watershed relative to the Upper White River study.

The information gained from this collection of studies has allowed for an increased understanding of nutrient and contaminant concentration patterns as they occur throughout the entirety of a storm, as well as the differences found between individual events, including the timing of concentration peaks relative to discharge and the levels that concentrations are able to reach as a result of discharge. Each of these factors is crucial in the development and success of best management practices (BMPs), remediating drinking water supplies, and ensuring the safety of recreationists.

Additionally, by comparing the patterns of nutrients and contaminants to those of cations and anions acting as tracers, one is able to better associate them with specific sources and flow pathways which is crucial in the protection of downstream areas.

The detailed concentration patterns captured in these studies have additionally allowed for the quantification of the rates and amounts of nutrients and contaminants that are transported through these systems during significant storm events. These values are directly influenced by the amount of nutrients supplied to the area as well as the climate and landscape characteristics of the area that may affect their ability to be delivered to surrounding bodies of water (Robertson et al., 2009). This aids in the understanding of the relationship between significant storm events and nutrient and contaminant loads thereby allowing water quality managers to be more prepared for, and react accordingly to, situations in reservoirs and water treatment facilities as well as gain an understanding of their roles on total maximum daily load (TMDL) values. By estimating nutrient and contaminant fluxes and loads, one can identify the size, location, and timing of the source load which can aid in developing restoration and reduction strategies (EPA, 2005).

Finally, this group of studies illustrates the differences in nutrient and contaminant export behavior as they relate to watershed scale and draws attention to the challenges associated with modeling increasingly larger-scale watersheds. A comparison of these three studies suggests that all nutrients and contaminants are likely not all similarly affected by watershed scale. Similarly, additional variation is likely found amongst varying landscapes. Further research of this nature will greatly contribute to the understanding of the effects of discharge, antecedent hydrological conditions, and watershed scale on concentration patterns and transport pathways observed during

significant storm events and aid in the development of accurate prediction models as well as optimizing sampling strategies (Vidon et al., 2009; Johnstone et al., 2010).

Land Use	Percent Area (%)	Area (km ²)
Agricultural	66	1943.70
Herbaceous	21	618.45
High-Mid Density Development	5	147.25
Forested	4	117.80
Other	4	117.80

Table 1: Summary of land use in the Upper White River Watershed upstream of the 146th Street study site according to a 2007 land cover/crop data remote sensing image provided by the U.S. Department of Agriculture’s National Cartography and Geospatial Center.

Storm/Event	Date/Time Range	# Samples Collected/Analyzed	# Duplicates Analyzed
Event 1-1	5/7/08, 21:00 – 5/11/08, 9:45	17	1
Event 1-2	5/11/08, 10:00 – 5/14/08, 3:30	14	2
Event 1-3	5/14/08, 3:45 – 5/26/08, 13:30	31	3
Storm 1 Total	5/7/08, 21:00 – 5/26/08, 13:30	62	6
Event 2-1	6/3/08, 8:00 – 6/7/08, 14:45	20	2
Event 2-2	6/7/08, 15:00 – 6/9/08, 22:00	11	1
Event 2-3	6/9/08, 22:15 – 6/19/08, 4:45	22	2
Storm 2 Total	6/3/08, 8:00 – 6/19/08, 4:45	53	5

Table 2: Storm event descriptions and sampling summary including date and time ranges and numbers of samples and duplicates collected and analyzed for Storms 1 and 2 and their events.

<u>Ions</u>	<u>Analytical Method</u>	<u>Detection Limit</u>	<u>Method Description</u>
Cl ⁻ (mg/L)	EPA (300.0)	8.0	Ion Chromatograph
Mg ²⁺ (mg/L)	EPA (300.7)	1.0	Ion Chromatograph
Na ⁺ (mg/L)	EPA (300.7)	1.0	Ion Chromatograph
SO ₄ ⁻ (mg/L)	EPA (300.0)	8.0	Ion Chromatograph
K ⁺ (mg/L)	EPA (300.7)	0.05	Ion Chromatograph
<u>Nutrients</u>			
Nitrate (mg/L)	EPA (300.0)	0.1	Ion Chromatograph
TOC/DOC (mg/L)	SM (5310C)	0.5	Persulfate Oxidation
Total P (mg/L)	SM (4500-P E.)	0.01	Colorimeter Ascorbic
TKN (mg/L)	EPA (351.4)	0.3	Digestion ISE
<u>Contaminants</u>			
TSS (mg/L)	EPA (160.2)	-	Dry Weight
Atrazine (µg/L)	EPA (525.2)	0.05	Enzyme Immunoassay
2-MIB (ng/L)	SM (6040D)	3.0	Solid-phase Microextraction
Geosmin (ng/L)	SM (6040D)	3.0	Solid-phase Microextraction

Table 3: Analytical methods, detection limits, and method descriptions associated with each of the collected samples.

	<u>Latitude</u>	<u>Longitude</u>	<u>Elevation</u>	<u>Hardware</u>
KINNOBLE3	N 40° 1' 3" (40.018°)	W 85° 59' 21" (-85.989°)	816	1-Wire AAG
KINWESTF1	N 40° 0' 10" (40.003°)	W 86° 7' 57" (-86.133°)	885	Davis Vantage Pro
KINCICER1	N 40° 7' 28" (40.125°)	W 86° 1' 40" (-86.028°)	835	Davis Vantage Pro 2
KINANDER5	N 40° 3' 36" (40.060°)	W 85° 48' 22" (-85.806°)	847	LaCrosse WS-2317
KINANDER6	N 40° 6' 40" (40.111°)	W 85° 39' 52" (-85.664°)	911	Davis Vantage Pro 2
KINYORKT2	N 40° 9' 37" (40.161°)	W 85° 31' 7" (-85.519°)	918	LaCrosse WS-2315

Table 4: Locations and descriptions of precipitation gages utilized during the study.

May	Calculated from Hourly (mm)	Reported by NOAA (mm)	June	Calculated from Hourly (mm)	Reported by NOAA (mm)
01	0	0	01	0.589	0.406
02	4.657	6.435	02	0	0
03	6.524	7.239	03	24.849	30.988
04	0	0	04	33.106	31.242
05	0.132	0.127	05	0	0
06	0.210	0.254	06	2.125	3.404
07	15.749	19.558	07	25.174	24.486
08	20.016	23.029	08	0	0
09	5.483	6.350	09	7.707	14.732
10	0.095	0.085	10	23.316	22.454
11	24.821	27.347	11	0	0
12	0	0	12	0	0
13	0	0	13	13.145	16.087
14	21.398	20.362	14	0.044	0.042
15	0	0.152	15	6.516	7.705
16	1.102	1.473	16	0.049	0.127
17	0.393	0.406	17	0	0
18	1.621	2.455	18	0	0
19	0.635	1.058	19	0.348	0.339
20	0.131	0.169	20	0	0
21	0	0	21	0.021	0.169
22	0	0	22	0.606	0.847
23	4.610	5.673	23	0.137	0.381
24	0.119	0.169	24	0	0
25	0	0	25	0.191	0.169
26	0.403	0.381	26	10.333	11.726
27	1.012	1.228	27	9.018	8.890
28	0	0	28	6.084	8.975
29	0	0	29	10.336	12.065
30	3.826	6.900	30	2.312	2.794
31	2.189	1.219			
Total	115.128	132.072	Total	176.008	198.027

Table 5: Comparison of total daily precipitation data sources as calculated from NOAA hourly precipitation readings and taken directly from the NOAA total daily precipitation calculations for the Upper White River Watershed upstream of the 146th Street study site (03350800), May-June, 2008.

	Jan	Feb	Mar	Apr	May	Jun	Jul	Aug	Sept	Oct	Nov	Dec
<u>1971-2000</u>												
Avg. Q (m ³ /s)	35.87	45.56	58.24	50.39	35.89	35.09	21.30	12.65	10.14	8.18	25.06	32.93
Avg. Q (cfs)	1266.89	1608.87	2056.68	1779.60	1267.39	1239.10	752.26	446.88	358.10	288.83	884.94	1162.00
<u>2007</u>												
Avg. Q (m ³ /s)	134.90	30.42	172.45	61.14	18.77	7.08	4.74	5.56	2.38	2.65	9.21	66.33
Avg. Q (cfs)	4764.08	1074.21	6089.97	2159.13	662.79	250.19	167.36	196.43	83.94	93.51	325.32	2342.54
% 30 Year Normal	376.05	66.77	296.11	121.33	52.30	20.19	22.25	43.96	23.44	32.37	36.76	201.42
<u>2008</u>												
Avg. Q (m ³ /s)	52.91	103.99	130.51	54.32	51.80	81.28	29.42	9.92	3.10	N/A	N/A	N/A
Avg. Q (cfs)	1868.39	3672.34	4608.95	1918.14	1829.36	2870.36	1039.09	350.49	109.51	N/A	N/A	N/A
% 30 Year Normal	147.48	228.26	224.10	107.78	144.34	231.65	138.13	78.43	30.58	N/A	N/A	N/A

Table 6: Comparison of 2007-2008 streamflow to 30-year normal (1971-2000) at 146th Street study site (03350800) as extrapolated from USGS streamflow records at Nora, IN (03351000) site.

	Storm 1				Storm 2			
	Event 1-1	Event 1-2	Event 1-3	Total	Event 2-1	Event 2-2	Event 2-3	Total
Recurrence Interval (days)	11.3	33.8	28.5	33.8	54.4	27.5	73.1	73.1
Avg. Rainfall Intensity (mm/hr)	1.10	1.24	2.63	1.66	1.93	1.24	1.41	1.53
Max Rainfall Intensity (mm/hr)	5.56	6.14	4.09	6.14	6.57	7.63	9.18	9.18
Bulk Precipitation (mm)	33.09	24.82	21.04	78.95	57.95	27.30	31.02	116.27
7 day Antecedent Precipitation (mm)	33.6	49.4	76.4	33.6	9.8	90.5	104.9	9.8
30 day Antecedent Precipitation (mm)	68.9	82.6	99.3	68.9	118.8	166.4	174.3	118.8
90 day Antecedent Precipitation (mm)	346.4	375.8	401.9	346.4	387.2	364.5	378.8	387.2
7 day Antecedent Discharge (mm/hr)	0.025	0.048	0.107	0.025	0.025	0.117	0.162	0.025
30 day Antecedent Discharge (mm/hr)	0.042	0.045	0.051	0.042	0.065	0.086	0.092	0.065
90 day Antecedent Discharge (mm/hr)	0.107	0.090	0.089	0.107	0.089	0.088	0.090	0.089
Pre-event Flow (mm/hr)	0.021	-	-	0.021	0.022	-	-	0.022
Time to Maximum Peak (hrs)	56.00	33.00	23.50	89.00	86.25	24.00	36.75	147.00
Mean Stormflow (mm/hr)	0.076	0.174	0.074	0.089	0.166	0.175	0.132	0.148
Peak Discharge (mm/hr)	0.116	0.223	0.207	0.223	0.288	0.204	0.304	0.304
Runoff Ratio	0.145	0.476	0.746	0.420	0.238	0.390	0.686	0.417

Table 7: Summary of precipitation events and hydrological responses associated with the storms/events captured during the study period.

	Storm 1			Storm 2		
	15-min (mm/hr)	Average Daily Discharge (mm/hr)	% Difference	15-min (mm/hr)	Average Daily Discharge (mm/hr)	% Difference
7 Day	0.0248	0.0248	-0.0007	0.0245	0.0247	0.0085
30 Day	N/A	0.0424	-	0.0649	0.0650	0.0018
90 Day	N/A	0.1072	-	N/A	0.0893	-

Table 8: Comparison of antecedent discharge data sources calculated from USGS 15-minute data and USGS average daily discharge values for the 146th Street study site (03350800).

		Storm 1				Storm 2			
		Event 1-1	Event 1-2	Event 1-3	Total	Event 2-1	Event 2-2	Event 2-3	Total
Mg²⁺ (mg/L)	N	17	14	31	62	20	11	22	53
	Mean	24.28	18.81	23.15	22.48	17.58	17.43	17.65	17.58
	Geo. Mean	24.10	18.80	22.92	22.22	16.67	17.38	17.32	17.08
	Median	24.14	18.69	23.65	21.43	16.66	17.94	16.84	17.23
	Max	29.44	20.20	28.14	29.44	29.70	19.74	25.10	29.70
Na⁺ (mg/L)	N	17	14	31	62	20	11	22	53
	Mean	25.09	12.74	18.33	18.92	15.59	11.51	11.85	13.19
	Geo. Mean	24.14	12.57	17.57	17.77	13.18	11.50	11.44	12.08
	Median	27.80	12.45	17.62	17.07	13.44	11.70	10.99	11.45
	Max	32.76	16.95	29.88	32.76	34.10	12.18	20.25	34.10
SO₄⁻ (mg/L)	N	17	13	26	56	20	11	22	53
	Mean	46.51	25.59	36.87	37.18	30.20	22.91	24.09	26.15
	Geo. Mean	45.36	25.40	35.47	35.37	26.36	22.89	23.41	24.37
	Median	51.28	24.91	36.80	34.65	26.82	23.40	21.69	23.40
	Max	58.60	32.13	55.39	58.60	79.80	24.16	38.04	79.80
Cl⁻ (mg/L)	N	16	13	31	60	20	11	22	53
	Mean	36.65	25.18	29.11	30.27	24.03	21.41	21.37	22.38
	Geo. Mean	36.32	25.01	28.79	29.71	22.10	21.36	20.99	21.48
	Median	36.16	24.03	28.54	30.26	21.75	22.00	20.73	21.05
	Max	45.48	32.74	38.26	45.48	42.35	23.13	30.91	42.35
K⁺ (mg/L)	N	17	14	31	62	20	11	22	53
	Mean	2.64	2.84	2.51	2.62	3.67	3.07	3.30	3.39
	Geo. Mean	2.63	2.83	2.50	2.61	3.62	3.05	3.26	3.34
	Median	2.58	2.84	2.49	2.64	3.65	3.03	3.26	3.29
	Max	2.97	3.10	2.79	3.10	4.74	3.83	4.40	4.74

Table 9: Mean, geometric mean, median and maximum concentration values for ion, nutrient, and contaminant concentration values.

		Storm 1				Storm 2			
		Event 1-1	Event 1-2	Event 1-3	Total	Event 2-1	Event 2-2	Event 2-3	Total
NO₃⁻ (mg/L)	N	17	13	26	56	20	11	22	53
	Mean	3.73	5.30	4.43	4.42	4.21	5.63	4.54	4.64
	Geo. Mean	3.36	5.30	4.38	4.22	4.08	5.58	4.52	4.55
	Median	3.85	5.30	4.44	4.84	4.60	6.00	4.44	4.60
	Max	6.17	5.65	5.42	6.17	5.65	6.24	5.85	6.24
DOC (mg/L)	N	9	8	17	34	11	6	11	28
	Mean	4.39	5.32	3.99	4.41	5.63	5.28	5.49	5.50
	Geo. Mean	4.28	5.31	3.96	4.33	5.47	5.27	5.41	5.40
	Median	3.81	5.31	3.83	4.19	5.45	5.18	5.07	5.24
	Max	5.85	5.78	5.11	5.85	7.30	5.97	7.27	7.30
TP (mg/L)	N	17	14	31	62	20	11	22	53
	Mean	0.21	0.31	0.20	0.22	0.45	0.28	0.39	0.39
	Geo. Mean	0.20	0.30	0.19	0.21	0.42	0.27	0.35	0.36
	Median	0.22	0.31	0.17	0.23	0.43	0.26	0.36	0.35
	Max	0.28	0.39	0.33	0.39	0.81	0.41	0.79	0.81
TKN (mg/L)	N	17	14	31	62	19	11	22	52
	Mean	1.29	1.73	1.16	1.32	1.97	1.47	1.39	1.62
	Geo. Mean	1.23	1.72	1.13	1.27	1.90	1.46	1.31	1.53
	Median	1.33	1.74	1.08	1.37	2.01	1.51	1.20	1.56
	Max	1.85	2.21	1.72	2.21	3.23	1.79	2.58	3.23
TSS (mg/L)	N	13	12	31	56	20	11	22	53
	Mean	30.08	58.73	24.39	33.07	107.42	62.56	98.44	94.38
	Geo. Mean	25.79	57.59	19.33	26.11	73.76	59.97	82.78	74.13
	Median	30.40	60.25	19.04	31.00	97.67	53.61	80.50	71.07
	Max	54.00	77.60	61.00	77.60	218.67	94.12	204.33	218.67
Atrazine (µg/L)	N	17	14	31	62	20	11	22	53
	Mean	4.73	9.74	4.15	5.57	10.31	9.60	4.85	7.89
	Geo. Mean	2.60	9.25	3.62	4.09	6.89	9.35	4.51	6.16
	Median	2.70	9.53	3.50	4.50	7.80	8.55	5.10	5.70
	Max	11.60	14.74	8.90	14.74	23.50	14.80	8.10	23.50
2-MIB (ng/L)	N	17	14	31	62	20	11	21	52
	Mean	3.01	3.45	8.34	5.78	12.52	5.75	3.15	7.30
	Geo. Mean	2.25	2.65	6.25	3.89	8.25	3.60	2.99	4.59
	Median	1.25	2.61	8.82	4.58	6.53	4.02	3.38	4.03
	Max	7.70	7.85	19.60	19.60	57.18	28.19	4.54	57.18
Geosmin (ng/L)	N	17	14	31	62	20	11	21	52
	Mean	18.76	10.65	6.59	10.84	5.50	3.91	4.40	4.72
	Geo. Mean	18.21	10.14	6.47	9.51	5.34	3.85	4.21	4.53
	Median	20.19	9.53	6.30	8.13	5.40	3.77	4.32	4.56
	Max	24.91	16.91	9.63	24.91	10.56	6.00	5.78	10.56

Table 9 (cont.): Mean, geometric mean, median and maximum concentration values for ion, nutrient, and contaminant concentration values.

		Storm 1	Storm 2	Total
Mg²⁺	N	6	5	11
	Min	0.00	0.00	0.00
	Max	0.78	0.67	0.78
	(%) Mean	0.37	0.24	0.31
	Median	0.35	0.27	0.27
Na⁺	N	6	5	11
	Min	0.00	0.00	0.00
	Max	1.52	0.46	1.52
	(%) Mean	0.58	0.09	0.36
	Median	0.46	0.00	0.29
SO₄⁻	N	4	5	9
	Min	0.00	0.00	0.00
	Max	3.76	23.56	23.56
	(%) Mean	1.14	4.80	3.17
	Median	0.41	0.00	0.30
Cl⁻	N	5	5	10
	Min	0.18	0.00	0.00
	Max	4.79	0.66	4.79
	(%) Mean	1.35	0.25	0.80
	Median	0.48	0.00	0.40
K⁺	N	6	5	11
	Min	0.34	0.15	0.15
	Max	1.01	1.01	1.01
	(%) Mean	0.55	0.54	0.54
	Median	0.46	0.42	0.42

Table 10: Minimum, maximum, mean, and median error percentages for ion, nutrient, and contaminant concentrations as determined from duplicate samples.

		Storm 1	Storm 2	Total
NO₃⁻	N	4	5	9
	Min	0.35	0.00	0.00
	Max	5.48	0.62	5.48
	(%) Mean	1.82	0.25	0.95
	Median	0.72	0.19	0.35
DOC	N	3	3	6
	Min	1.72	0.91	0.91
	Max	5.55	5.22	5.55
	(%) Mean	3.10	2.59	2.84
	Median	2.03	1.64	1.87
TP	N	6	5	11
	Min	0.00	0.00	0.00
	Max	13.04	29.77	29.77
	(%) Mean	5.35	7.67	6.41
	Median	4.64	2.70	2.70
TKN	N	6	5	11
	Min	0.68	0.00	0.00
	Max	4.89	7.53	7.53
	(%) Mean	2.93	3.75	3.31
	Median	3.17	4.55	3.42
TSS	N	3	5	8
	Min	2.00	0.47	0.47
	Max	27.78	1.69	27.78
	(%) Mean	17.33	0.91	7.07
	Median	22.22	0.60	1.46
Atrazine	N	6	5	11
	Min	0.53	1.75	0.53
	Max	22.67	18.30	22.67
	(%) Mean	9.21	7.65	8.50
	Median	7.33	6.25	6.67
2-MIB	N	3	4	7
	Min	2.02	0.77	0.77
	Max	47.61	2.94	47.61
	(%) Mean	28.45	1.95	13.31
	Median	35.73	2.04	2.47
Geosmin	N	5	5	10
	Min	0.36	0.87	0.36
	Max	11.14	6.89	11.14
	(%) Mean	4.73	3.56	4.14
	Median	2.39	4.25	3.32

Table 10 (cont.): Minimum, maximum, mean, and median error percentages for ion, nutrient, and contaminant concentrations as determined from duplicate samples.

		Storm 1				Storm 2			
		Event 1-1	Event 1-2	Event 1-3	Total	Event 2-1	Event 2-2	Event 2-3	Total
Mg²⁺	Total Load (kg)	4.266 x 10 ⁵	6.252 x 10 ⁵	1.478 x 10 ⁶	2.530 x 10⁶	7.306 x 10 ⁵	4.985 x 10 ⁵	1.485 x 10 ⁶	2.714 x 10⁶
	Yield (kg/ha)	1.449	2.123	5.018	8.589	2.481	1.693	5.044	9.217
	Rate (kg/ha/hr)	0.017	0.032	0.017	0.019	0.024	0.091	0.024	0.025
Na⁺	Total Load (kg)	4.194 x 10 ⁵	4.148 x 10 ⁵	1.124 x 10 ⁶	1.958 x 10⁶	5.523 x 10 ⁵	3.288 x 10 ⁵	9.884 x 10 ⁵	1.870 x 10⁶
	Yield (kg/ha)	1.424	1.408	3.816	6.649	1.875	1.117	3.356	6.348
	Rate (kg/ha/hr)	0.017	0.021	0.013	0.015	0.018	0.061	0.016	0.017
SO₄⁻	Total Load (kg)	7.976 x 10 ⁵	8.370 x 10 ⁵	2.395 x 10 ⁶	4.209 x 10⁶	1.112 x 10 ⁶	6.542 x 10 ⁵	2.022 x 10 ⁶	3.788 x 10⁶
	Yield (kg/ha)	2.709	2.842	8.132	13.682	3.776	2.221	6.865	12.862
	Rate (kg/ha/hr)	0.032	0.043	0.027	0.030	0.037	0.124	0.033	0.035
Cl⁻	Total Load (kg)	6.392 x 10 ⁵	8.192 x 10 ⁵	1.858 x 10 ⁶	3.317 x 10⁶	9.482 x 10 ⁵	6.125 x 10 ⁵	1.792 x 10 ⁶	3.353 x 10⁶
	Yield (kg/ha)	2.170	2.782	6.310	11.262	3.220	2.080	6.084	11.384
	Rate (kg/ha/hr)	0.026	0.042	0.021	0.025	0.031	0.110	0.029	0.031
K⁺	Total Load (kg)	4.988 x 10 ⁴	9.586 x 10 ⁴	1.704 x 10 ⁵	3.162 x 10⁵	1.975 x 10 ⁵	8.645 x 10 ⁴	2.853 x 10 ⁵	5.692 x 10⁵
	Yield (kg/ha)	0.169	0.326	0.579	1.074	0.670	0.294	0.969	1.933
	Rate (kg/ha/hr)	1.992 x 10 ⁻³	4.951 x 10 ⁻³	1.944 x 10 ⁻³	2.383 x 10⁻³	6.510 x 10 ⁻³	0.018	4.603 x 10 ⁻³	5.242 x 10⁻³

Table 11: Total loads, yields, and yield rates of all ions, nutrients, and contaminants transported during each storm/event.

		Storm 1				Storm 2			
		Event 1-1	Event 1-2	Event 1-3	Total	Event 2-1	Event 2-2	Event 2-3	Total
NO₃⁻	Total Load (kg)	8.092 x 10 ⁴	1.783 x 10 ⁵	3.691 x 10 ⁵	6.283 x 10⁵	2.331 x 10 ⁵	1.623 x 10 ⁵	3.851 x 10 ⁵	7.804 x 10⁵
	Yield (kg/ha)	0.275	0.605	1.253	2.133	0.791	0.551	1.308	2.650
	Rate (kg/ha/hr)	3.233 x 10 ⁻³	9.208 x 10 ⁻³	4.209 x 10 ⁻³	4.736 x 10⁻³	7.683 x 10 ⁻³	0.024	6.212 x 10 ⁻³	7.186 x 10⁻³
DOC	Total Load (kg)	8.441 x 10 ⁴	1.800 x 10 ⁵	2.816 x 10 ⁵	5.460 x 10⁵	2.990 x 10 ⁵	1.477 x 10 ⁵	4.915 x 10 ⁵	9.383 x 10⁵
	Yield (kg/ha)	0.287	0.611	0.956	1.854	1.015	0.502	1.669	3.186
	Rate (kg/ha/hr)	3.372 x 10 ⁻³	9.293 x 10 ⁻³	3.212 x 10 ⁻³	4.115 x 10⁻³	9.859 x 10 ⁻³	0.030	7.928 x 10 ⁻³	8.640 x 10⁻³
TP	Total Load (kg)	4.200 x 10 ³	1.057 x 10 ⁴	1.399 x 10 ⁴	2.876 x 10⁴	2.506 x 10 ⁴	7.832 x 10 ³	3.401 x 10 ⁴	6.690 x 10⁴
	Yield (kg/ha)	0.014	0.036	0.048	0.098	0.085	0.027	0.115	0.227
	Rate (kg/ha/hr)	1.678 x 10 ⁻⁴	5.460 x 10 ⁻⁴	1.595 x 10 ⁻⁴	2.168 x 10⁻⁴	8.262 x 10 ⁻⁴	2.090 x 10 ⁻³	5.486 x 10 ⁻⁴	6.161 x 10⁻⁴
TKN	Total Load (kg)	2.672 x 10 ⁴	5.914 x 10 ⁴	8.315 x 10 ⁴	1.690 x 10⁵	1.035 x 10 ⁵	4.182 x 10 ⁴	1.190 x 10 ⁵	2.643 x 10⁵
	Yield (kg/ha)	0.091	0.201	0.282	0.574	0.352	0.142	0.404	0.897
	Rate (kg/ha/hr)	1.068 x 10 ⁻³	3.054 x 10 ⁻³	9.482 x 10 ⁻⁴	1.274 x 10⁻³	3.143 x 10 ⁻³	7.311 x 10 ⁻³	1.919 x 10 ⁻³	2.434 x 10⁻³
TSS	Total Load (kg)	6.997 x 10 ⁵	2.044 x 10 ⁶	1.931 x 10 ⁶	4.675 x 10⁶	6.275 x 10 ⁶	1.775 x 10 ⁶	8.646 x 10 ⁶	1.670 x 10⁷
	Yield (kg/ha)	2.376	6.941	6.557	15.874	21.308	6.028	29.357	56.693
	Rate (kg/ha/hr)	0.028	0.106	0.022	0.035	0.207	0.531	0.140	0.154
Atrazine	Total Load (kg)	116.90	338.67	327.36	782.92	681.34	266.12	412.38	1359.84
	Yield (kg/ha)	3.969 x 10 ⁻⁴	1.150 x 10 ⁻³	1.112 x 10 ⁻³	2.658 x 10⁻³	2.314 x 10 ⁻³	9.036 x 10 ⁻⁴	1.400 x 10 ⁻³	4.617 x 10⁻³
	Rate (kg/ha/hr)	4.670 x 10 ⁻⁶	1.749 x 10 ⁻⁵	3.733 x 10 ⁻⁶	5.901 x 10⁻⁶	2.246 x 10 ⁻⁵	2.534 x 10 ⁻⁵	6.652 x 10 ⁻⁶	1.252 x 10⁻⁵
2-MIB	Total Load (kg)	0.060	0.114	0.547	0.721	0.533	0.142	0.261	0.936
	Yield (kg/ha)	2.030 x 10 ⁻⁷	3.878 x 10 ⁻⁷	1.858 x 10 ⁻⁶	2.449 x 10⁻⁶	1.809 x 10 ⁻⁶	4.833 x 10 ⁻⁷	8.854 x 10 ⁻⁷	3.178 x 10⁻⁶
	Rate (kg/ha/hr)	2.389 x 10 ⁻⁹	5.898 x 10 ⁻⁹	6.241 x 10 ⁻⁹	5.436 x 10⁻⁹	1.757 x 10 ⁻⁸	1.603 x 10 ⁻⁸	4.206 x 10 ⁻⁹	8.619 x 10⁻⁹
Geosmin	Total Load (kg)	0.333	0.350	0.430	1.113	0.285	0.110	0.366	0.760
	Yield (kg/ha)	1.131 x 10 ⁻⁶	1.190 x 10 ⁻⁶	1.459 x 10 ⁻⁶	3.779 x 10⁻⁶	9.665 x 10 ⁻⁷	3.719 x 10 ⁻⁷	1.243 x 10 ⁻⁶	2.582 x 10⁻⁶
	Rate (kg/ha/hr)	1.331 x 10 ⁻⁸	1.809 x 10 ⁻⁹	4.899 x 10 ⁻⁹	8.389 x 10⁻⁹	9.383 x 10 ⁻⁹	2.250 x 10 ⁻⁸	5.907 x 10 ⁻⁹	7.001 x 10⁻⁹

Table 11 (cont.): Total loads, yields, and yield rates of all ions, nutrients, and contaminants transported during each storm/event.

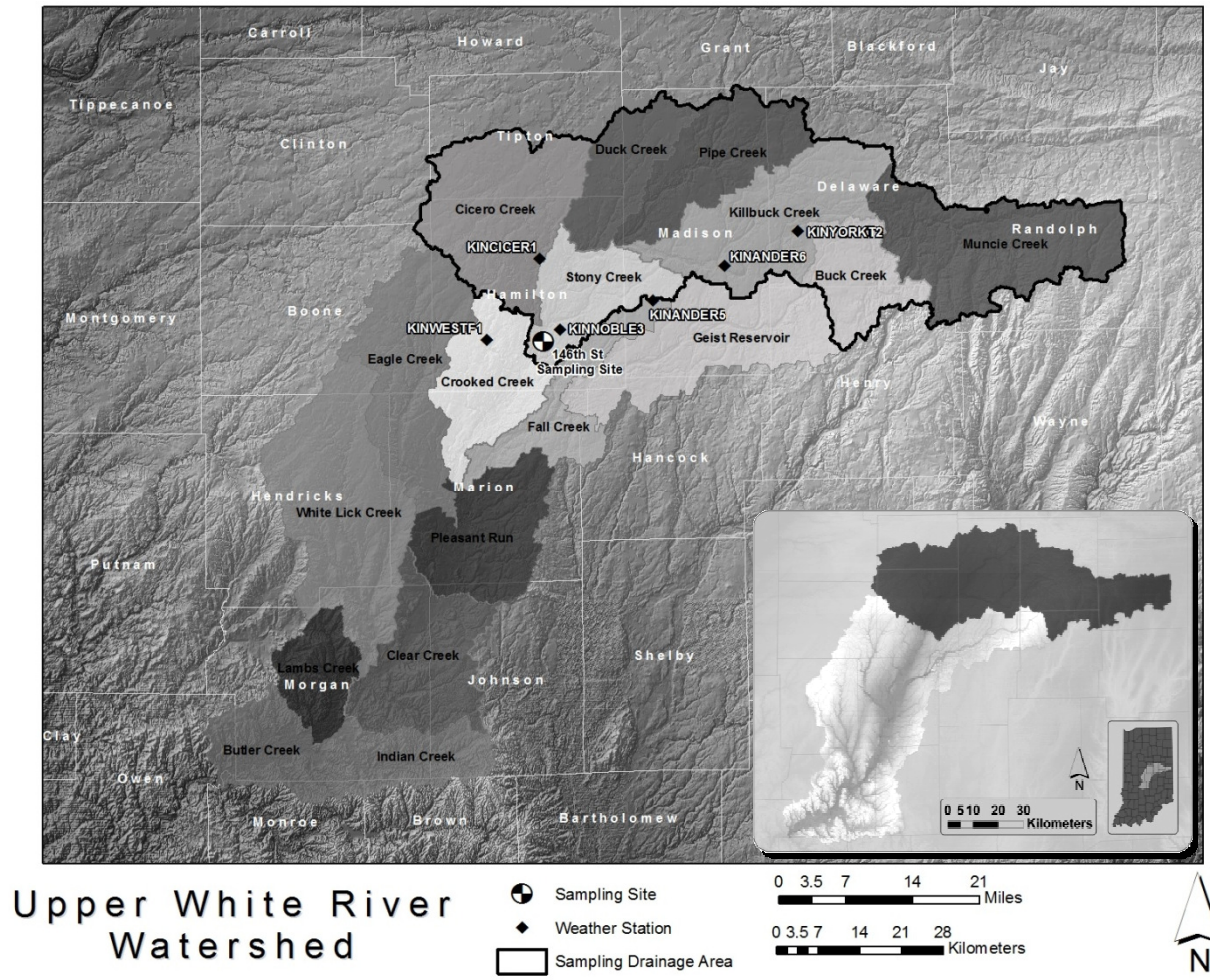


Figure 1: Map of the Upper White River Watershed (HUC8) and its 17 HUC10 tributaries, the six contributing NOAA weather stations, and the study site location, Central Indiana (upper left) and delineation of watershed area contributing to the study site located at 146th Street near Fishers, IN (03350800) (bottom right).

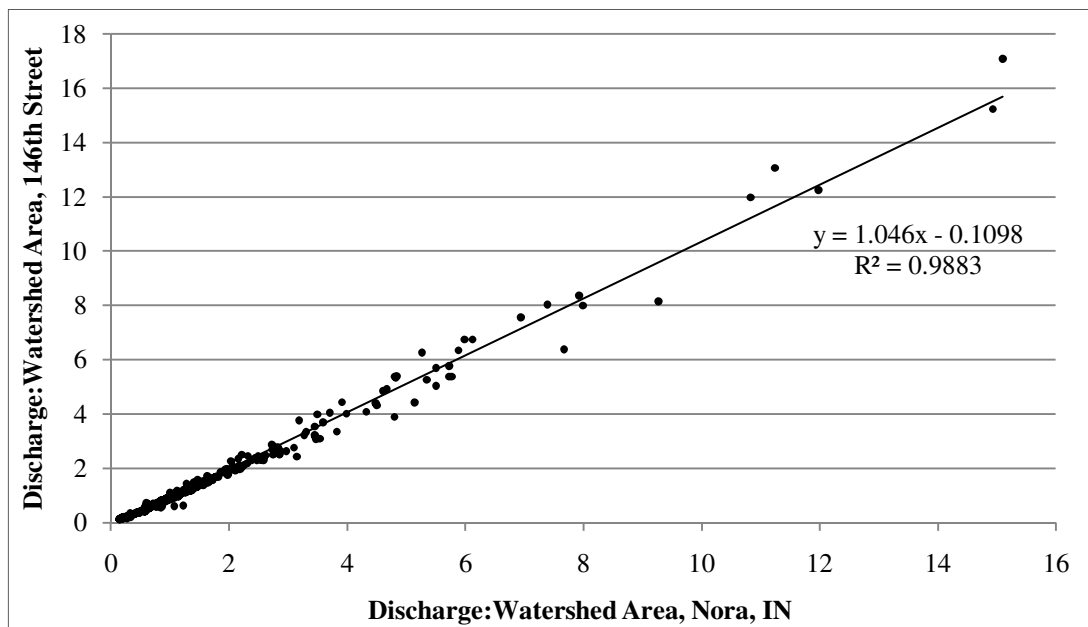


Figure 2: Linear regression analysis of discharge to contributing watershed area ratios for the USGS gaging stations located at Nora, IN (03351000) and 146th Street near Fishers, IN (03350800) between October 28, 2007 and October 27, 2008.

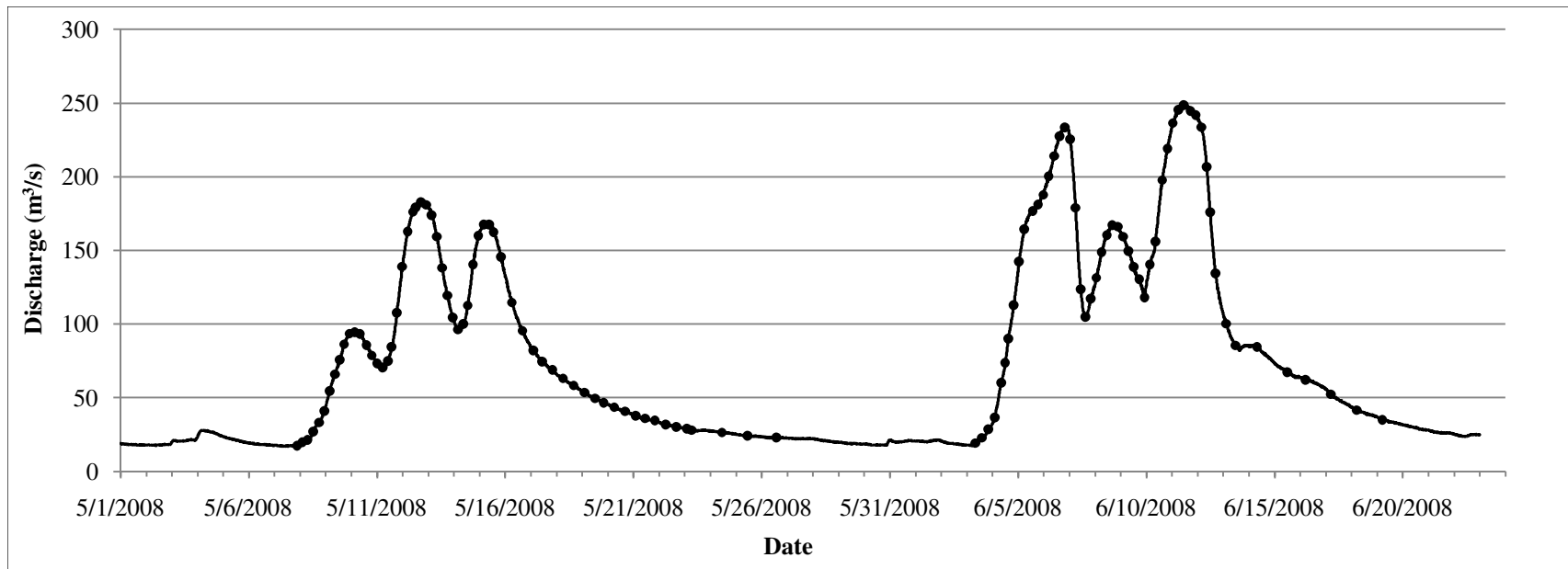


Figure 3: Hydrograph of study period overlain with all points at which samples were collected for Storms 1 (May 7 – May 26, 2008) and 2 (June 3 – June 19, 2008).

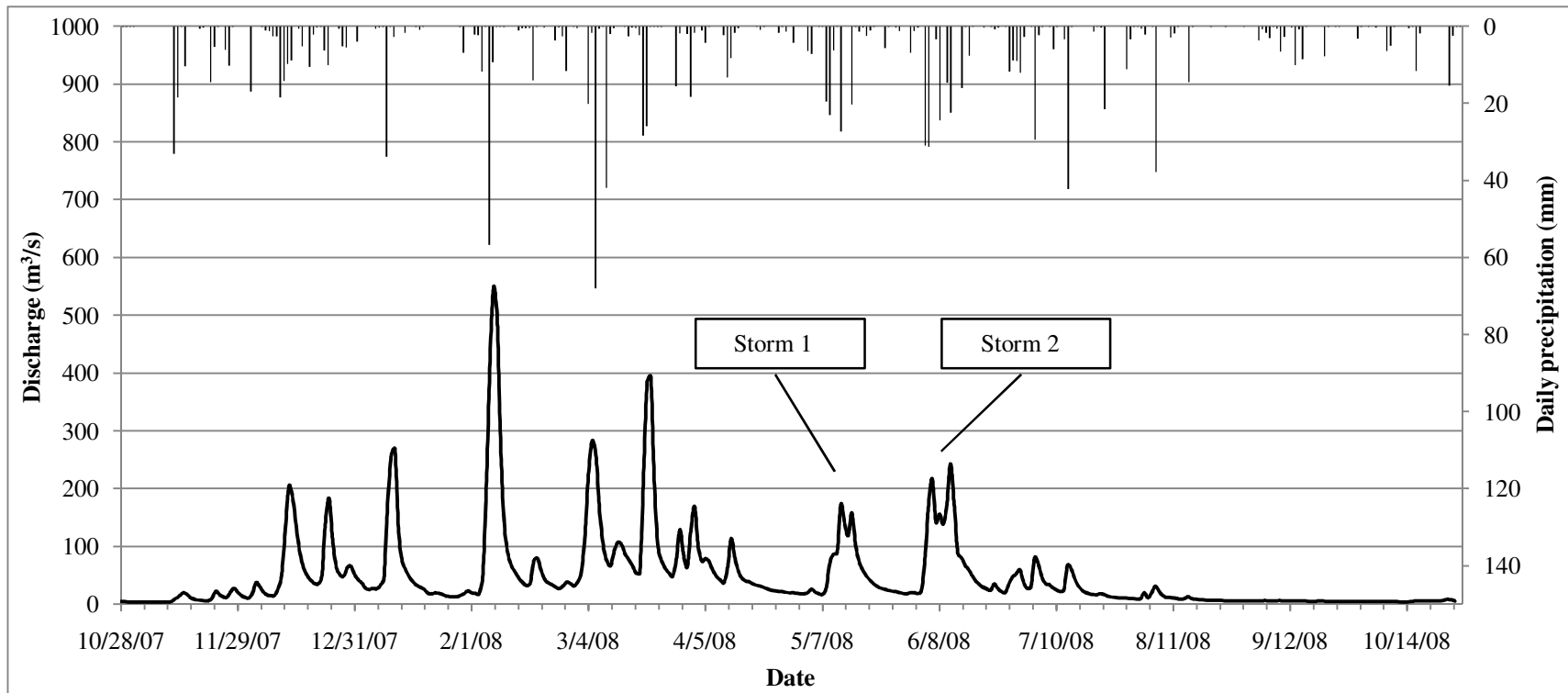


Figure 4: Hydrograph of average daily discharge (bottom) and daily contributing precipitation (top) at the study site located at 146th Street near Fishers, IN (03350800) between October 28, 2007 and October 27, 2008.

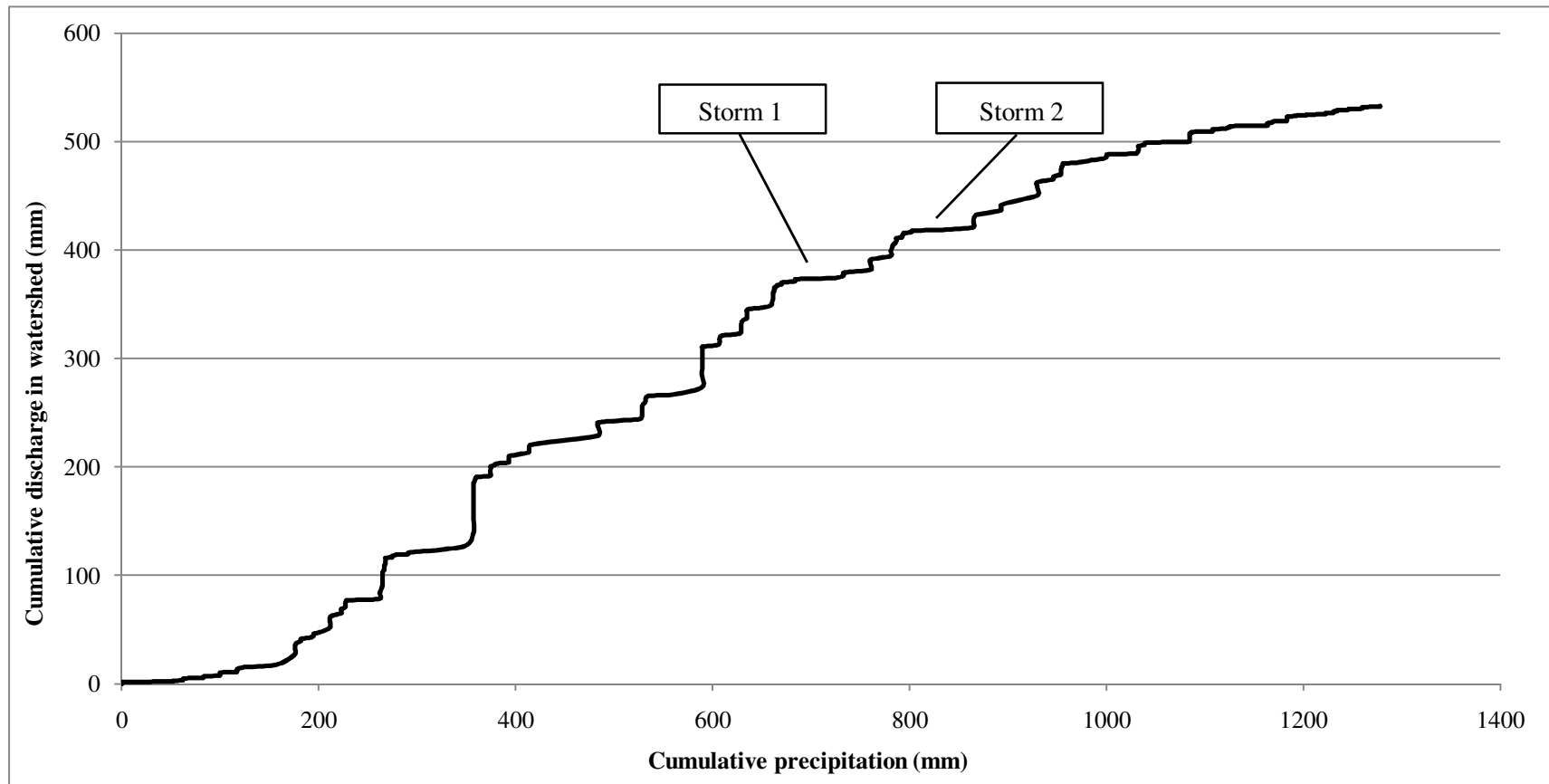


Figure 5: Double-mass curve based on cumulative watershed delivery of water to the Upper White River and cumulative precipitation collected by the Upper White River Watershed between October 28, 2008 and October 27, 2008.

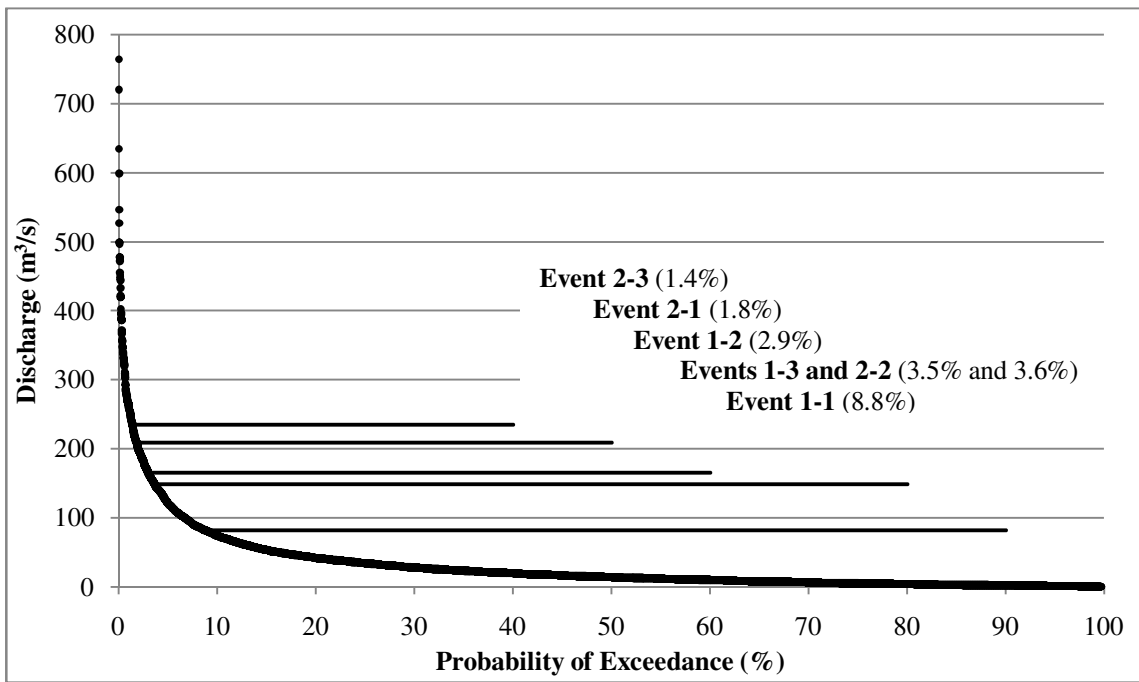
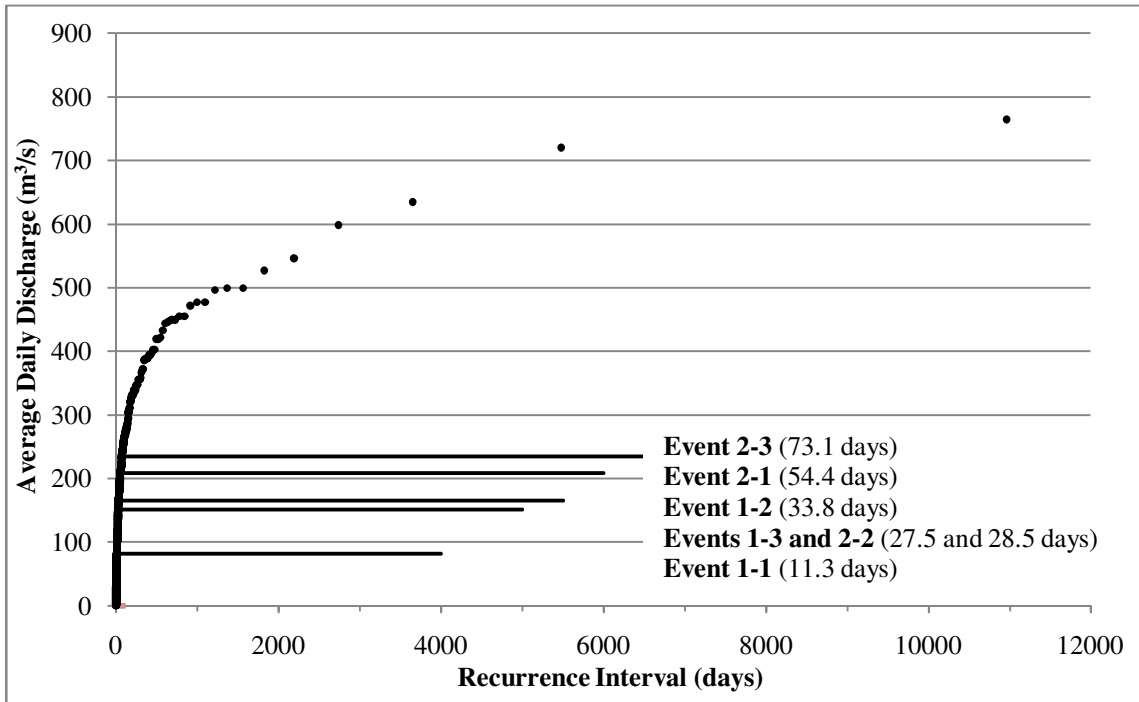


Figure 6: 30-year discharge recurrence interval (top) and exceedance probability curves (bottom) based on USGS average daily discharge values (between 1971-2000) at the 146th Street study site (03350800) as extrapolated from data collected at the Nora, IN station (03351000).

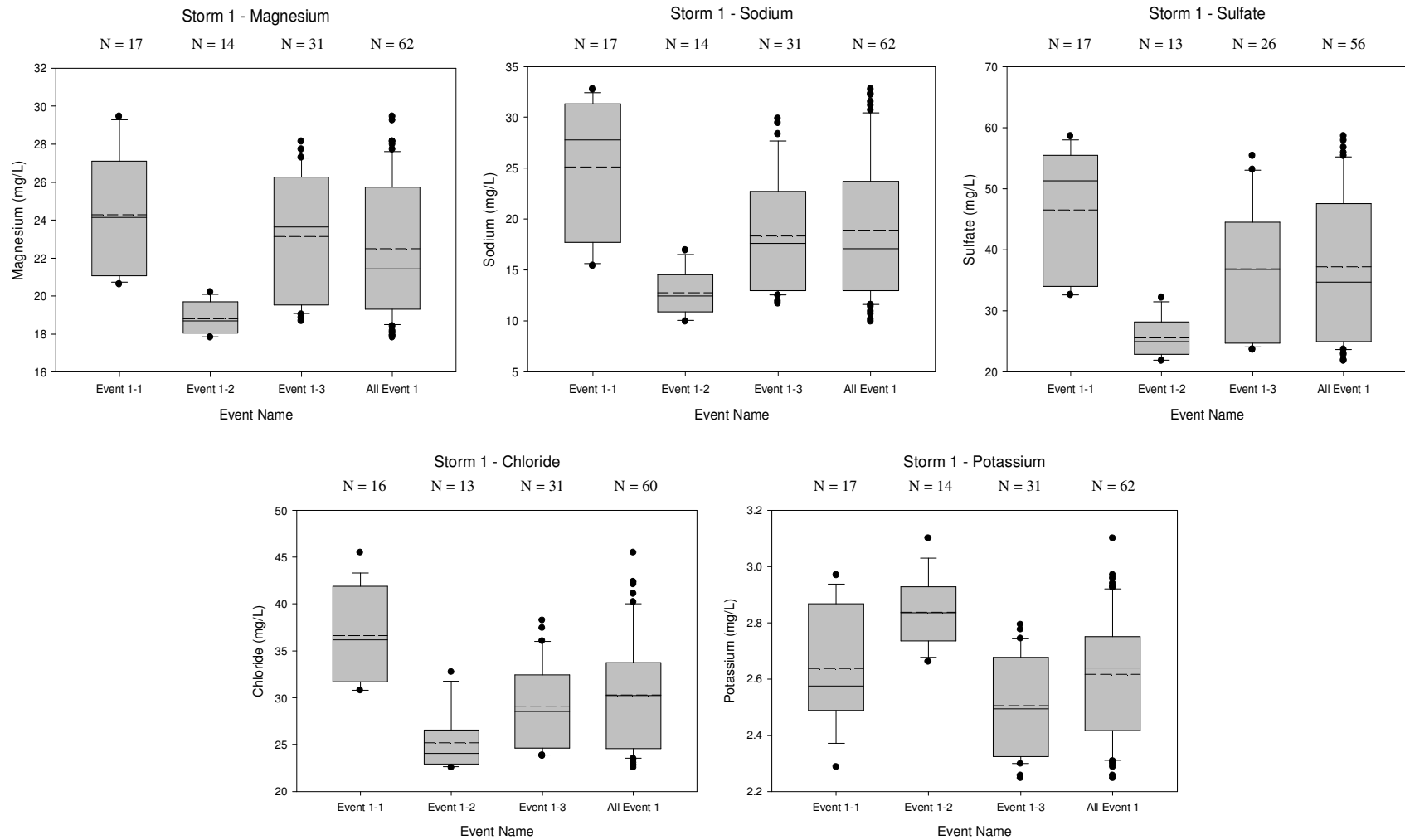


Figure 7: Box plots of ion concentrations for each storm/event. Mean and median concentrations are indicated by dashed and solid lines, 25th and 75th percentiles by the lower and upper box boundaries, 5th and 95th percentile by the extent of the lower and upper whiskers, and the outliers by dots, respectively.

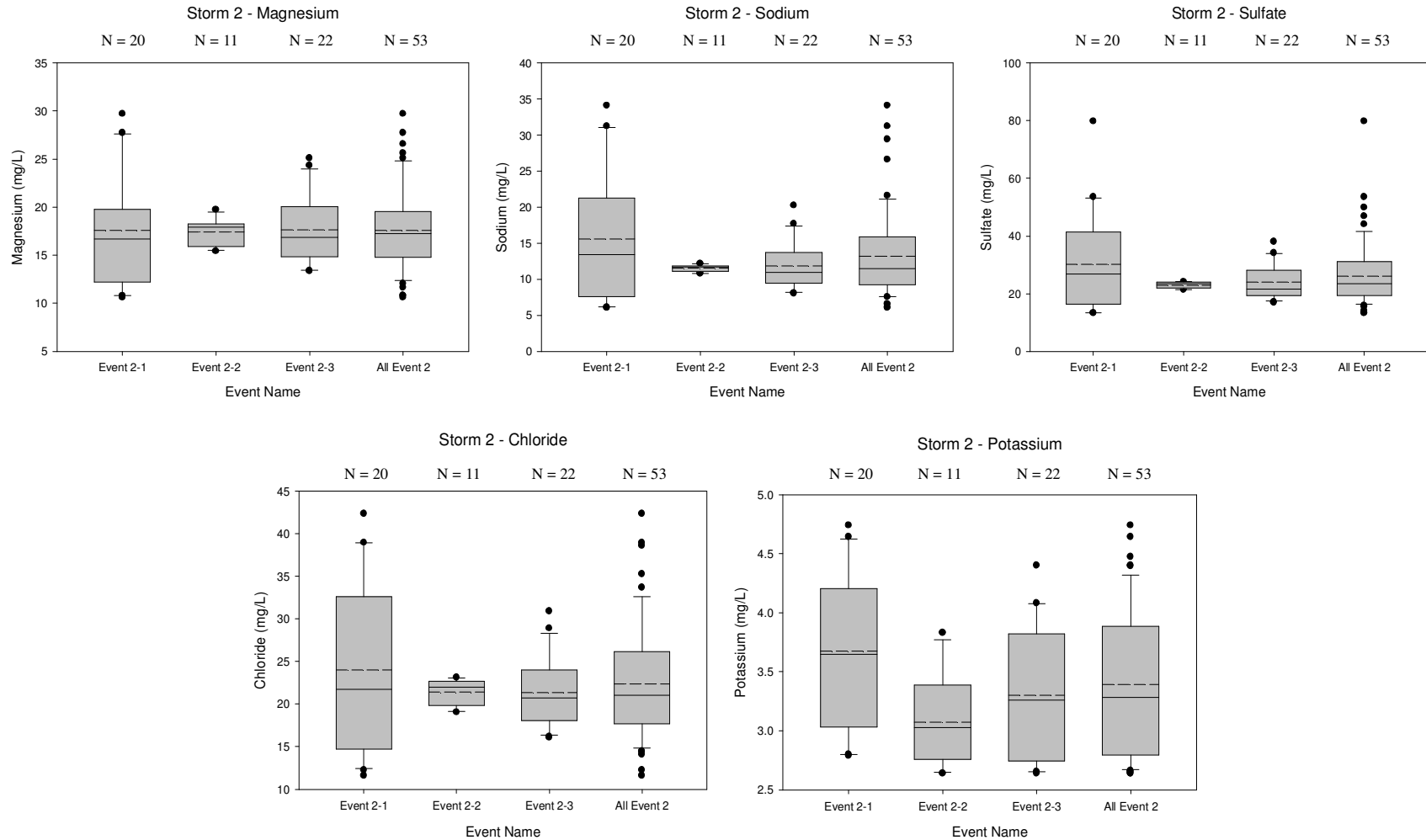


Figure 7 (cont.): Box plots of ion concentrations for each storm/event. Mean and median concentrations are indicated by dashed and solid lines, 25th and 75th percentiles by the lower and upper box boundaries, 5th and 95th percentile by the extent of the lower and upper whiskers, and the outliers by dots, respectively.

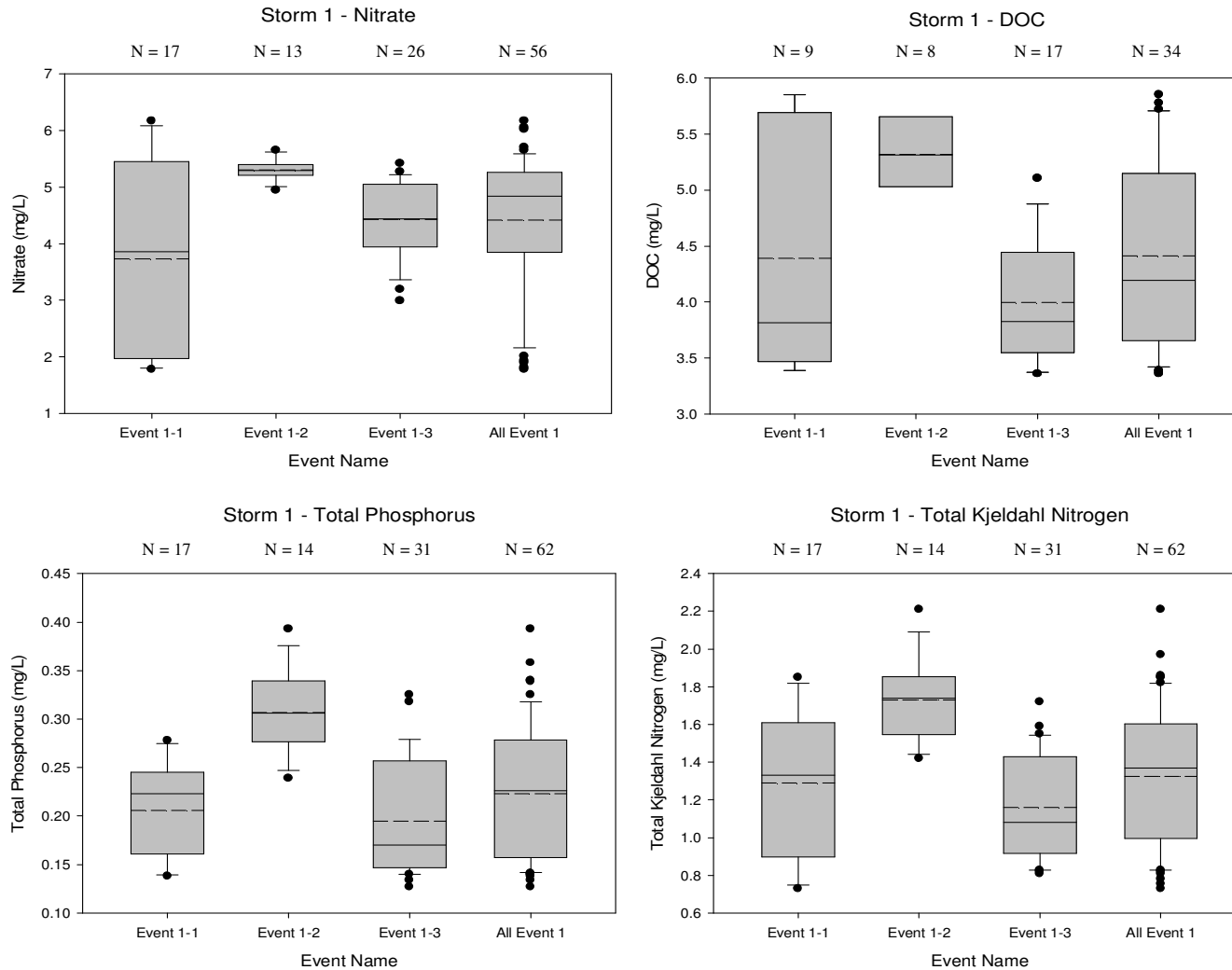


Figure 8: Box plots of nutrient concentrations for each storm/event. Mean and median concentrations are indicated by dashed and solid lines, 25th and 75th percentiles by the lower and upper box boundaries, 5th and 95th percentile by the extent of the lower and upper whiskers, and the outliers by dots, respectively.

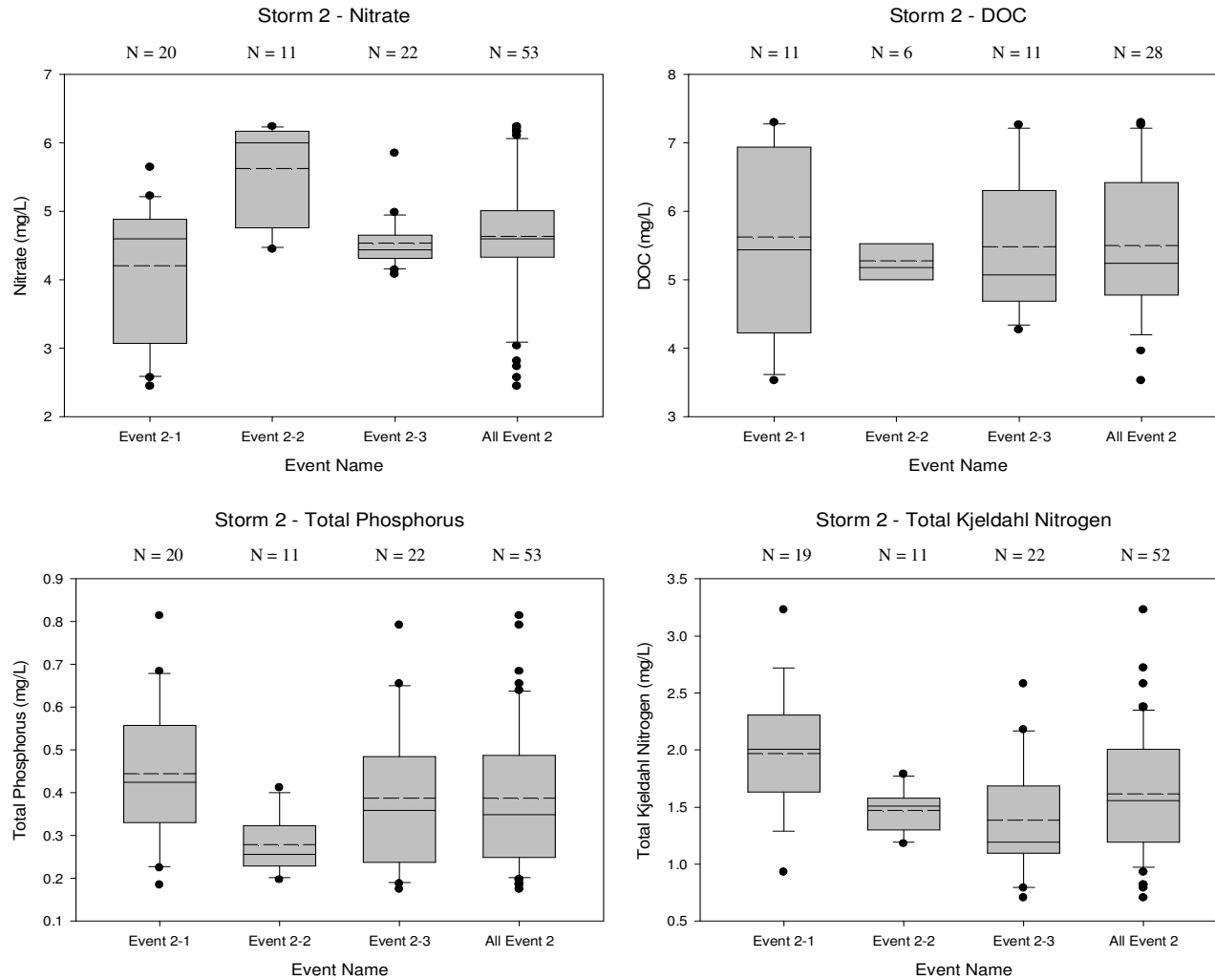


Figure 8 (cont.): Box plots of nutrient concentrations for each storm/event. Mean and median concentrations are indicated by dashed and solid lines, 25th and 75th percentiles by the lower and upper box boundaries, 5th and 95th percentile by the extent of the lower and upper whiskers, and the outliers by dots, respectively.

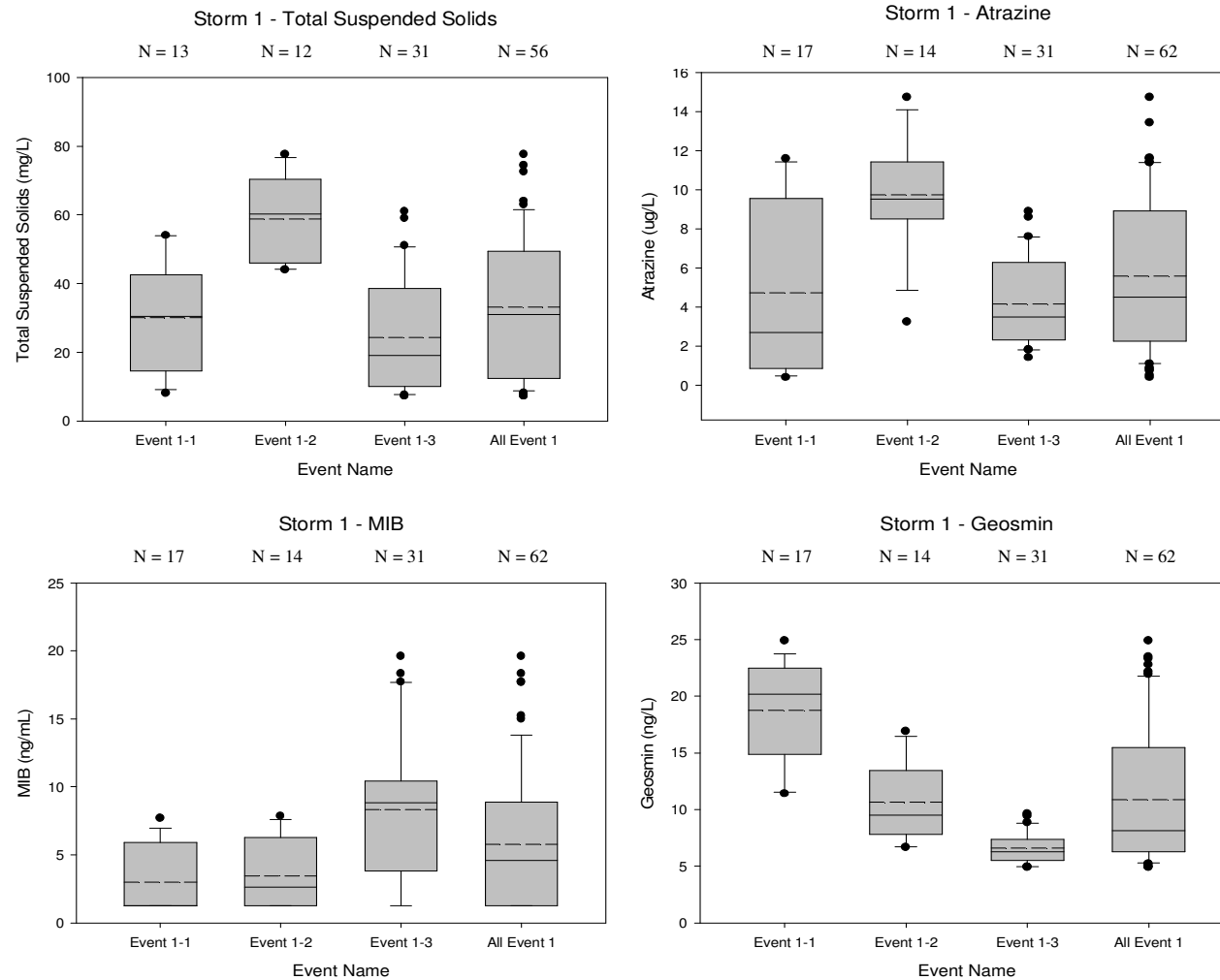


Figure 9: Box plots of contaminant concentrations for each storm/event. Mean and median concentrations are indicated by dashed and solid lines, 25th and 75th percentiles by the lower and upper box boundaries, 5th and 95th percentile by the extent of the lower and upper whiskers, and the outliers by dots, respectively.

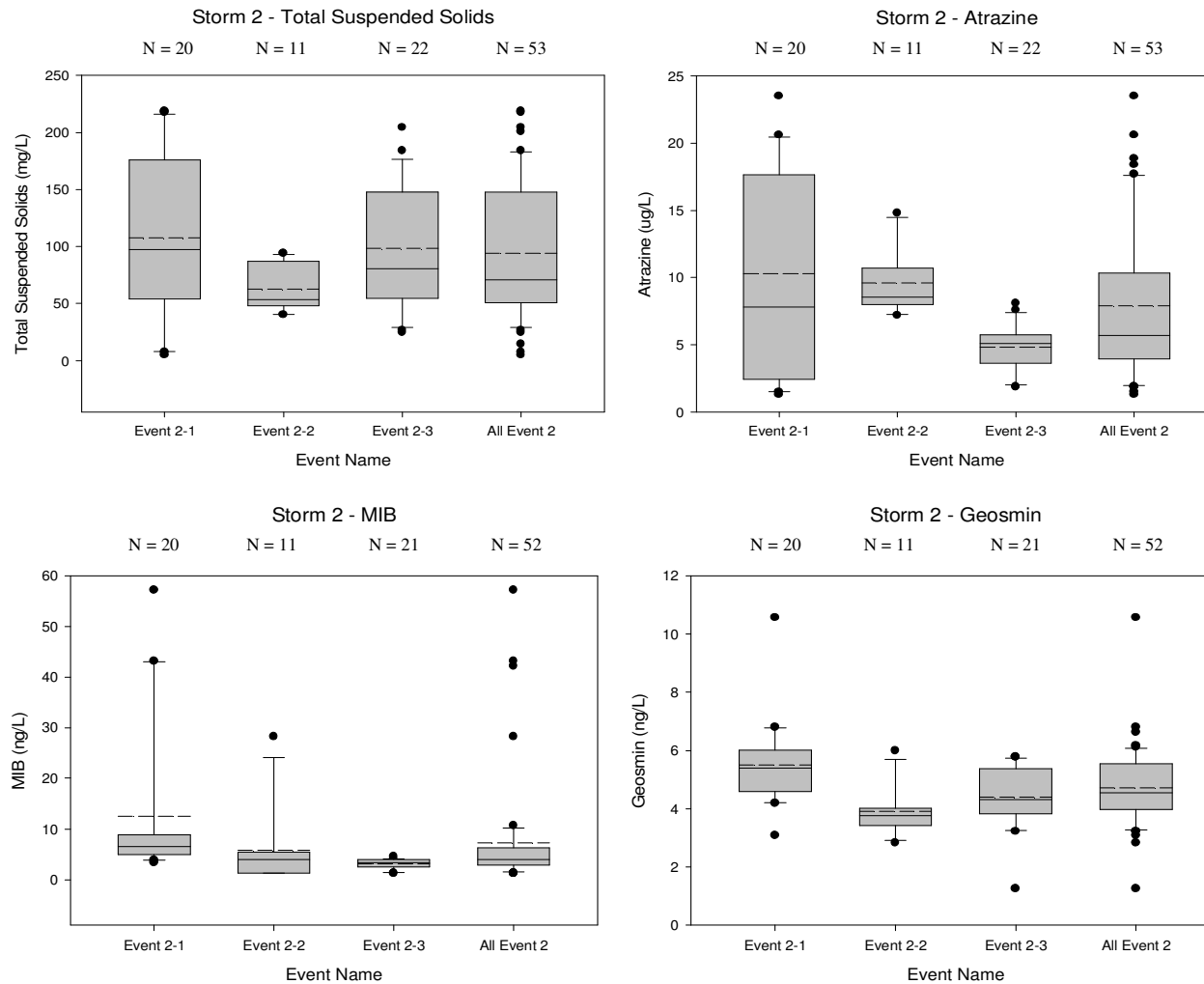


Figure 9 (cont.): Box plots of contaminant concentrations for each storm/event. Mean and median concentrations are indicated by dashed and solid lines, 25th and 75th percentiles by the lower and upper box boundaries, 5th and 95th percentile by the extent of the lower and upper whiskers, and the outliers by dots, respectively.

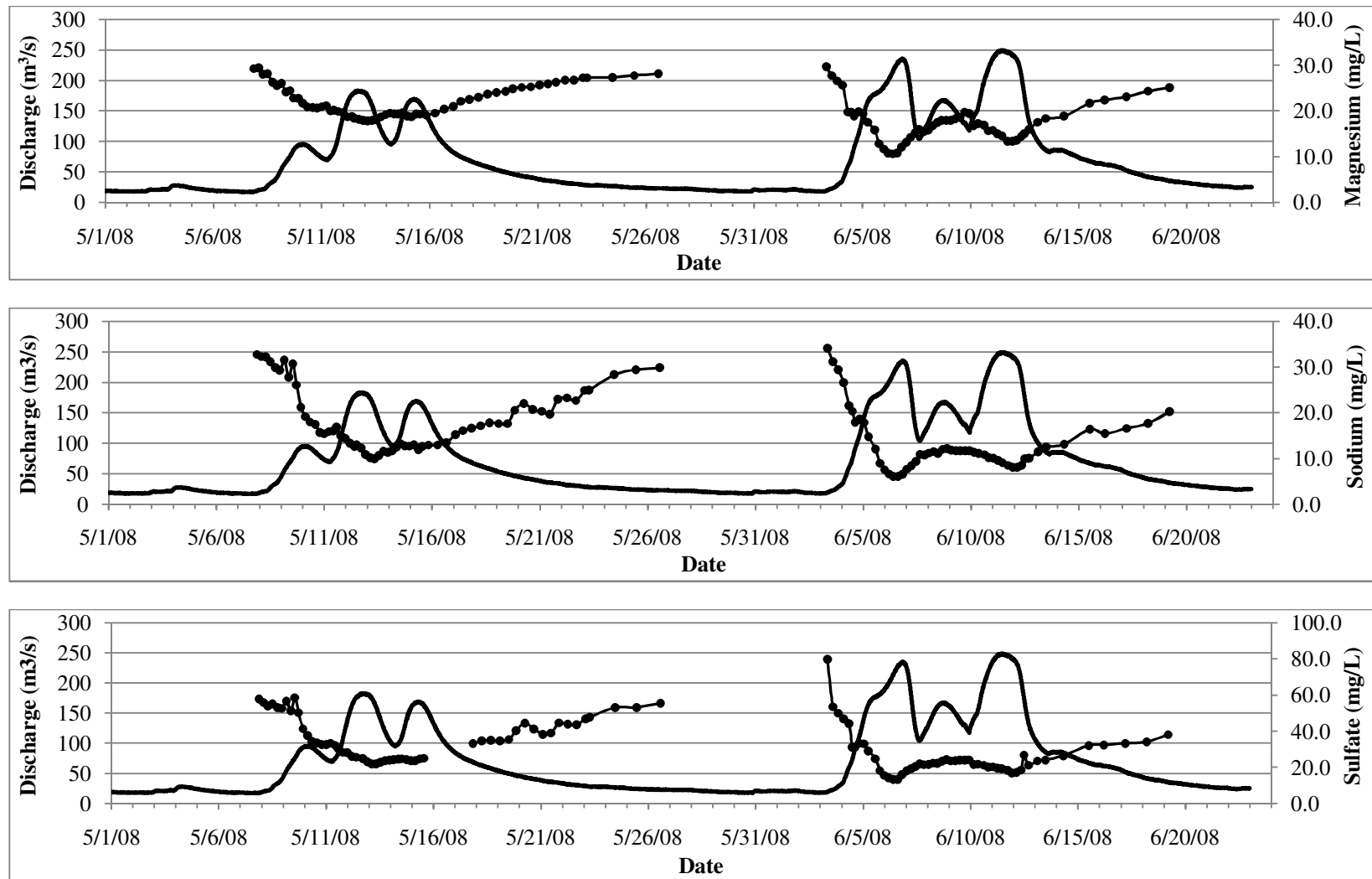


Figure 10: Ion concentration curves (Mg^{2+} , Na^+ , SO_4^- , Cl^- , K^+) plotted against discharge for Storm 1 (left) and Storm 2 (right).

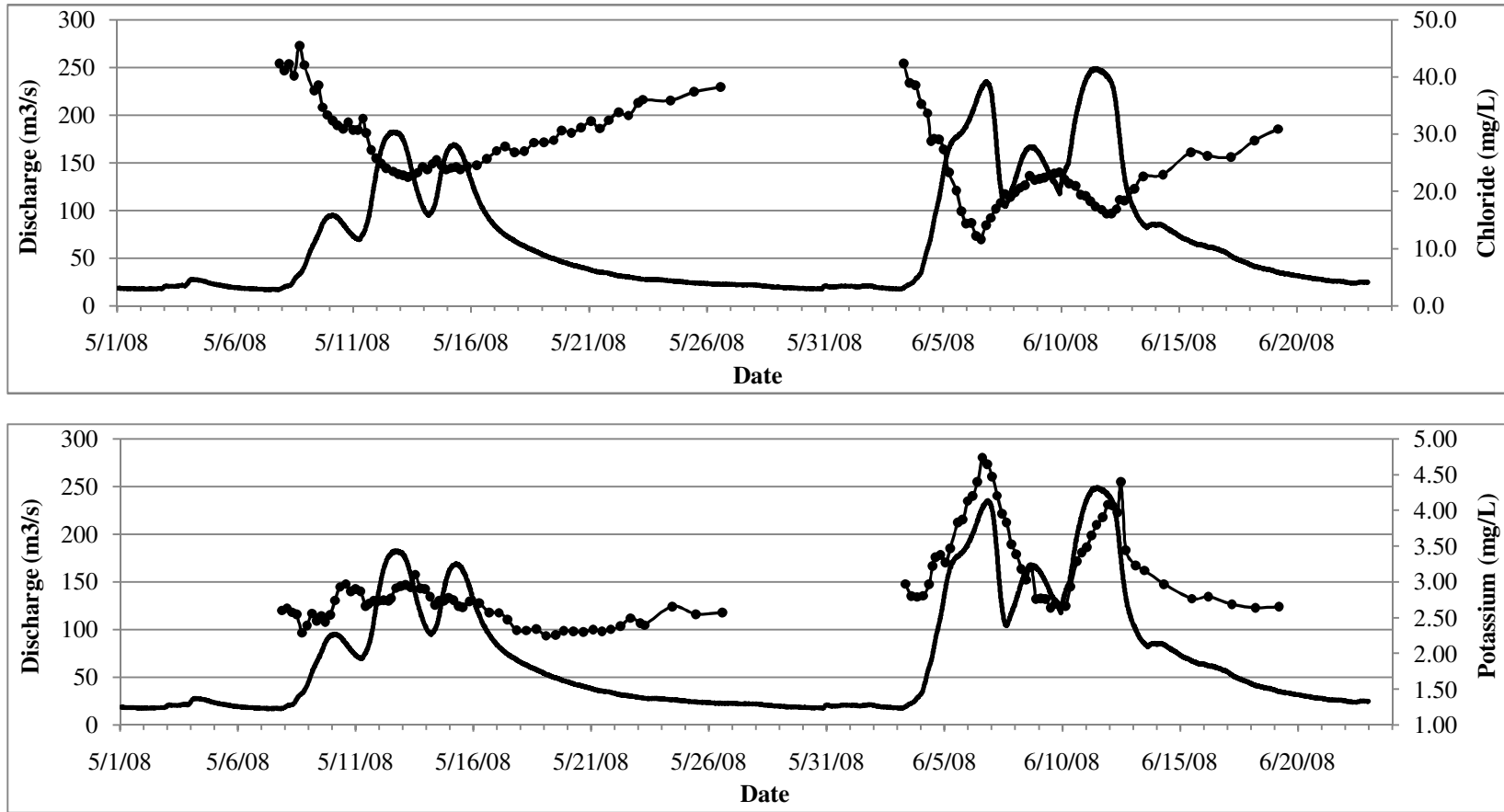


Figure 10 (cont.): Ion concentration curves (Mg^{2+} , Na^+ , SO_4^- , Cl^- , K^+) plotted against discharge for Storm 1 (left) and Storm 2 (right).

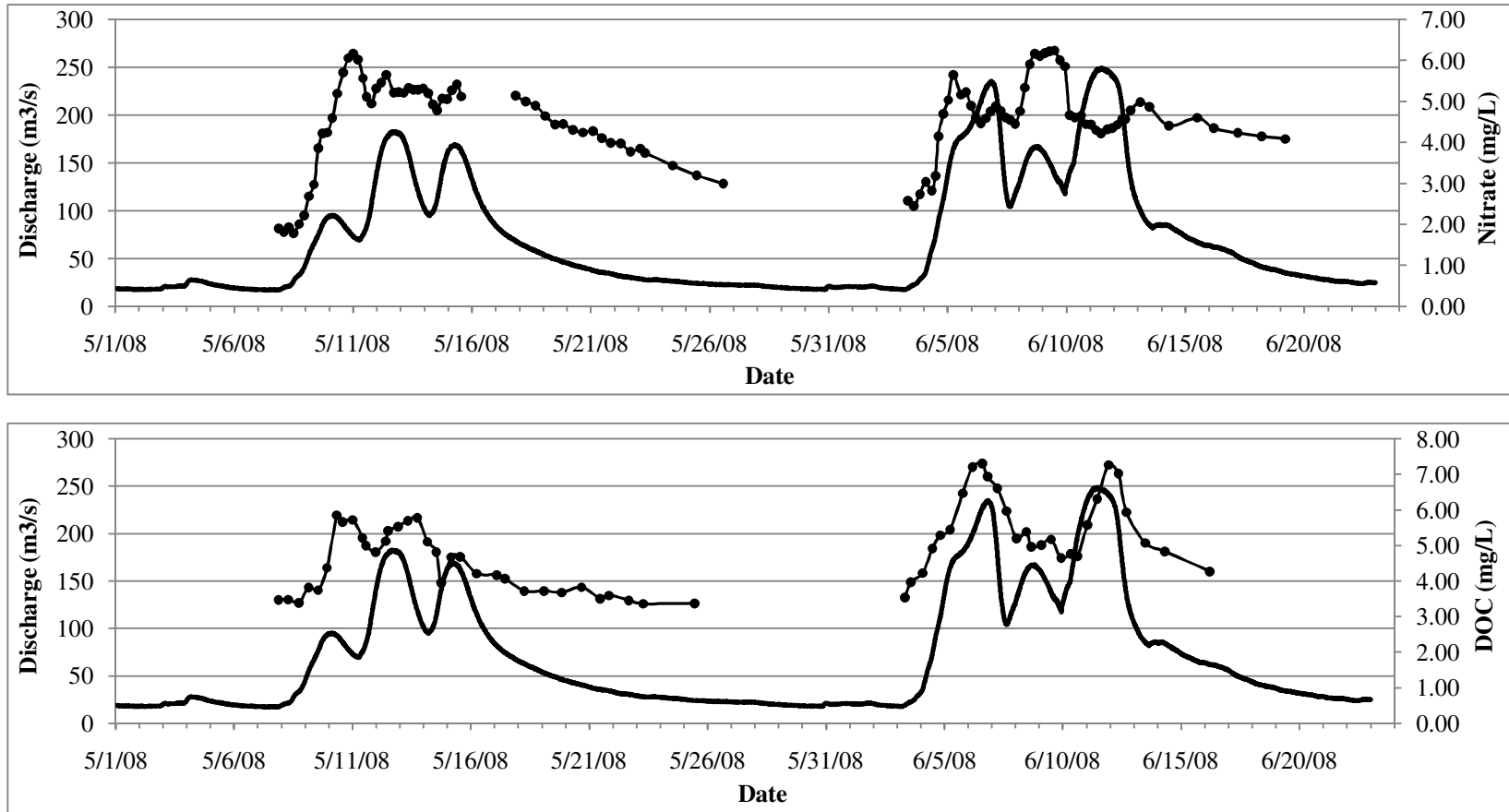


Figure 11: Nutrient concentration curves (nitrate, DOC, total phosphorus, TKN) plotted against discharge for Storm 1 (left) and Storm 2 (right).

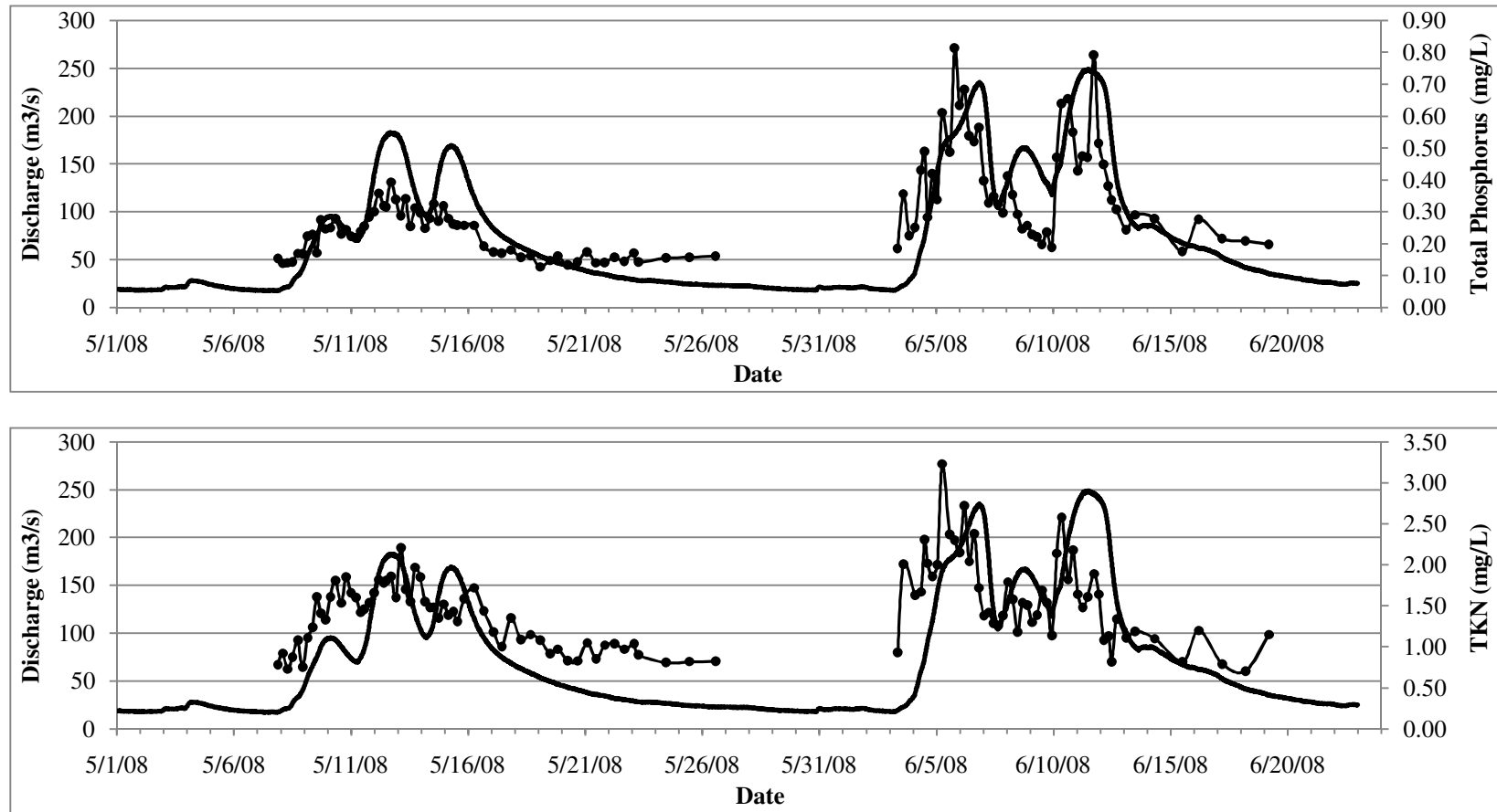


Figure 11 (cont.): Nutrient concentration curves (nitrate, DOC, total phosphorus, TKN) plotted against discharge for Storm 1 (left) and Storm 2 (right).

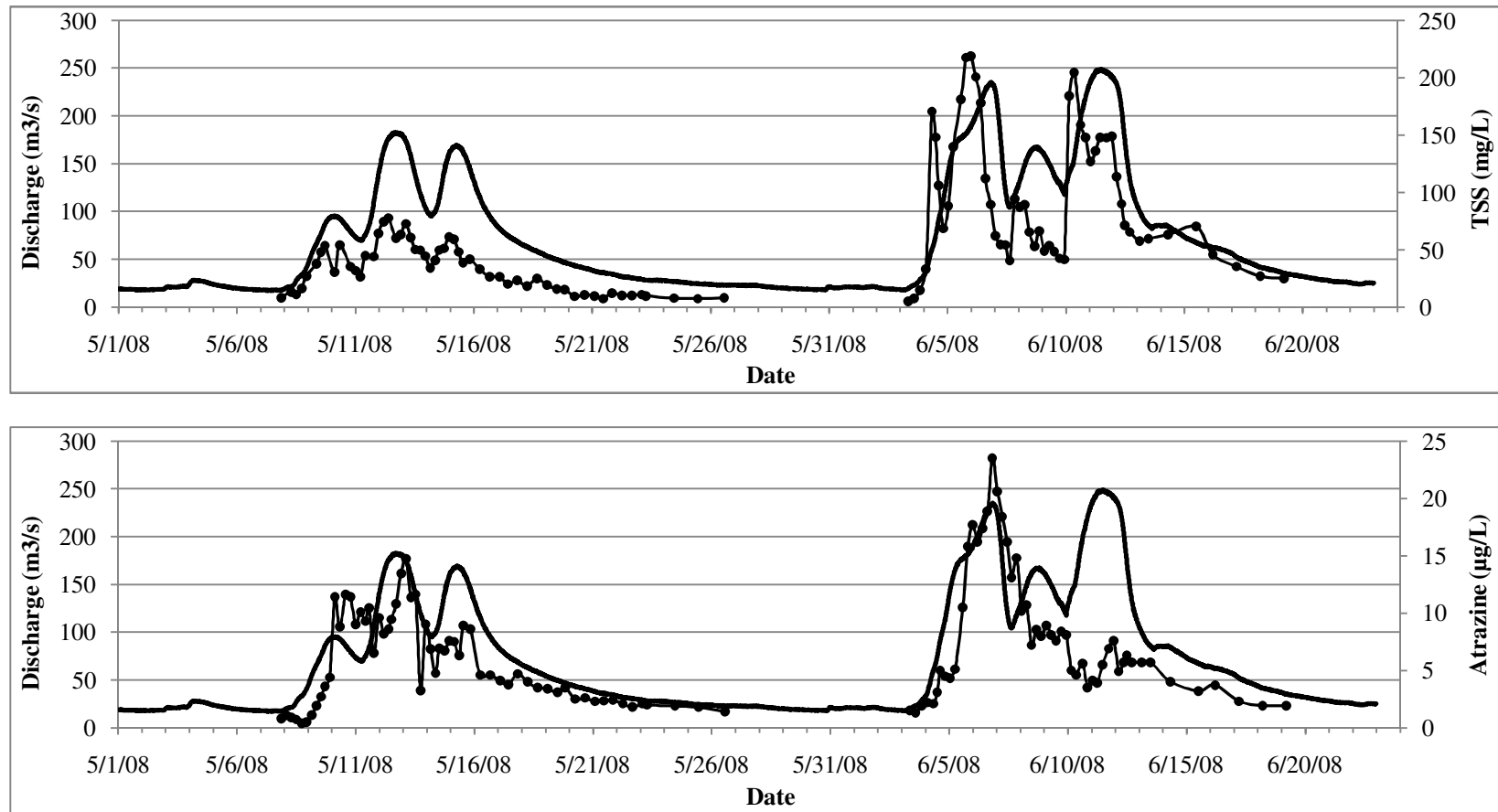


Figure 12: Contaminant concentration curves (TSS, atrazine, 2-MIB, geosmin) plotted against discharge for Storm 1 (left) and Storm 2 (right).

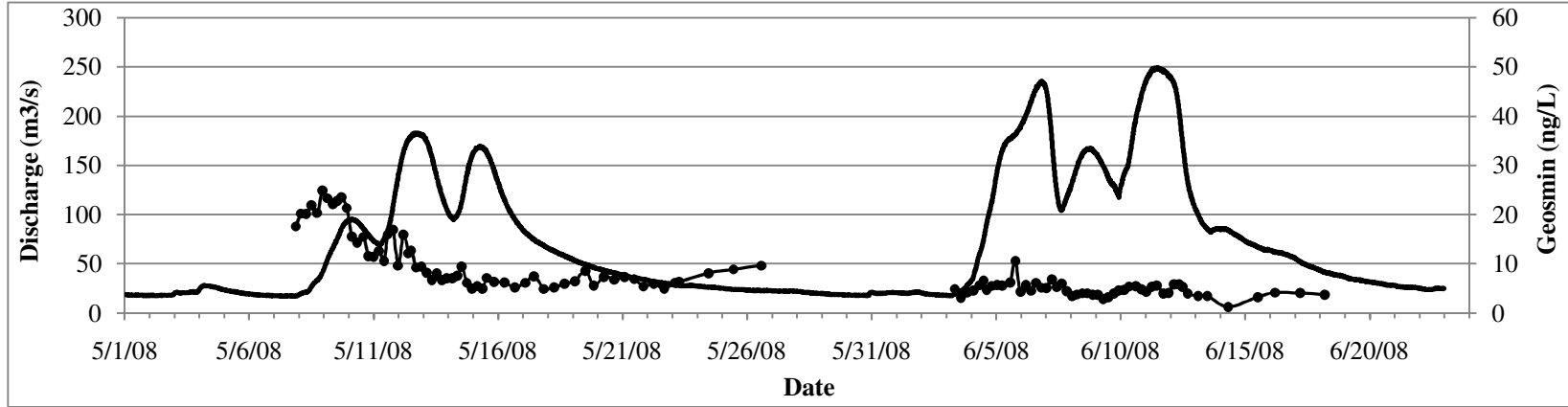
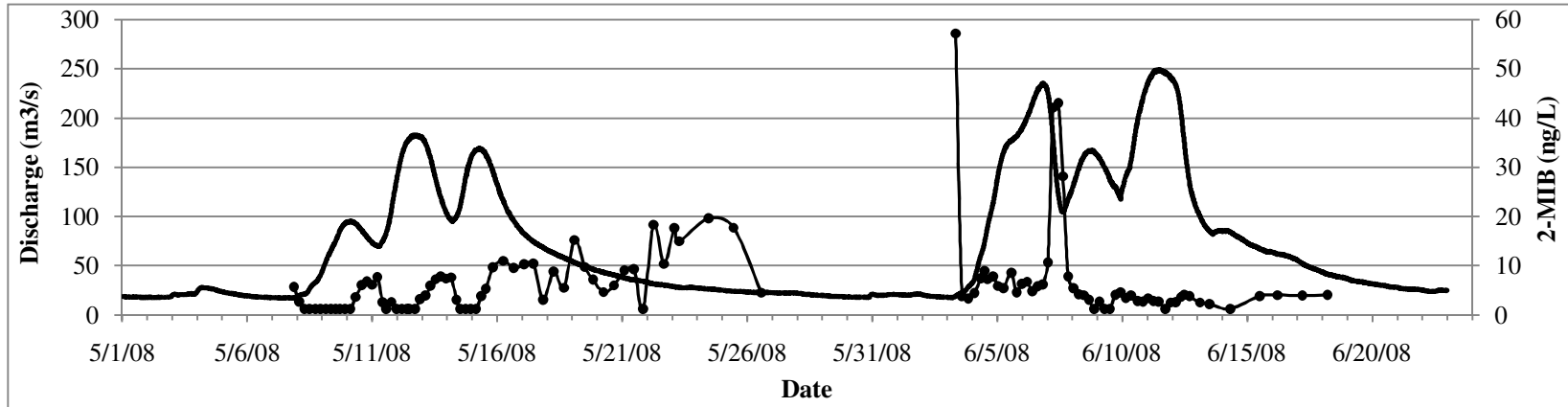


Figure 12 (cont.): Contaminant concentration curves (TSS, atrazine, 2-MIB, geosmin) plotted against discharge for Storm 1 (left) and Storm 2 (right).

References

- Alexander, B.R., Smith, R.A., Schwarz, G.E., Boyer, E.W., Nolan, J.V., and Brakebill, J.W., 2008. Differences in phosphorus and nitrogen delivery to the Gulf of Mexico from the Mississippi River Basin. *Environmental Science and Technology* 42(3):822-830.
- Bachman, L.J., Lindsey, B., Brakebill, J., and Powars, D.S., 1998. Ground-water discharge and base-flow nitrate loads of nontidal streams, and their relation to a hydrogeomorphic classification of the Chesapeake Bay Watershed, middle Atlantic coast. U.S. Geological Survey Water Investigations Report 98-4059, 71 pp.
- Baker, N.T., Stone, W.W., Wilson, J.T., and Meyer, M.T., 2006. Occurrence and transport of agricultural chemicals in Leary Weber Ditch Basin, Hancock County, Indiana, 2003-04. U.S. Geological Survey Scientific Investigations Report 2006-5251, 44 pp.
- Barr, R.C., Hall, B.E., Wilson, J.S., Souch, C., Lindsey, G., Bacone, J.A., Campbell, R.K., and Tedesco, L.P., 2002. Documenting changes in the natural environment of Indianapolis-Marion County between the time of European settlement (ca. 1820) and the present. *Ecological Restoration* 20:37-46.
- Beaulac, M.N. and Reckhow, K.H., 1982. An examination of land use – nutrient export relationships. *Water Resources Bulletin* 18(6):1013-1024.
- Bernhardt, E.S. and Palmer, M.A., 2007. Restoring streams in an urbanizing world. *Freshwater Biology* 52:738-751.
- Bonnell, M., 1993. Progress in the understanding of runoff generation dynamics in forests. *Journal of Hydrology* 150:217-275.
- Booth, D.B. and Jackson, R., 1997. Urbanization of aquatic systems: Degradation thresholds, stormwater detection, and the limits of mitigation. *Journal of the American Water Resources Association* 33(5):1077-1090.
- Brown, V.A., McDonnell, J.J., Burns, D.A., and Kendall, C., 1999. The role of event water, a rapid shallow flow component, and catchment size in summer stormflow. *Journal of Hydrology* 217:171-190.
- Burns, D.A., Hooper, R.P., McDonnell, J.J., Freer, J., Kendall, C., and Beven, K., 1998. Base cation concentrations in subsurface flow from a forested hillslope – the role of flushing frequency. *Water Resources Research* 34:3535-3544.

- Burns, D.A., McDonnell, J.J., Hooper, R.P., Peters, N.E., Freer, J.E., Kendall, C., and Beven, K., 2001. Quantifying contributions to storm runoff through end-member mixing analysis and hydrologic measurements at the Panola Mountain Research Watershed (Georgia, USA). *Hydrological Processes* 15:1903-1924.
- Burns, D., Vitvar, T., McDonnell, J., Hassett, J., Duncan, J., and Kendall, C., 2005. Effects of suburban development on runoff generation in the Croton River Basin, New York, USA. *Journal of Hydrology* 311:266-281.
- Buttery, R.G. and Garibaldi, J.A., 1976. Geosmin and methylisoborneol in garden soil. *Journal of Agricultural and Food Chemistry* 24:1246-1247.
- Butturini, A. and Sabater, F., 2002. Nitrogen concentrations in a small Mediterranean stream: 1. Nitrate 2. Ammonium. *Hydrology and Earth System Sciences* 6(3):539-550.
- Carpenter, S.R., Caraco, N.F., Correll, D.L., Howarth, R.W., Sharpley, A.N., and Smith, V.H., 1998. Nonpoint pollution of surface waters with phosphorus and nitrogen. *Ecological Applications* 8(3):559-568.
- Castillo, M.M., Allan, J.D., and Brunzell, S., 2000. Nutrient concentrations and discharges in a Midwestern agricultural catchment. *Journal of Environmental Quality* 29(4):1142-1151.
- Christopher, S.F., Mitchell, M.J., McHale, M.R., Boyer, E.W., Burns, D.A., and Kendall, C., 2008. Factors controlling nitrogen release from two forested catchments with contrasting hydrochemical responses. *Hydrological Processes* 22:46-62.
- Clark, G.D., ed., 1980. *The Indiana water resource—availability, uses, and needs: Indianapolis, Indiana Department of Natural Resources, 508 pp.*
- Cooke, J.G. and Cooper, A.B., 1988. Sources and sinks of nutrients in a New Zealand hill pasture catchment III. Nitrogen. *Hydrological Processes* 2:135-149.
- Cooke, S.E. and Prepas, E.E., 1998. Stream phosphorus and nitrogen export from agricultural and forested watersheds on the Boreal Plain. *Canadian Journal of Fisheries and Aquatic Sciences* 55:2292-2299.
- Coulter, C.B., Kolka, R.K., and Thompson, J.A., 2004. Water quality in agricultural, urban, and mixed land use watersheds. *Journal of the American Water Resources Association* 40(6):1593-1601.

- Craig, L.S., Palmer M.A., Richardson D.C., Filoso S., Bernhardt E.S., Bledsoe B.P., Doyle, M.W., Groffman P.M., Hassett B.A., Kaushal, S.S., Mayer P.M., Smith S.M., and Wilcock P.R., 2008. Stream restoration strategies for reducing river nitrogen loads. *Frontiers in Ecology and the Environment* 6(10):529-538.
- Creed, I.F. and Band, L.E., 1998. Export of nitrogen from catchments within a temperate forest: Evidence for a unifying mechanism regulated by variable source area dynamics. *Water Resources Research* 34(11):3105-3120.
- Dalzell, B.J., Filley, T.R., and Harbor, J.M., 2005. Flood pulse influences on terrestrial organic matter export from an agricultural watershed. *Journal of Geophysical Research* 110, G02011, doi:10.1029/2005JG000043
- Dalzell, B.J., Filley, T.R., and Harbor, J.M., 2007. The role of hydrology in annual organic carbon loads and terrestrial organic matter export from a Midwestern agricultural watershed. *Geochimica et Cosmochimica Acta* 71:1448-1462.
- David, M.B., Gentry, L.E., Kovacic, D.A., and Smith, K.M., 1997. Nitrogen balance in and export from an agricultural watershed. *Journal of Environmental Quality* 26:1038-1048.
- Devito, K.J., Fitzgerald, D., Hill, A.R., and Aravena, R., 2000. Nitrate dynamics in relation to lithology and hydrologic flow path in a river riparian zone. *Journal of Environmental Quality* 29:1075-1084.
- Dinnes, D.L., Karlen, D.L., Jaynes, D.B., Kaspar, T.C., Hatfield, J.L., Colvin, T.S., and Cambardella, C.A., 2002. Nitrogen management strategies to reduce nitrate leaching in tile-drained Midwestern soils. *Agronomy Journal* 94:153-171.
- Dosskey, M.G., Helmers, M.J., Eisenhaur, D.E., Franti, T.G., and Hoagland, K.D., 2002. Assessment of concentrated flow through riparian buffers. *Journal of Soil and Water Conservation* 57(6):336-343.
- Dunne, T.D. and Leopold, L.B., 1978. *Water in Environmental Planning*. W.H. Freeman and Company, New York. 818 pp.
- Environmental Protection Agency, 2008. Handbook for developing watershed plans to restore and protect our waters. EPA 841-B-08-002.
<http://epa.gov/nps/watershed_handbook>
- Fausey, N.R., Brown, L.C., Belcher, H.W., and Kanwar, R.S., 1995. Drainage and water quality in Great Lakes and Cornbelt states. *Journal of Irrigation and Drainage Engineering* 121:238-288.

- Franzmeier, D.P., Steinhardt, G.C., Sinclair Jr., H.R., and Hosteter, W.D., 1989. Taxonomic and environmental factor keys to the soils of Indiana: West Lafayette, Ind., Purdue University Cooperative Extension Service, 20 pp.
- Gächter, R., Ngatiah, J.M., and Stamm, C., 1998. Transport of phosphate from soil to surface waters by preferential flow. *Environmental Science Technology* 32:1865-1869.
- Gentry, L.E., David, M.B., Royer, T.V., Mitchell, C.A., and Starks, K.M., 2007. Phosphorus transport pathways to streams in tile-drained agricultural watersheds. *Journal of Environmental Quality* 36:408-415.
- Goolsby, D.A., Battaglin, W.A., Aulenbach, B.T., and Hooper, R.P., 2001. Nitrogen input to the Gulf of Mexico. *Journal of Environmental Quality* 30:329-336.
- Gray, H.H., 1989. Quaternary geologic map of Indiana: Bloomington, Ind., Indiana Geological Survey Miscellaneous Map 49, scale 1:500,000.
- Gray, H.H., Ault, C.H., and Keller, S.J., 1987. Bedrock geologic map of Indiana: Bloomington, Ind., Indiana Geological Survey, Miscellaneous Map 48, scale 1:500,000.
- Hancock, T.C., Sandstrom, M.W., Vogel, J.R., Webb, R.M.T., Bayless, E.R., and Barbash, J.E., 2008. Pesticide fate and transport throughout unsaturated zones in five agricultural settings, USA. *Journal of Environmental Quality* 37:1086-1100.
- Hill, A.R., 1993. Base cation chemistry of storm runoff in a forested headwater wetland. *Water Resources Research* 29(8):2663-2673.
- Hood, E., Gooseff, M.N., and Johnson, S.L., 2006. Changes in the character of stream water dissolved organic carbon during flushing in three small watersheds, Oregon. *Journal of Geophysical Research* 111, G01007, doi:10.1029/2005JG000082
- Hook, A.M. and Yeakley, J.A., 2005. Stormflow dynamics of dissolved organic carbon and total dissolved nitrogen in a small urban watershed. *Biogeochemistry* 75(3):409-431.
- Howarth, R.W., Boyer, E.W., Pabich, W.J., and Galloway, J.N., 2002. Nitrogen use in the United States from 1961 to 2000 and potential future trends. *Ambio* 31:88-96.
- Hyer, K.E., Hornberger, G.M., and Herman, J.S., 2001. Processes controlling the episodic streamwater transport of atrazine and other agrichemicals in an agricultural watershed. *Journal of Hydrology* 254:47-66.

- Inamdar, S.P., Christopher, S.F., and Mitchell, M.J., 2004. Export mechanisms for dissolved organic carbon and nitrate during summer storm events in a glaciated forested catchment in New York, USA. *Hydrological Processes*, 18:2651-2661.
- Inamdar, S.P. and Mitchell, M.J., 2006. Hydrologic and topographic controls on storm-event exports of dissolved organic carbon (DOC) and nitrate across catchment scales. *Water Resources Research* 42, W03421, doi:10.1029/2005WR004212
- Indiana State Climate Office, 2003. 1971-2000 precipitation normals for Indiana by climate division. Purdue University School of Agronomy. <<http://shadow.agry.purdue.edu/sc.norm-geog.html>>.
- Inwood, S.E., Tank, J.L., and Bernot, M.J., 2005. Patterns of denitrification associated with land use in 9 Midwestern headwater streams. *Journal of North American Benthological Society* 24(2):227-245.
- Jensen, S.E., Anders, C.L., Goatcher, L.J., Perley, T., Kenefick, S., and Hruday, S.E., 1994. Actinomycetes as a factor in odour problems affecting drinking water from the North Saskatchewan River. *Water Resources* 28:1393-1401.
- Johnson, A.H., Bouldin, D.R., Goyette, E.A., and Hedges, A.M., 1976. Phosphorus loss by stream transport from a rural watershed: Quantities, processes, and sources. *Journal of Environmental Quality* 5:148-157.
- Johnstone, J., Vidon, P., Tedesco L.P., and Soyeux, E. Nitrogen, phosphorus, and carbon dynamics in a third-order stream of the U.S. Midwest. *Proceedings of the Indiana Academy of Science* 119(1) (in press), 2010.
- Jüttner, F., 1990. Monoterpenes and microbial metabolites in the soil. *Environmental Pollution* 68:377-382.
- Jüttner, F. and Watson, S.B., 2007. Biochemical and ecological control of geosmin and 2-methylisoborneol in sources waters. *Applied and Environmental Microbiology* 73(14):4395-4406.
- Kauffman, J.B., Beschta, R.L., Otting, N., and Lytjen, D., 1997. An ecological perspective of riparian and stream restoration in the western United States. *Fisheries* 22(5):12-24.
- Kladivko, E.J., Van Scoyoc, G.E., Monke, E.J., Oates, K.M., and Pask, W., 1991. Pesticide and nutrient movement into subsurface tile drains on a silt loam soil in Indiana. *Journal of Environmental Quality* 20:264-270.

- Kladivko, E.J., Brown, L.C., and Baker, J.L., 2001. Pesticide transport to subsurface tile drains in humid regions of North America. *Critical Reviews in Environmental Science and Technology* 31(1):1-62.
- Kladivko, E.J., Frankenberger, J.R., Jaynes, D.B., Meek, D.W., Jenkinson, B.J., and Fausey, N.R., 2004. Nitrate leaching to subsurface drains as affected by drain spacing and changes in crop production system. *Journal of Environmental Quality* 33:1803-1813.
- Kovacic, D.A., David, M.B., Gentry, L.E., Starks, K.M., and Cooke, R.A., 2000. Effectiveness of constructed wetlands in reducing nitrogen and phosphorus export from agricultural tile drainage. *Journal of Environmental Quality* 29:1262-1274.
- Kronvang, B., Laubel, A., and Grant, R., 1997. Suspended sediment and particulate phosphorus transport and delivery pathways in an arable catchment, Gelbæk Stream, Denmark. *Hydrological Processes* 11:627-642.
- Kronvang, B., Bechmann, M., Lundekvam, H., Behrendt, H., Rubæk, G.H., Schoumans, O.F., Syversen, N., Andersen, H.E., and Hoffman, C.C., 2005. Phosphorus losses from agricultural areas in river basins: effects and uncertainties of targeted mitigation measures. *Journal of Environmental Quality* 34:2129-2144.
- Leopold, L.B. and Maddock, T., Jr., 1953. The hydraulic geometry of stream channels and some physiographic implications: U.S. Geological Survey Professional Paper 252, 57 pp.
- Lindsey, B.D., Breen, K.J., Bilger, M.D., and Brightbill, R.A., 1998. Water quality in the Lower Susquehanna River Basin, Pennsylvania and Maryland, 1992-95. U.S. Geological Survey Circular 1168, 38 pp.
- Mitsch, W.J. and Gosselink, J.G., 2000. *Wetlands*, 3rd ed. John Wiley & Sons, Inc., New York. 920 pp.
- Ochoa-Acuña, H., Frankenberger, J., Hahn, L., and Carbajo, C., 2009. Drinking water herbicide exposure in Indiana and prevalence of small-for-gestational-age and preterm delivery. *Environmental Health Perspectives* 117:1619-1624.
- Osborne, L.L. and Kovacic, D.A., 1993. Riparian vegetated buffer strips in water-quality restoration and stream management. *Freshwater Biology* 29:243-258.
- Pascual, D.L., Raftis, R., Filippelli, G.M., Tedesco, L.P., and Seillier, JM., 2006. Run-off and tile drainage verses internal recycling: Three year mass balance approach to understanding phosphorous loading and productivity in a small, urban reservoir, Eagle Creek Reservoir, IN, USA. 26th International Symposium of the North American Lake Management Society Program, 58 pp.

- Peter, A. and von Gunten, U., 2007. Oxidation kinetics of selected taste and odor compounds during ozonation of drinking water. *Environmental Science and Technology* 41:626-631.
- Poor, C.J. and McDonnell, J.J., 2007. The effects of land use on stream nitrate dynamics. *Journal of Hydrology* 332:54-68.
- Randall, G.W. and Mulla, D.J., 2001. Nitrate nitrogen in surface waters as influenced by climatic conditions and agricultural practices. *Journal of Environmental Quality* 30:337-344.
- Ricklefs, R.E., 2001. *The Economy of Nature*. W.H. Freeman and Company, New York. 550 pp.
- Rienhardt, M., Gächter, R., Wehrli, B., and Müller, B., 2005. Phosphorus retention in small constructed wetlands treating agricultural drainage water. *Journal of Environmental Quality* 34:1251-1259.
- Reinhardt, M., Müller, B., Gächter, R., and Wehrli, B., 2006. Nitrogen removal in a small constructed wetland: an isotope mass balance approach. *Environmental Science and Technology* 40:3313-3319.
- Robertson, D.M., Schwarz, G.E., Saad, D.A., and Alexander, R.B., 2009. Incorporating uncertainty into the ranking of SPARROW model nutrient yields from Mississippi/Atchafalaya River Basin Watersheds. *Journal of the American Water Resources Association* 45(2):534-549.
- Royer, T.V. and David, M.B., 2005. Export of dissolved organic carbon from agricultural streams in Illinois, USA. *Aquatic Sciences* 67:465-471.
- Royer, T.V., David M.B., and Gentry L.E., 2006. Timing of riverine export of nitrate and phosphorus from agricultural watersheds in Illinois: Implications for reducing nutrient loading to the Mississippi River. *Environmental Science and Technology* 40:4126-4131.
- Schipper, L.A., Cooper, A.B., Harfoot, C.G., and Dyck, W.J., 1993. Regulators of denitrification in an organic riparian soil. *Soil Biology and Biochemistry* 25(7):925-933.
- Schneider, A.F., 1966. Physiography, in Lindsey, A.A., ed., *Natural Features of Indiana: Indianapolis, Indiana Academy of Science*, p. 46-56.

- Schnoebelen, D.J., Fenelon, J.M., Baker, N.T., Martin, J.D., Bayless, E.R., Jacques, D.V., and Crawford, C.G., 1999. Environmental setting and natural factors and human influences affecting water quality in the White River Basin, Indiana: U.S. Geological Survey Water-Resources Investigations Report 97-4260, 66 pp.
- Seaber, P.R., Kapinos, F.P., and Knapp, G.L., 1987. Hydrologic Unit Maps: U.S. Geological Survey Water-Supply Paper 2294, 63 pp.
- Shampine, W.J., 1975. A river-quality assessment of the Upper White River, Indiana: U.S. Geological Survey Water-Resources Investigations Report 75-10, 68 pp.
- Sharpley, A.N., Gburek, W.J., Folmar, G., and Pionke, H.B., 1999. Sources of phosphorus exported from an agricultural watershed in Pennsylvania. *Agricultural Water Management* 41:77-89.
- Shaver, R.H., Ault, C.H., Burger, A.M., Carr, D.D., Droste, J.B., Eggert, D.L., Gray, H.H., Harper, D., Hasenmueller, N.R., Hasenmueller, W.A., Horowitz, A.S., Hutchinson, H.C., Keith, B.D., Keller, S.J., Patton, J.B., Rexroad, C.B., and Wier, C.E., 1986. Compendium of Paleozoic rock-unit stratigraphy in Indiana – a revision. Bloomington, Ind., Indiana Geological Survey Bulletin 59, 203 pp.
- Sherwood, J.M. and Huitger, C.A., 2005. Bankfull characteristics of Ohio streams and their relation to peak streamflows: U.S. Geological Survey Scientific Investigations Report 2005-5153, 38 pp.
- Sidle, R.C., Tsuboyama, Y., Noguchi, S., Hosoda, I., Fujieda, M., and Shimizu, T., 2000. Stormflow generation in steep forested headwaters: A linked hydrogeomorphic paradigm. *Hydrological Processes* 14:369-385.
- Smith, D.R., Warnemuende, E.A., Haggard, B.E., and Huang, C., 2006. Dredging of drainage ditches increase short-term transport of soluble phosphorus. *Journal of Environmental Quality* 35:611-616.
- Snyder, N.J., Mostaghimi, D.F., Berry, D.F., Reneau, R.B., Hong, S., McClellan, P.W., and Smith, E.P., 1998. Impact of riparian forest buffers on agricultural nonpoint source pollution. *Journal of the American Water Resources Association* 34(2):385-394.
- Soller, D.R., 1993. Map showing the thickness and character of Quaternary sediments in the glaciated United States east of the Rocky Mountains – northeastern states, the Great Lakes, and parts of southern Ontario and the Atlantic offshore area: U.S. Geological Survey Miscellaneous Investigations Series Map I-1970-A, scale 1:1,000,000.

- Stamm, C., Flühler, H., Gächter, R., Leuenberger, J., and Wunderli, H., 1998. Preferential transport of phosphorus in drained grassland soils. *Journal of Environmental Quality* 27:515-522.
- Tedesco, L.P., Pascual, D.L., Shrake, L.K., Casey, L.R., Vidon, P.G.F., Hernly, F.V., Salazar, K.A., Barr, R.C., Ulmer, J., and Pershing, D., 2005. Eagle Creek Watershed Management Plan: An integrated approach to improved water quality. Eagle Creek Watershed Alliance, CEES publication 2005-07, IUPUI, Indianapolis, 182 pp.
- Triska, F.J., Kennedy, V.C., Avanzino, R.J., Zellweger, G.W., and Bencala, K.E., 1989. Retention and transport of nutrients in a third-order stream in northwestern California: Hyporheic processes. *Ecology* 70(6):1893-1905.
- Ulrich, H.P., 1966. Soils, *in* Lindsey, A.A., ed., *Natural features of Indiana*: Indianapolis, Indiana Academy of Science, p. 57-90.
- U.S. Department of Agriculture, 1987. *Farm drainage in the United States – history, status, and prospects*: U.S. Department of Agriculture Economic Research Service, Washington, D.C. Miscellaneous Publication No. 1455, 186 pp.
- U.S. Geological Survey, 1999. *The quality of our nation's waters – nutrients and pesticides*: U.S. Geological Survey Circular 1225, 82 pp.
- Uusitalo, R., Turtola, E., Puustinen, M., Paasonen-Kivekäs, M., and Uusi-Kämpä, J., 2003. Contribution of particulate phosphorus to runoff phosphorus bioavailability. *Journal of Environmental Quality* 32:2007-2016.
- Vanni, M.J., Renwick, W.H., Headworth, J.L., Auch, J.D., and Schaus, M.H., 2001. Dissolved and particulate nutrient flux from three adjacent agricultural watersheds: A five-year study. *Biogeochemistry* 54:85-114.
- Vidon, P., Wagner, L.E., and Soyeux, E., 2008. Changes in the character of DOC in streams during storms in two Midwestern watersheds with contrasting land uses. *Biogeochemistry* 88:257-270.
- Wagner, L.E., Vidon, P., Tedesco, L.P., and Gray, M., 2008. Stream nitrate and DOC dynamics during three spring storms across land uses in glaciated landscapes of the Midwest. *Journal of Hydrology* 362:177-190.
- Watson, S.B., 2004. Aquatic taste and odour: A primary signal of drinking water integrity. *Journal of Toxicology and Environmental Health, Part A: Current Issues* 67:1779-1795.

- Westerhoff, P., Nalinakumari, B., and Pei, P., 2006. Kinetics of MIB and geosmin oxidation during ozonation. *Ozone Science and Engineering* 28:277-286.
- Willet, V.B., Reynolds, B.A., Stevens, P.A., Ormerod, S.J., and Jones, D.L., 2004. Dissolved organic nitrogen regulation in freshwaters. *Journal of Environmental Quality* 33:201-209.
- Williams, M., Hopkinson, C., Rastetter, E., and Vallino, J., 2004. N budgets and aquatic uptake in the Ipswich River Basin, northeastern Massachusetts. *Water Resources Research* 40, W11201, doi:10.1029/2004WR003172
- Winchester, P.D., Huskins, J., and Ying, J., 1999. Agrichemicals in surface water and birth defects in the United States. *Acta Pædiatrica* 98:664-669.
- Wolman, M.G. and Leopold, L.B., 1957. River flood plains – some observations on their formation: U.S. Geological Survey Professional Paper 282-C, 107 pp.
- Wolman, M.G. and Miller, J.P., 1960. Magnitude and frequency of forces in geomorphic processes. *Journal of Geology* 68:54-74.
- Worrall, F., Burt, T., and Adamson, J., 2003. Controls on the chemistry of runoff from an upland peat catchment. *Hydrological Processes* 17:2063-2083.
- Xue, Y., David, M.B., Gentry, L.E., and Kovacic, D.A., 1998. Kinetics and modeling of dissolved phosphorus export from a tile-drained agricultural watershed. *Journal of Environmental Quality* 27:917-922.

Curriculum Vitae

Michael David Wayne Stouder

Education

Master of Science, January 2008 to August 2010

Indiana University, IUPUI, Indianapolis, IN

Major: Earth Sciences with concentration in surface water hydrology

Thesis: *Nutrient and contaminant export dynamics in a larger-order Midwestern watershed: Upper White River, Central Indiana, USA*

GPA: 4.0/4.0

Bachelor of Arts, August 2003 to December 2007

Indiana University, IUPUI, Indianapolis, IN

Major: Earth Sciences

GPA: 3.1/4.0

Professional Experience

Graduate Research Assistant, January 2008 – August 2010

Department of Earth Sciences, IUPUI, Indianapolis, IN

Intern, August 2007 – December 2007

Center for Earth and Environmental Science, IUPUI, Indianapolis, IN

Drill Helper, May 2007 – August 2007

ATC Associates, Inc., Indianapolis, IN

Publications and Presentations

Tedesco, L.P., Clercin, N., Cowan, A., Stouder, M., and Gray, M., 2010. Microcystin and Taste and Odor Compound Occurrence, Fate and Transport in central Indiana Surface Waters. Abstract submitted to the 7th National Water Monitoring Conference, Denver, April 2010.

Stouder, M., Tedesco, L.P., and Jacinthe, P-A., 2009. The Utility of Agricultural Constructed Wetlands, Project Aquisafe. Kompetenzzentrum Wasser Berlin (Berlin Center of Competence in Water), Berlin, Germany, 29 pp. Available at: <http://cees.iupui.edu/Publications/Abstracts_Papers/Water_Resources/2009_Aug_KWB_Aquisafe_Stouder_Tedesco_Jacinthe.pdf>

Stouder, M., Tedesco, L.P., Johnstone, J., Vidon, P., and Gray, M., 2009. Contaminant export dynamics in larger-order Midwestern watersheds: Upper White River, Central Indiana. Poster presented at the Indiana Environmental Health Summit: Water Quality and Human Health in Indiana, Indianapolis, May 2009.

Stouder, M., Johnstone, J.A., Vidon, P., and Tedesco, L.P., 2009. Nutrient export dynamics in larger order Midwestern watersheds: Upper White River, Central Indiana. Research presented at the Central Indiana Water Resources Partnership Annual Meeting, Indianapolis, March 2009.

Hack, E., Morel-Fatio, A., Tedesco, L.P., Barr, R.C., Grützmacher, G., Bacqueroet, A., Stouder, M., Woolems, B., 2008. Assessment of risks to surface water from diffuse contaminants. CEES Spring Science Meeting, Center for Earth and Environmental Science, Indiana University-Purdue University, Indianapolis, April 2008.

Stouder, M. and Barr, R.C. 2008. Bibliography of Data Resources Relative to Physical, Chemical, and Biological Water Quality in the Upper White River Watershed, Central and East-Central Indiana. Upper White River Watershed Alliance Homepage, 136 pp. Available at:
<http://76.12.238.58/docs/00Final_bibliography.pdf>